# Speciation of selenium (IV, VI) in urine and serum of thyroid patients by ultrasound-assisted dispersive liquid-liquid microextraction

**Elham Mosafayian Jahromy**[a] and **Negar Motakef Kazemi** [a,*]

*[a] Department of Medical Nanotechnology, Faculty of Advanced Sciences and Technology, Tehran Medical Sciences, Islamic Azad University, Tehran, Iran*

**A B S T R A C T**

In-vitro speciation of inorganic selenium (Se$^{IV}$ and Se$^{VI}$) in serum blood and urine of hyperthyroidism and hypothyroidism patients based on isopropyl 2-[(isopropoxycarbothiolyl) disulfanyl] ethane thioate (IICDET) as a complexing agent were studied by ultrasound-assisted dispersive liquid-liquid bio-microextraction procedure (USA-DLLMBE). In first stage, 100 μL (≈0.1 g) of hydrophobic ionic liquid of [C$_8$MIM][PF$_6$] mixed with IICDET ligand and 100 μL of acetone. Then, the mixture injected to 10 mL of human samples at pH=4. After shacking, the Se (IV) ions were complexed by IICDET and extracted to IL at pH=4 (R-S: …Se). The IL phase was separated from sample by centrifuging and inorganic selenium (Se $_{IV}$) in remained samples was determined by electro thermal atomic absorption spectrometry (ET-AAS) after back extraction of Se (IV). As speciation, the Se (VI) reduced to Se (IV) in acidic pH (HCl, 130$^O$C) and the total Se(T-Se) was obtained at pH=4. Therefore, the Se (VI) was calculated by difference of T-Se and Se (IV). After optimized conditions, the enrichment factor (EF), Linear range and limit of detection (LOD) for inorganic Se (IV) were obtained 20.1, 0.75- 20 μg L$^{-1}$ and 0.18 μg L$^{-1}$ in serum and urine samples respectively. The results showed us, the concentration of selenium was decreased in thyroid patients as compared to healthy peoples. The validation of methodology was achieved by certified reference material (CRM) and ICP-MS.

## 1. Introduction

Selenium is an essential trace element in humans. The soluble selenium compounds can be easily absorbed through the lungs and the gastrointestinal tract. Selenium is mainly excreted in human urine [1]. When the exposure is very high it can also be excreted in exhaled air as dimethylselenide vapor (DMSe). Normal selenium concentrations in serum and urine are dependent on daily intake, which may vary considerably in different parts of the world but are usually below 15 μg per 100 mL$^{-1}$ and 25 μg g$^{-1}$ creatinine, respectively [2-5]. The concentration of selenium in urine is mainly a reflection of recent exposure. The relationship between the intensity of exposure and selenium concentration in urine has not been established yet. It seems that the concentration in plasma (or serum) and urine mainly reflects to short-term exposure, whereas the selenium content of erythrocytes reflects more long-term exposure

*Corresponding Author: Negar Motakef Kazemi
Email: negar.motakef@gmail.com

[6]. Measuring selenium in blood or urine gives some information on selenium status. Currently it is more often used to detect a deficiency rather than an overexposure. Since the available data concerning the health risk of long-term exposure to selenium and the relationship between potential health risk and levels in biological media are too limited. So, the biological threshold value for Se wasn't reported [7]. The thyroid is the organ with the highest selenium content per gram of tissue because it expresses specific selenoproteins. The value of selenium supplementation in autoimmune thyroid disorders has been emphasized. Most authors attribute the effect of supplementation on the immune system to the regulation of the production of reactive oxygen species and their metabolites [8-10]. The mechanism and role of selenium in inflammation, immunity and hepatocytes was reported [11, 12] In patients with Hashimoto's disease and in pregnant women with anti-TPO antibodies, selenium supplementation decreases anti-thyroid antibody levels and improves the ultrasound structure of the thyroid gland [13]. Although clinical applications still need to be defined for Hashimoto's disease, they are very interesting for pregnant women given that supplementation significantly decreases the percentage of postpartum thyroiditis and definitive hypothyroidism. In Graves' disease, selenium supplementation results in euthyroidism being achieved more rapidly and appears to have a beneficial effect on mild inflammatory orbitopathy [14]. A risk of diabetes has been reported following long-term selenium supplementation, but few data are available on the side effects associated with such supplementation and further studies are required. One of the diseases that affect the thyroid gland is subclinical hypothyroidism, which is characterized by elevated serum levels of thyroid-stimulating hormone (TSH) at a concentration recommended for prohormone thyroxine (T4) and active hormone triiodothyronine (T3). The decompensated levels of thyroid hormones may contribute to atherosclerotic events and an increase in cardiovascular-related mortality [15]. Also, observational longitudinal studies have shown an inverse association between selenium exposure and risk of some cancer types but still to be confirmed [16]. It is estimated that subclinical hypothyroidism affects 3–8% of the general population and is more common in women than in men. In Brazil, an epidemiological study in elderly reported that prevalence of subclinical hypothyroidism was 6.5%. The thyroid gland contains high levels of selenium (Se) and expresses a variety of selenoproteins that are involved in protection of oxidative stress and metabolism of thyroid hormones (TH) [17]. Selenium deficiency impairs regular synthesis of selenoproteins and adequate TH metabolism. Therefore selenium species in serum and urine must be evaluated and determined by favorite techniques. The different methods such as, flame atomic absorption spectrometry [18], electrothermal atomic absorption spectrometry [19], liquid chromatography and liquid chromatography inductively coupled plasma mass spectrometry (LC and LC-ICP- MS) [20-22] and high-performance liquid chromatography coupled to hydride generation atomic fluorescence spectrometry [23,24] were used for Se determination in different human and water samples. A sample preparation is required to extract metals ions in different biological samples. The sample preparation such as microextraction techniques [25], suspended dispersive solid phase microextraction [26], ultrasonic assisted dispersive liquid-liquid microextraction method [27] and ultrasound assisted-ionic liquid-solid phase microextraction [28] were used for extraction metals in human samples. In this study, the mixture of hydrophobic ionic liquid of [$C_8$MIM] [$PF_6$], IICDET ligand and acetone was used for selenium speciation /extraction based on ultrasound-assisted dispersive liquid-liquid bio-microextraction procedure (USA-DLLMBE) and determined by ET-AAS. The Se (IV) ions were complexed by IICDET and extracted to IL at pH=4. Then speciation of Se was obtained by total determination of selenium. Validation methodology was confirmed by spiking of standard samples and ICP-MS.

## 2. Experimental
### 2.1. Instrument and Reagents
The electrothermal atomic absorption spectrophotometer (ET-AAS, GBC932plus, Australia)

equipped with a graphite furnace (Pal GF3000) were used for the validation and determination of selenium (Se) in samples (Wavelength 349.9 nm; slit 0.2 nm; current 10 mA). The working range as peak area and height was obtained 15- 400 $\mu g\ L^{-1}$ and 15-210 $\mu g\ L^{-1}$, respectively. The linear range was achieved for peak area of 0.3 Abs for sample injection. Based on the manual book of ET-AAS, the Se determination was achieved by injecting 20 $\mu L$ of sample to graphite tube with auto-sampler in three steps of drying, ashing, and atomization for Se. The ICP-MS (Perkin Elmer, USA) as ultra-trace analysis with high sensitivity was used for determining of Se(IV) and Se(VI) in human blood and water samples (1100 W; 15 L $min^{-1}$; 1.5 sec per mass; auxiliary gas 1.12 L $min^{-1}$). The Metrohm pH meter based on the glass electrode was used for measuring pH in serum, urine and blood samples (E-744, Switzerland). The vortex mixer were used for shaking of human samples based on 300 rpm speeds and centrifuged by Falcon accessory by 4000 rpm speeds (Thermo, USA). An ultrasonic bath was used for blood and urine samples with heat controller between 30- 120$^o$C (Thomas, USA). The standard solution of Se (VI, VI) was purchased from Merck CO. (Germany) with a concentration of 1000 mg $L^{-1}$ in 1 % $HNO_3$. The different concentration of Selenium was prepared by dilution of deionized water (DW) and ultrapure water was purchased from Millipore Company. The 1-Hexyl-3-methylimidazolium hexafluorophosphate as hydrophobic ionic liquid was purchased from Sigma Aldrich ([HMIM][$PF_6$], CAS N: 304680-35). Isopropyl 2-[(isopropoxycarbothioyl) disulfanyl] ethane thioate was synthesized and purified by Azad university laboratories (IICDET; $(CH3)_4$ $(CO)_2 S_4$). The acetate ($CH_3COOH$/ $CH_3COONa$) and phosphate buffer was used to adjust the pH between 2.8–6.2 and 6.2–8.2, respectively. The analytical grade of reagents such as polyoxyethylene octyl phenyl ether (TX-100) as the anti-sticking agent, $HNO_3$, HCl, acetone, and ethanol were purchased from Sigma Aldrich, Germany.

## 2.2. Preparation of human samples

All glass or PCV tubes were cleaned with a 1.0 mol $L^{-1}$ $HNO_3$ solution for at least one day and then washed for ten times with ultrapure water. As low concentrations of Se(IV) and Se(VI) in human serum, blood and urine samples, the cations or anions contamination at any stage of sample preparation, saving and analytical processes can be affected on the results accuracy. Heparin was used as anticoagulants for human blood samples into Eppendorf (5 mL) tubes and kept at -20$^o$C for two weeks. Each blood samples were prepared by 10 $\mu L$ of pure heparin (free Se) to blood sample. The serum, blood and urine samples were collected from hypothyroidism patients (50) and healthy peoples (50) with aged between 25 - 60 years, Tehran (IRAN). In this study, the world medical association declaration of Helsinki (WMADH) based on guiding physicians in human body research was obtained by the Ethical Committee of Azad University (E.C.: R.IAU.PS.REC.1399.106). The human samples were prepared based on WMADH law and absolutely protected the life and health of the human subject.

## 2.3. Synthesis of IICDET ligand

The 2.0×$10^{-3}$ mol of potassium O-isopropyl (ditiocarbomate) was dissolved in 20 mL of DW and cooled in an ice bath for 10 minutes. The 2.0×$10^{-3}$ mol of iodine solution and potassium iodide as drop wise was added to 20 ml of DW. After stirring of mixture for 1h, the aqueous phase was extracted with $CH_2Cl_2$ and washed with 30 mL of aqueous $Na_2S_2O_3$(10%) and DW. The organic phase was dried and evaporated with powder anhydrous calcium chloride Ca $Cl_2$ (99.99%; CAS Number: 10043-52-4). The purification was obtained by recrystallization in hexane. A pale yellowish crystal of isopropyl 2-[(isopropoxycarbothiolyl) disulfanyl] ethane thioate with a yield of 95% was achieved. The structure and isopropyl 2-[(isopropoxycarbothiolyl) disulfanyl] ethane thioate were confirmed by NMR spectroscopic methods (Fig. 1). $^1$H NMR ($CDCl_3$). $\delta$ (ppm): 1.43 (d, 12H, $CH_3$), 5.63 (m, 2H, CH). $^{13}$C NMR ($CDCl_3$). $\delta$ (ppm): 22.2, 80.6, 207.1. $^{IR}$ (KBr). vmax (cm−1): 2979.8 (s), 2869.9 (w), 1463.9 (s), 1442.7 (s), 1373.0 (s), 1271.1 (s, b), 1145.6 (s), 1082.2 (s), 1048.0 (s, b) 898.8 (s), 796. 5 (s), 690. 5 (m).
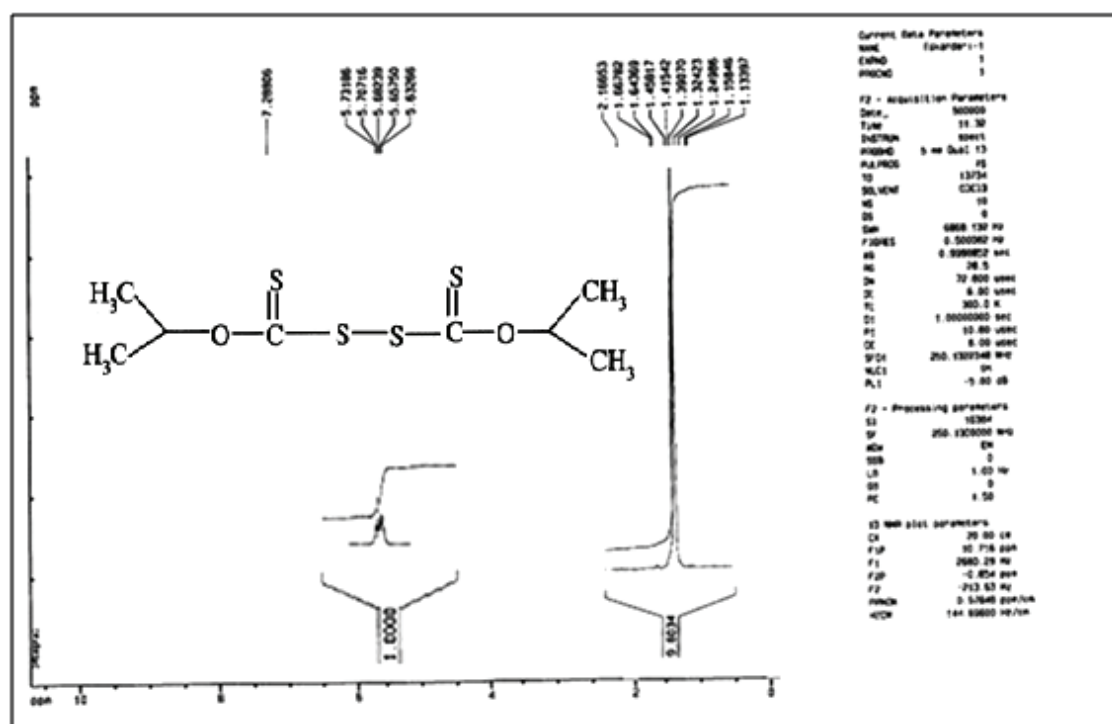
**Fig.1.** NMR spectroscopic for isopropyl 2-[(isopropoxycarbothiolyl) disulfanyl] ethane thioate

### 2.4. Extraction Procedure

The Se (IV) based on IICDET ligand was extracted by ultrasound-assisted dispersive liquid-liquid bio-microextraction procedure (USA-DLLMBE). By procedure, 100 μL (≈0.1 g) of hydrophobic ionic liquid of [$C_8$MIM][$PF_6$] mixed with $0.35 \times 10^{-6}$ mol $L^{-1}$ of IICDET solution and 100 μL of acetone at pH of 4. The mixture based on Triton X-100, an emulsifier and anti-sticking agent was injected to 5 mL of blood, serum and urine samples which was diluted with 5 mL of DW. For optimizing, 1.0 μg $L^{-1}$ and 20 μg $L^{-1}$ of standard solution of Se (IV) as LLOQ and ULOQ was used instead of the blood and serum samples. After shacking, the Se (IV) ions were complexed by IICDET and extracted to IL at pH=4 (R-S: …Se). By centrifuging (3 min), the IL phase was separated from sample and inorganic selenium (Se $_{IV}$) was back- extracted from IL phase in basic pH (0.25 mL of 1.0 mol $L^{-1}$ NaOH). Finally, the remained samples was determined by electro thermal atomic absorption spectrometry (ET-AAS). the Se (VI) reduced to Se (IV) in acidic pH (HCl, 130°C) and the total Se(T-Se) was obtained at pH=4. Therefore, the Se (VI) was calculated by difference of T-Se and Se (IV) amount (Fig.2).

### 3. Results and Discussion

The human blood, serum and urine samples based on IICDET was used for selenium speciation with high accuracy by USA-DLLMBE procedure. The results showed us, the mean concentrations of Se (IV and VI) in human biological samples in hypothyroidism patients (50) were significantly higher than the healthy peoples (50). As linear range of selenium between 0.75-20 μg $L^{-1}$, the human samples can be diluted before using by proposed procedure. Based on results, the mean concentration of total selenium in urine and serum of hypothyroidism patients was obtained 11.8 μg $g^{-1}$ creatinine and 52.6 μg $L^{-1}$, respectively which was less than 25 μg $g^{-1}$ creatinine for urine samples and 150 μg $L^{-1}$ for serum samples as TLVs in standard references.
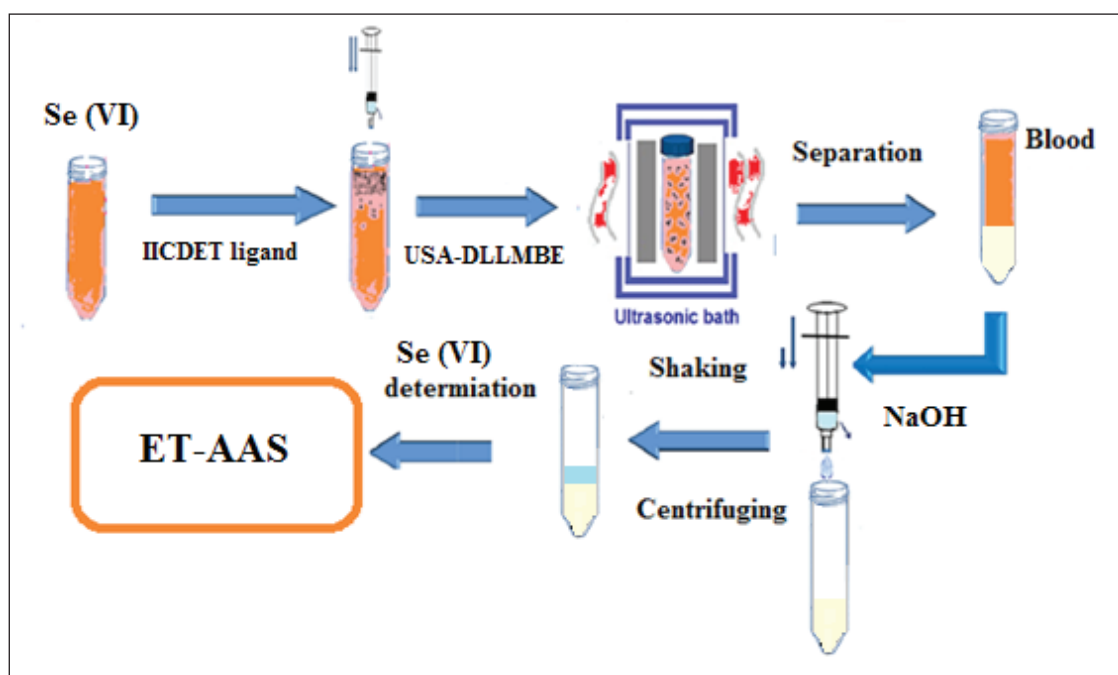
**Fig. 2.** Separation of selenium (IV) by ultrasound-assisted dispersive liquid-liquid bio-microextraction procedure (USA-DLLMBE)

### 3.1. Effect of ETAAS

The effect of pyrolysis temperature on the absorbance of Se was studied up to 1000 $^{\circ}$C. The maximum absorbance was achieved within a range of 600–800 $^{\circ}$C. Therefore, 700 $^{\circ}$C was selected as the working pyrolysis temperature for selenium by nickel nitrate as modifier at concentration of 0.05 to 0.1% Ni. In addition, a drying as a 25 s was chosen for water evaporation, and a long ramp time of 40 s was chosen as it allowed gradual elimination of trace ionic liquid solution in liquid phase (350 $^{\circ}$C) and avoided Se loss in pyrolysis temperature. The effect of atomization temperature on chromium signal was studied within the range of 2000–2500 $^{\circ}$C, and the maximum signal was obtained at approx. 2400 $^{\circ}$C. Cleaning time and temperature were ordered at 2 s and 2500 $^{\circ}$C, respectively, and argon flow rate was 350 mL min$^{-1}$

### 3.2. Optimization of pH

The sample pH for extraction Se(IV) ions based on IICDET ligand was studied and optimized in different pH ranges between 2-11 for 0.75μg L$^{-1}$ as a lower limit of quantification (LLOQ) and 20 μg L$^{-1}$ selenium as upper limit of quantification (ULOQ). The complexation Se with sulfur of IICDET ligand was strongly depended on the pH of serum, blood and urine samples and caused to increase the recovery of extraction by ligand. Based on experimental results, the extraction efficiency of Se(IV) ions was perfectly achieved at pH =3.5-4.5. Therefore, the USA-DLLMBE procedure was used to speciation of selenium at pH=4 by IICDET ligand. The mechanism of Se extraction was obtained based on the complex formation of IICDET ligand between Se(IV) ions and sulfur covalence bonding of IICDET at optimized pH. The sulfur groups can be deprotonated (SH$^{-}$) at pH range of 3.5-8 and pH=4 was used as favorite pH for extraction of Se(IV) from human biological samples which was shown in Figure 3. As hydroxyl form of Se(OH)$_4$ in above pH (more than 6), the extraction capacity of Se(IV) in basic pH may be attributed to the affinities of OH groups.
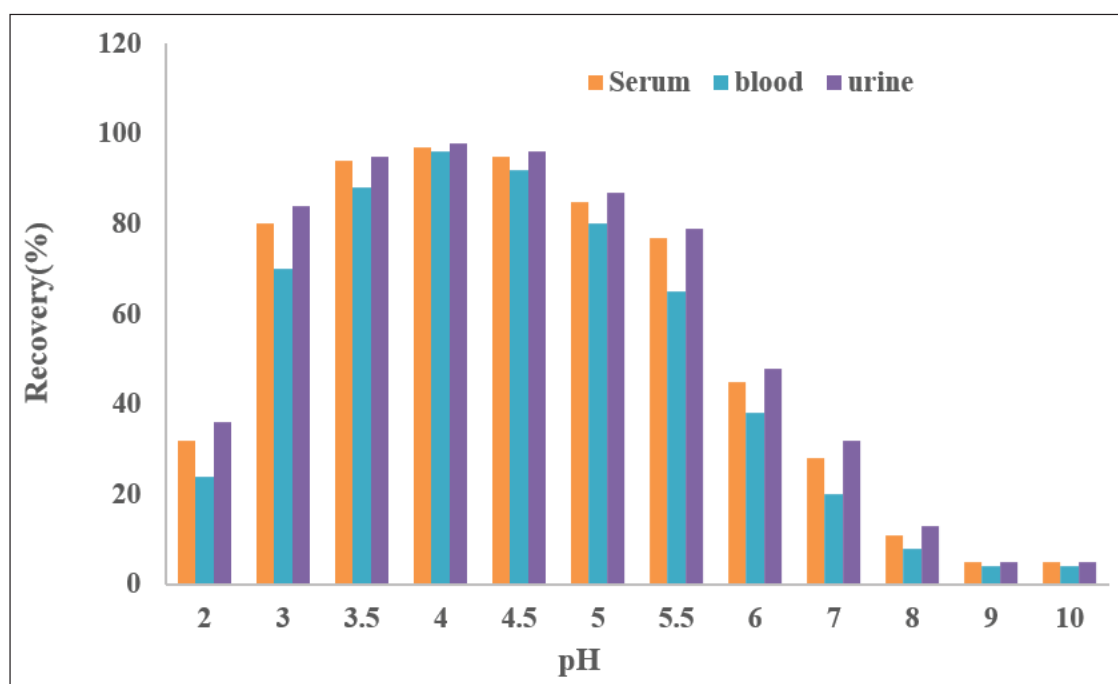
**Fig.3.** The effect of pH on Extraction Se(IV) based on IICDET ligand by USA-DLLMBE procedure

### 3.3. Optimization of IICDET ligand

The concentration of IICDET ligand as important parameters must be studied and optimized by USA-DLLMBE procedure. For optimizing, the concentration of $0.1 \times 10^{-6}$-$1.0 \times 10^{-6}$ mol $L^{-1}$ of IICDET ligand was used for evaluation. Due to results, the more concentration of $0.33 \times 10^{-6}$ mol $L^{-1}$ of IICDET, has no effect on recoveries. So, the concentration of $0.35 \times 10^{-6}$ mol $L^{-1}$ of IICDET was selected as optimum ligand concentration for high extraction efficiency. The signal remained constant from $0.35 \times 10^{-6}$ mol $L^{-1}$ up to at least $1.0 \times 10^{-6}$ mol $L^{-1}$ IICDET for $0.75 \mu g$ $L^{-1}$ Se as a LLOQ range. Therefore $0.35 \times 10^{-6}$ mol $L^{-1}$ of IICDET concentration was used for further works. As 20 μg $L^{-1}$ of Se as a ULOQ range, the signal remained constant from $0.4 \times 10^{-6}$ mol $L^{-1}$ up to at least $1.0 \times 10^{-6}$ mol $L^{-1}$ and $0.4 \times 10^{-6}$ mol $L^{-1}$ was selected as an optimized IICDET concentration. By adjusting pH, the best performance of the Se extraction was achieved between 0.3-0.4 μmol $L^{-1}$ (Fig. 4).

### 3.4. Optimization of volume and ionic liquid amount

The sample volume as main parameters for Se extraction based on IICDET ligand and must be optimized at pH=4. So, the different volume of sample urine, blood and serum from 1-20 mL was used for extraction of Se ions by USA-DLLMBE procedure as 0.75 μg $L^{-1}$ and 20 μg $L^{-1}$ of selenium (IV). Perfect extraction more than 95% was achieved by sample volume of 1 - 10 mL. By increasing of sample volumes, the extraction efficiency was reduced. On the other hand, in high sample volumes, the partially solubilized the ionic liquid phase was increased and decreased accuracy and precision of results. So, a sample volume of 5 mL was selected as optimum volume for Se(IV) extraction based on ICDET ligand by USA-DLLMBE procedure (Fig. 5). Furthermore, the amount of ionic liquid effected on extraction recovery of Se in serum, blood, urine samples. Therefore, the different amount of ([C$_8$MIM][PF$_6$] as hydrophobic ionic liquid was studied from the range of 0.05–0.35 g. Quantitative extraction was observed at higher than 0.08 g. So, 0.1 g of
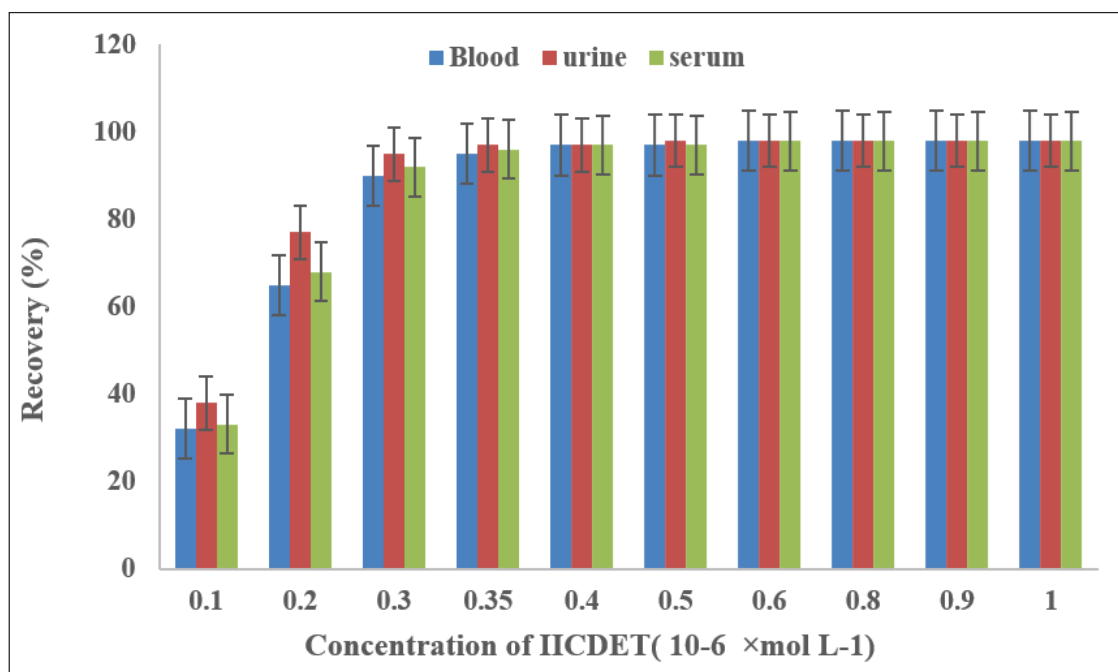
**Fig. 4.** The effect of IICDET ligand on Extraction Se(IV) by USA-DLLMBE procedure
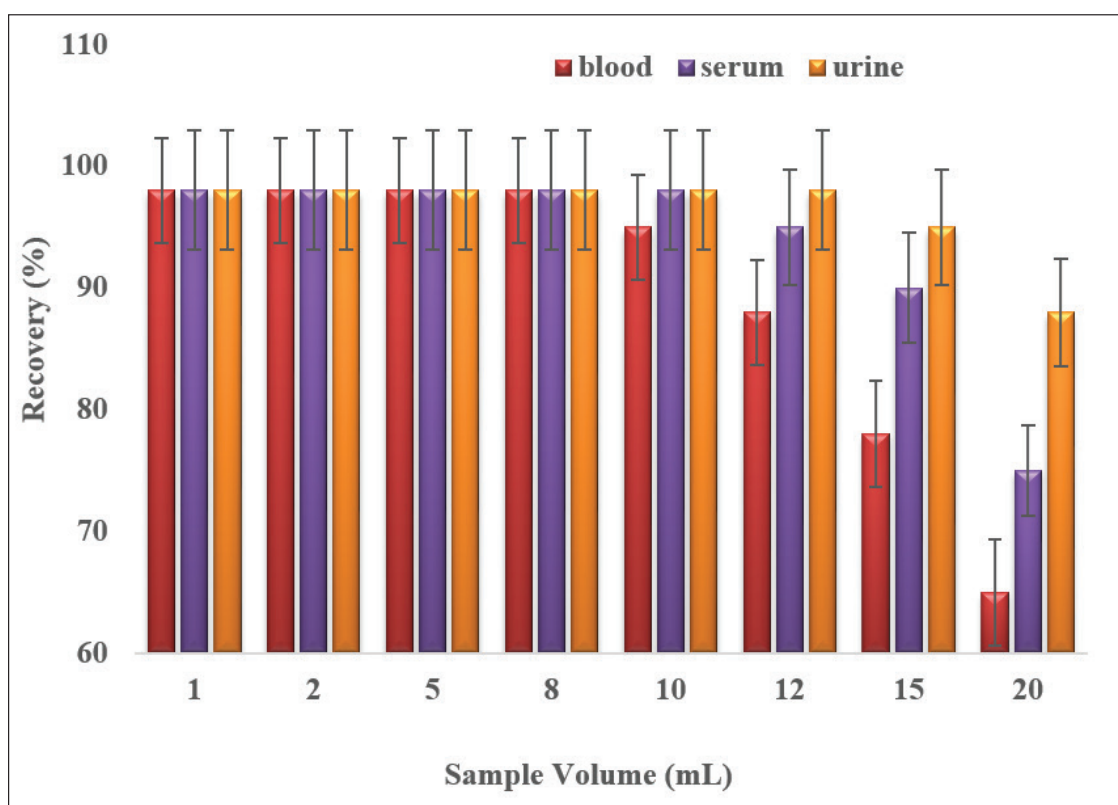


**Fig. 5.** The effect of sample volume on Extraction Se(IV) by USA-DLLMBE procedure
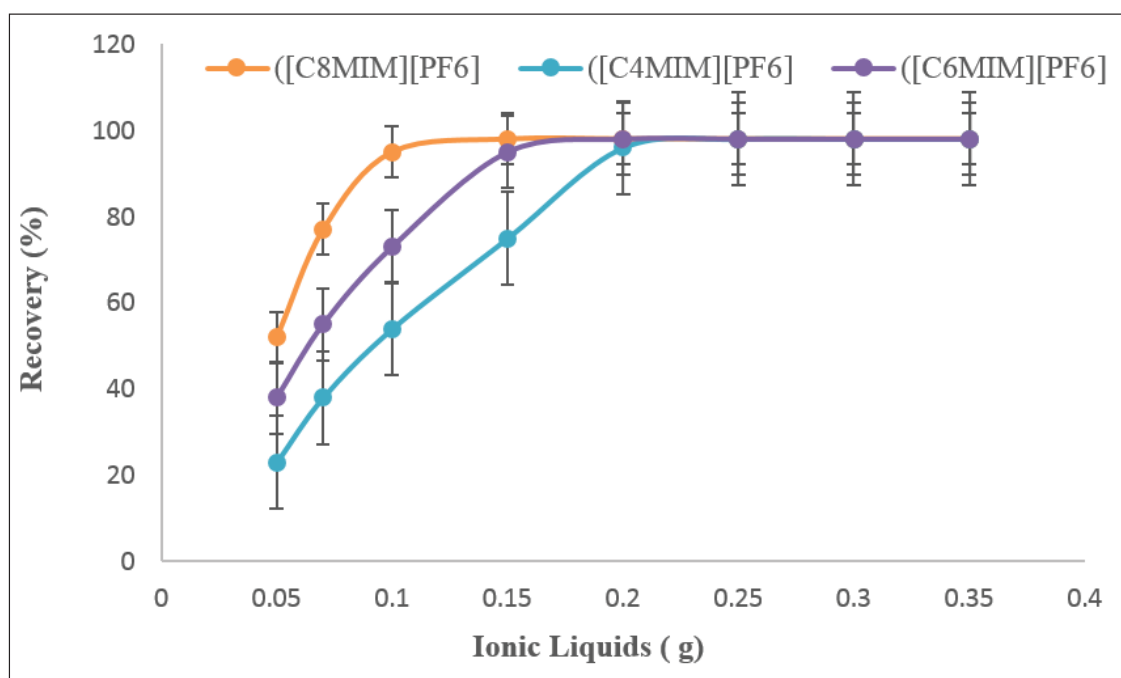
**Fig. 6.** The effect of amount of ionic liquid on Extraction Se(IV) based on IICDET ligand by USA-DLLMBE procedure

$[C_8MIM][PF_6]$ was chosen as optimum mass for Se extraction in 10 mL of samples at pH=4 (Fig. 6). The results showed, the amounts of IL have changes a little mass in different samples. The amounts of IL for serum, blood and urine samples were obtained 0.09 g, 0.1 g and 0.07 g, respectively.

### 3.5. Optimization of Eluent
The ionic liquids cannot apply directly by ETAAS as a viscose solution with high ash point temperature. So, the se ions were back-extracted from $[C_8MIM][PF_6]$ by different eluents such as a mineral acidic/basic solution. By changing pH, the complexation of Se-ligand leads to dissociation and Se ions release into the aqueous phase. Therefore, the varying concentration of mineral reagents such as HCl, $HNO_3$, $H_2SO_4$, KOH and NaOH from 0.5─3 mol $L^{-1}$ were used for Se back-extraction from IL by elution processes (Fig. 7). Based on results, 1.0 mol $L^{-1}$ of NaOH at 25°C can be back-extracted Se (IV) from the IL phase). By procedure, 0.25 mL of 1.0 mol $L^{-1}$ of NaOH was added and shacked for I minute at 25 °C. Finally, Se(IV) the remain solution determining by ET-AAS after dilution

with DW up to 0.5 mL.

### 3.6. Effect of ultrasound and matrix
By procedure, the different ultrasound times was studied for selenium extraction in urine, blood and serum samples from 30 to 300 seconds. The results showed us, the extraction efficiency of Se improved by increasing the ultra-sonication time and then the relative response increased. Based on results, the maximum extraction was shown at 132 seconds and then remained constant. So, 2.2 minutes was selected as optimum time as ligand complexation (IICDET). Many techniques such as ETAAS have low sensitivity to metal interference ions. Therefore, the most interference ions can be occurred during the pre-concentration or extraction processes which was effected on accuracy of results. So, the important metals based on potential interfering ions for selenium determination were studied and optimized by procedure. 10 mL sample containing 20 μg $L^{-1}$ of Se and 1–4 mg $L^{-1}$ different concentration of matrix ions was used. The tolerate amounts of each ion were tested and results showed the absorbance alteration of interfering metals
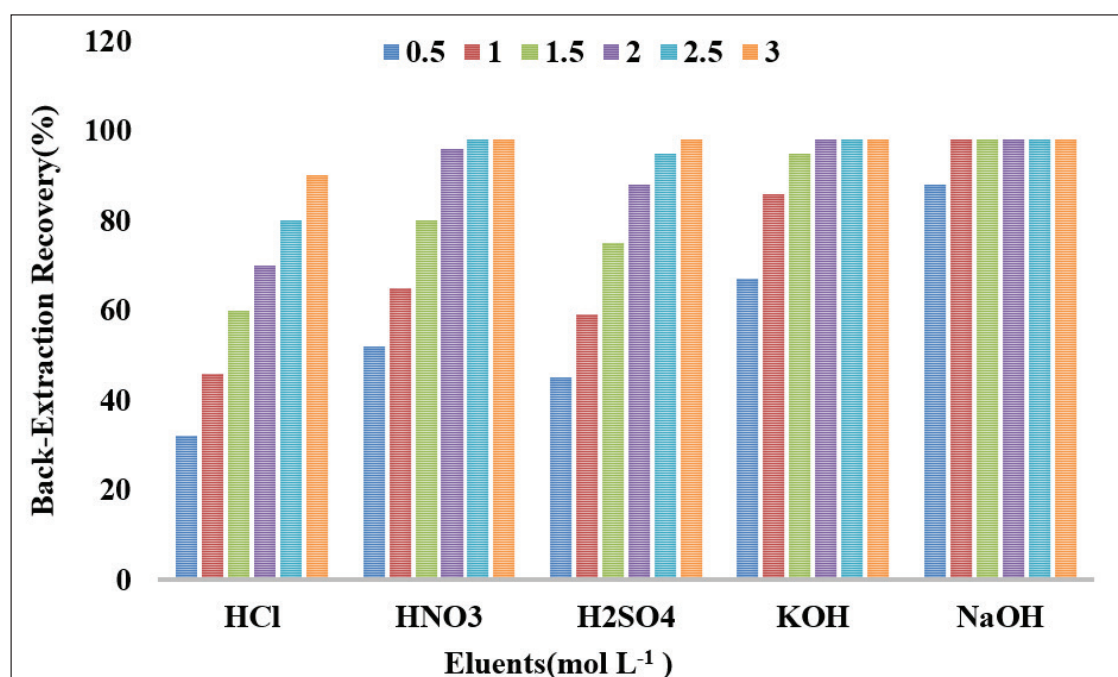
**Fig. 7.** The effect of different eluents on Extraction Se(VI) based on IICDET ligand by USA-DLLMBE procedure

were less than 5%. So, the interfering metals don't effected on extraction Se in optimized conditions (Table 1).

### 3.7. Analytical features

Analytical figures of merit were evaluated by USA-DLLMBE procedure for 10 mL of standard aqueous solutions, serum, urine and blood samples at pH=4 (Table 2). After preconcentration steps, the calibration curve was linear from $0.75 - 20$ μg $L^{-1}$ as a lower limit of quantification (LLOQ) and upper limit of quantification (ULOQ). Detection limits (LOD) and precision (RSD %) was evaluated for selenium extraction by proposed ligand. The LOD were calculated as the concentration providing an analytical signal three times higher than the background noise. The LOD was obtained 186 ng $L^{-1}$ and 174 ng $L^{-1}$ for 10 mL of human and standard samples, respectively (MLOD=180 ng $L^{-1}$). As precision (RSD %), it was calculated from ten individual standards. The RSD (%) of Se (IV) in different concentrations of 0.75, 1.0 5.0, 10, and 20 μg $L^{-1}$ were obtained 3.8, 3.2, 2.7, 2.6 and 2.45, respectively (MRSD% =2.95). The

enrichment factor (EF), calculated as the ratio of the concentration of Se after preconcentration to that prior preconcentration based on curve fitting calibration rule. The EF of 21.2 and 18.9 for human and standard samples, respectively (M PF=20.1).

### 3.8. Validation of Results

The selenium was extracted and determined in human samples based on IICDET ligand with USA-DLLMBE procedure for 10 mL of hypothyroidism patients (50) and healthy peoples (50) with aged between 25 - 60 years (Table 3). The mean concentration of Se(IV) more than Se(VI) in human samples and the mean concentration of Se(IV) and Se(VI) in hypothyroidism patients lower than healthy peoples. The coloration analysis (r) of total Se(IV and VI) in hypothyroidism patients and healthy peoples were less than 0.19 in blood samples. The spiked urine, serum and blood were used to demonstrate the reliability of the method for determination of Se(IV) and Se(VI) in hypothyroidism patients by USA-DLLMBE procedure (Table 4). The recovery of spiked samples showed a satisfactorily results with the

**Table 1.** The effect of interferences ions on extraction of Se(IV) in human samples by USA-DLLMBE procedure

| Blood, Serum (I) | Mean ratio $(C_I/C_{Se(IV)})$ | Recovery (%) |
|---|---|---|
| | Se(IV) | Se(IV) |
| $Al^{3+}$ , $Cr^{3+}$ | 550 | 96.8 |
| $Zn^{2+}$, $Cu^{2+}$, $Ni^{2+}$, $Co^{2+}$, $Pb^{2+}$ | 750 - 850 | 97.6 |
| $I^-$ , $Br^-$, $F^-$, $Cl^-$ | 1250 | 98.9 |
| $Na^+$, $K^+$, $Ca^{2+}$, $Mg^{2+}$ | 1100 | 97.7 |
| $CO_3^{2-}$, $PO_4^{3-}$, $NH_4^+$ | 950 | 99.3 |
| $Mn^{2+}$, $As^{3+}$ | 150 - 250 | 98.1 - 97.5 |
| $Cd^{2+}$ | 200 | 98.4 |
| $Hg^{2+}$ | 45 | 97.3 |
| Urine (I) | Mean ratio $(C_I/C_{Se(IV)})$ | Recovery (%) |
| | Se(IV) | Se(IV) |
| $Cl^-$, $NO_3^-$ | 1200 | 98.2 |
| $Na^+$, $K^+$ | 1200 | 98.6 |
| $Ca^{2+}$, $Mg^{2+}$ | 1000 | 98.0 |
| $Zn^{2+}$, $Cu^{2+}$ | 700 | 97.5 |
| $CO_3^{2-}$, $PO_4^{3-}$, $NH_4^+$ | 900 | 96.9 |
| $Hg^{2+}$ | 50 | 97.4 |
| $Pb^{2+}$ | 800 | 98.3 |
| $Ni^{2+}$, $Co^{2+}$ | 700 | 97.2 |
| $Cd^{2+}$ | 150 | 98.5 |
| $Mn^{2+}$ | 100 | 96.6 |

**Table 2.** The analytical features for selenium determination by USA-DLLMBE procedure

| Features | value |
|---|---|
| Working pH | 4.0 |
| Concentration of IICDET | $0.35 \times 10^{-6}$ mol $L^{-1}$ |
| Sample volume of Blood, Serum, Urine (mL) | 10 .0 |
| Volume of sample injection | 20 μL |
| Linear range (Peak Area) | 0.75-20 μg $L^{-1}$ |
| Linear range (Peak Height) | 0.75-10.4 μg $L^{-1}$ |
| Mean RSD %, n=10 | 2.95 |
| LOD for human sample | 0.187 μg $L^{-1}$ |
| LOD for standard sample | 0.174 μg $L^{-1}$ |
| Enrichment factor for human blood or serum | 21.2 |
| Enrichment factor for standard | 18.9 |
| Volume and concentration of NaOH | 0.25 mL,1M |
| Shaking/Centrifuging time | 2.2 min, 3.0 min |
| Correlation coefficient | $R^2 = 0.9997$ |

ability of procedure for determination of Se(IV) and Se(VI) in hypothyroidism patients. Furthermore, the real blood, serum and urine samples were analyzed with ICP-MS and used as a CRM by USA-DLLMBE procedure. The results showed, the favorite efficiency and reliability of proposed method for determination and speciation of Se(IV) and Se(VI) in hypothyroidism patients (Table 5).

## 4. Conclusions

A simple and efficient method based on IICDET ligand was used for the speciation and determination of trace amount of Se(IV) and Se(VI) in hypothyroidism patients by USA-DLLMBE procedure coupled to ET-AAS. The main parameters such as sample volume, pH and ligand amount were optimized. This procedure introduced a sensitive, efficient and low cost method for speciation and separation of the Se(IV) and Se(VI) in human biological samples. The performance of USA-DLLMBE procedure for quantification extraction of Se(IV) and Se(VI) in blood, urine and serum samples was satisfactory. The favorite LOD, LOQ and RSD% achieved 0.18, 0.75 and 2.95, respectively and are comparable to previous reported methods. Based on results, the selenium concentration in thyroid patients was decreased as compared to healthy peoples. The method was validated by certified reference material (CRM) and ICP-MS analysis in real samples.

**Table 3.** Speciation and determination of Se(IV) and Se(VI) in serum, blood and urine samples based on IICDET ligand by USA-DLLMBE procedure (Serum and blood: $\mu gL^{-1}$, Urine: $\mu g\ g^{-1}$)

| Sample | Patients (n=50) | | Healthy peoples (n=50) | | Patients /healthy | |
| --- | --- | --- | --- | --- | --- | --- |
| | Se(IV) | Se(VI) | Se(IV) | Se(VI) | r | P value |
| **Serum** | 77.9 ± 11.9 | 16.8 ± 4.8 | 130.7 ± 21.7 | 21.8 ± 4.3 | 0.202 | <0.001 |
| **Urine** | 14.5 ± 3.7 | 2.7 ± 0.9 | 22.7 ± 7.8 | 3.6 ± 0.8 | 0.187 | <0.001 |
| **Whole Blood** | 81.8 ± 13.8 | 17.4 ± 5.6 | 122.4 ± 18.6 | 34.5 ± 6.6 | 0.194 | *<0.001* |

*Correlations are based on Pearson coefficients (r). Statistical significance will be observed if *P < 0.05*
Mean of three determinations of samples ± standard deviation (P = 0.95, n =10)

**Table 4.** Analytical results of Se(IV), Se(VI) and T-Se determination in serum, blood and urine samples with USA-DLLMBE procedure and ICP-MS ($\mu g\ L^{-1}$)

| Sample | Added | | *Found ($\mu g\ L^{-1}$) | | | * ICP-Ms | Recovery (%) | | |
| --- | --- | --- | --- | --- | --- | --- | --- | --- | --- |
| | Se(IV) | Se(VI) | Se(IV) | Se(VI) | T-Se | T-Se | Se(IV) | Se(VI) | T-Se |
| **Blood** | ----- | ----- | 67.5 ± 3.3 | 12.8± 0.6 | 80.3 ± 4.2 | 79.2 ± 2.7 | ---- | ---- | ---- |
| | 50 | ----- | 115.3 ± 5.6 | 12.6 ± 0.5 | 127.6 ± 6.1 | 129.3 ± 3.5 | 95.6 | ----- | 94.6 |
| | ----- | 10 | 67.3 ± 3.4 | 22.7 ± 1.1 | 90.0 ± 4.7 | 88.8 ± 2.9 | ----- | 99.0 | 97.0 |
| **Serum** | ----- | ----- | 81.6 ± 3.8 | 17.5 ± 0.8 | 99.1 ± 5.1 | 100.3 ± 3.4 | ----- | ----- | ---- |
| | 100 | ----- | 180.2 ± 8.5 | 17.2 ± 0.7 | 197.4 ± 9.3 | 195.6 ± 5.8 | 98.6 | ----- | 98.3 |
| | ----- | 20 | 82.2 ± 4.2 | 37.2 ± 1.8 | 119.4 ± 5.5 | 120.5 ± 3.6 | ----- | 98.5 | 101.5 |
| **Urine** | ----- | ----- | 12.6 ± 0.6 | 3.8 ± 0.2 | 16.4 ± 0.8 | 15.8 ± 0.3 | ----- | ----- | ----- |
| | 10 | ----- | 22.4 ± 1.2 | 3.7 ± 0.2 | 26.1±1.3 | 26.5 ± 0.5 | 98.0 | ----- | 97.0 |
| | ----- | 5 | 12.7 ± 0.6 | 8.6 ± 0.4 | 21. 3 ± 1.1 | 20. 8 ± 0.6 | ----- | 96.0 | 98.0 |

* Mean of three determinations ± standard deviation (P= 0.95, n=5)

All blood and serum samples diluted with DW (1: 10)

**Table 5.** Validation of methodology for determination selenium based on certified reference material (CRM) by USA-DLLMBE procedure

| Sample | Certified ($\mu g\ L^{-1}$) | Added ($\mu g\ L^{-1}$) | *Found ($\mu g\ L^{-1}$) | Recovery (%) |
|---|---|---|---|---|
| **CRM1598a** | 13.44 ± 0.58 | 10 | 23.22 ± 1.14 | 97.8 |
| S-ICP-MS | 15.56 ± 0.46 | 10 | 25.13 ± 1.23 | 95.7 |

* Mean of three determinations ± standard deviation (P= 0.95, n=5)

All blood and serum samples diluted with DW (1: 10)

CRM1598a selenium in animal serum

S-ICP-MS: Human serum analyses with ICP-MS

## 5. Acknowledgment

## 6. References

[1] G. Bjørklund, J. Aaseth, A.V. Skalny, J. Suliburska, M.G. Skalnaya, A.A. Nikonorov, Interactions of iron with manganese, zinc, chromium, and selenium as related to prophylaxis and treatment of iron deficiency, J. Trace Elem. Med. Biol., 41(2017) 41–53.

[2] M. Kucharzewski, J. Braziewicz, U. Majewska, S. Góźdź, Concentration of selenium in the whole blood and the thyroid tissue of patients with various thyroid diseases, Biol. Trace Elem. Res., 88 (2002) 25–30.

[3] M.K. Gürgöze, A. Olçücü, A.D. Aygün, E. Taskin, M. Kiliç, Serum and hair levels of zinc, selenium, iron, and copper in children with iron-deficiency anemia, Biol. Trace Elem. Res., 111 (2006) 23-29.

[4] W. Chin-Thin, C. Wei-Tun, P. Tzu-Ming, W. Ren-Tse, Blood concentrations of selenium, zinc, iron, copper and calcium in patients with hepatocellular carcinoma, Clin. Chem. Lab. Med., 40 (2002) 1118-1122.

[5] A.K. Baltaci, R. Mogulkoc, M. Belviranli, Serum levels of calcium, selenium, magnesium, phosphorus, chromium, copper and iron--their relation to zinc in rats with induced hypothyroidism, Acta Clin. Croat., 52 (2013) 151- 156.

[6] G.F. Combs, Biomarkers of selenium status, Nutrients., 7 (2015) 2209–36

[7] P.P. Felix, E.L. Ander, Urine selenium concentration is a useful biomarker for assessing population level selenium status, Environ. Int., 134 (2020) 105218.

[8] D.L. Hatfield, P.A. Tsuji, B.A. Carlson, V.N. Gladyshev, Selenium and selenocysteine: Roles in cancer, health, and development, Trends Biochem. Sci., 39 (2014) 112–20.

[9] W. Yang, A.M. Diamond, Selenium-binding protein as a tumor suppressor and a prognostic indicator of clinical outcome, Biomark Res., 1 (2013) 15.

[10] Y. Wang, W. Fang, Y. Huang, F. Hu, Q. Ying, W. Yang, B. Xiong, Reduction of selenium-binding protein 1 sensitizes cancer cells to selenite via elevating extracellular glutathione: a novel mechanism of cancer-specific cytotoxicity of selenite, Free Radic. Biol. Med., 79 (2015) 186-196.

[11] S. Misra, R.W. Kwong, S. Niyogi, Transport of selenium across the plasma membrane of primary hepatocytes and enterocytes of rainbow trout, J. Exp. Biol., 215 (2012) 1491–501.

[12] Z. Huang, A.H. Rose, P.R. Hoffmann, The role of selenium in inflammation and immunity: from molecular mechanisms to therapeutic opportunities, Antioxid Redox

Sign. 16 (2012) 705-743

[13] N. Manevska, S. Stojanoski, T. Makazlieva, Selenium treatment effect in auto-immune hashimoto thyroiditis in macedonian population, J. Endocrinol. Metabol., 9 (2019) 22-28.

[14] M. Leo, L. Bartalena., G. Rotondo Dottore, Effects of selenium on short-term control of hyperthyroidism due to Graves' disease treated wif methimazole: results of a randomized clinical trial, J. Endocrinol. Invest., 40 (2017) 281–287.

[15] G. Ira Martin, R. James, Sowers thyroid and the heart, Am. J. Med., 127 (2014) 691–698.

[16] M. Outzen, A. Tjonneland, E.H. Larsen, S. Friis, S.B. Larsen, J. Christensen, Selenium status and risk of prostate cancer in a Danish population, Brit. J. Nutr., 115 (2016) 1669-77.

[17] A. Dalia, T. Loh, A. Sazili, M. Jahromi, A. Samsudin, The effect of dietary bacterial organic selenium on growth performance, antioxidant capacity, and selenoproteins gene expression in broiler chickens, BMC Vet. Res., 13 (2017). http://doi:10.1186/s12917-017-1159-4.

[18] S.S. Najim, Determination of some trace elements in breast cancer serum by atomic absorption spectroscopy, Int. J. Chem., 9 (2017) 1-6.

[19] M. Krawczyk-Coda, Determination of selenium in food samples by high-resolution continuum source atomic absorption spectrometry after preconcentration on halloysite nanotubes using ultrasound-assisted dispersive micro solid-phase extraction, Food Anal. Meth., 12 (2019) 128-135.

[20] A. Terol, F. Ardini, A. Basso, M. Grotti, Determination of selenium urinary metabolites by high temperature liquid chromatography-inductively coupled plasma mass spectrometry, J. Chromatogr., 1380 (2015) 112–119.

[21] K. Pyrzynska, A. Sentkowska, Liquid chromatographic analysis of selenium species in plant materials, TrAC, Trend Anal. Chem., 111 (2019) 128–138.

[22] C.K Su, W.C. Chen, 3D-printed, $TiO_2$ NP-incorporated minicolumn coupled with ICP-MS for speciation of inorganic arsenic and selenium in high-salt-content samples, Microchim. Acta., 185 (2018) 1–8.

[23] M. Pettine, T.J. McDonald, M. Sohn, G.A.K. Anquandah, R. Zboril, V.K.A Sharma, Critical review of selenium analysis in natural water samples, Trends Environ. Anal., 5 (2015) 1–7.

[24] T. Hu, L.P. Liu, S.Z. Chen, W.L. Wu, G.G. Xiang, Y.B. Guo, Determination of selenium species in cordyceps militaris by high-performance liquid chromatography coupled to hydride generation atomic fluorescence spectrometry, Anal. Lett., 51 (2018) 2316-2330.

[25] A.S.A. Ibrahim, R. Al-Farawati, U. Hawas,Y, Shaban, Recent microextraction techniques for determination and chemical speciation of selenium, Open Chem., 15 (2017) 103–122.

[26] L. Nyaba, J.M. Matong, K.M. Dimpe, P.N. Nomngongo, Speciation of inorganic selenium in environmental samples after suspended dispersive solid phase microextraction combined with inductively coupled plasma spectrometric determination, Talanta., 159 (2016) 174–180.

[27] A.H. Panhwar; M. Tuzen, T.G. Kazi, Ultrasonic assisted dispersive liquid-liquid microextraction method based on deep eutectic solvent for speciation, preconcentration and determination of selenium species (IV) and (VI) in water and food samples, Talanta, 175 (2017) 352–358.

[28] N. Motakef Kazemi, A novel sorbent based on metal–organic framework for mercury separation from human serum samples by ultrasound assisted- ionic liquid-solid phase microextraction, Anal. Methods Environ. Chem. J., 2 (2019) 67-78.

AMECJ
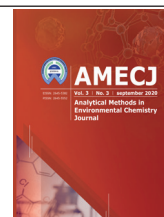
# Dispersive liquid–liquid microextraction technique combined with UV–Vis spectrophotometry for determination of zirconium in aqueous samples

**Ehsan Zolfonoun[a,*]**

*[a]Nuclear Fuel Cycle Research School, Nuclear Science & Technology Research Institute, Tehran, Iran*

**ABSTRACT**

Dispersive liquid–liquid microextraction coupled with UV–Vis spectrophotometry was applied for the determination of zirconium in aqueous samples. In this method a small amount of chloroform as the extraction solvent was dissolved in pure ethanol as the disperser solvent, then the binary solution was rapidly injected by a syringe into the water sample solution containing Zr(IV), xylenol orange and cetyltrimethylammonium bromide (CTAB). The formed ion-associate was extracted into the fine chloroform droplets. The detection limit for Zr(IV) was 0.010 µg mL$^{-1}$. The precision of the method, evaluated as the relative standard deviation obtained by analyzing of 10 replicates, was 2.7 %. The practical applicability of the developed method was examined using natural waters and ceramic samples.

## 1. Introduction

Zirconium is used in the nuclear industry as a fuel rod cladding, as a catalyst in organic reactions and, additionally, in the manufacture of water repellent textiles, in metal alloys and in dye pigments and ceramics [1, 2]. Most of zirconium compounds have low solubility and as a result have low toxicity. However, chronic exposure to the soluble compounds of zirconium such as zirconium tetrachloride may cause skin and lung granulomas [3, 4]. Industrial wastewater can increase the amount of zirconium in the environment. Contaminated soil and water can expose humans to this metal. Therefore, extraction and determination of trace levels of zirconium is necessary.

* Corresponding Author: Ehsan Zolfonoun
Email: ezolfonoun@aeoi.org.ir
https://doi.org/10.24200/amecj.v3.i03.107

Spectrophotometric methods are most commonly used for the determination of zirconium [5, 6]. However, the direct determination of zirconium at very low concentrations by traditional spectrophotometric techniques is difficult because of insufficient sensitivity of this technique as well as the matrix interferences occurring in real samples, and an initial sample pretreatment, such as preconcentration of the analyte and matrix separation, is often necessary.

Several methods have been reported for the separation and preconcentration of metal ions, such as liquid–liquid extraction (LLE) [7], coprecipitation [8], solid phase extraction (SPE) [9, 10] and cloud point extraction (CPE) [11], but the disadvantages such as time-consuming, unsatisfactory enrichment factors, large organic solvents and secondary wastes, limit their applications.

Dispersive liquid–liquid microextraction (DLLME) is a modified solvent extraction method

and provides the advantages of ease of operation, rapid extraction, and use of small volume of organic solvent [12, 13]. In DLLME, a water-immiscible organic extractant and a water-miscible dispersive solvent are two key factors to form fine droplets of the extractant, which disperse entirely in the aqueous solution, for extracting analytes. The cloudy sample solution is then subjected to centrifuge to obtain sedimented organic extractant containing target analytes. This method has been applied for the determination of trace organic pollutants and metal ions in the environmental samples [14-17].

Xylenol orange (XO) is a metal indicator, which is widely used for analytical determination [18, 19]. It can react with many metal ions in various oxidation states and the solution chemistry of its chelates is known to be complex [20]. However the utility of XO for extraction of metal ions is reported rarely. As the XO is a nonselective methallochromic indicator it's complexes with the cited ion has severe spectral interferences and this makes the determination to be very difficult or practically impossible. For a successful determination a prior separation step is mandatory for elimination of the cationic interferences.

In the present study we introduce a simple and fast dispersive liquid–liquid microextraction (DLLME) method for the separation and preconcentration of trace amounts of zirconium, prior to spectrophotometric determination. The point of the present method is using of an accessible and inexpensive reagent, XO, with a cationic surfactant as a new extractant.

## 2. 2. Experimental

### 2.1. Reagents

All reagents were of analytical grade, purchased from the Merck Company. Standard stock solution (1000 µg mL$^{-1}$) of Zr(IV) was prepared by dissolving appropriate amounts of ZrOCl$_2$·8H$_2$O, in water. Stock solutions of diverse elements were prepared from the high purity salts of the cations (all from Merck, Germany). A solution of $1.0\times10^{-3}$ mol L$^{-1}$ xylenol orange was prepared by dissolving

appropriate amounts of this reagent in distilled water.

### 2.2. Instrumentation

A Perkin Elmer (Lambda 25) spectrophotometer with 10 mm quartz cells (500 µL) was used for UV−Vis spectra acquisition. A Metrohm model 744 digital pH meter, equipped with a combined glass-calomel electrode, was employed for the pH adjustments. A Hettich centrifuge model EBA 20 (Oxford, England) was employed for phase separation.

### 2.3. Dispersive liquid–liquid microextraction procedure

A 5 mL sample or standard solution containing Zr(IV) (pH 3.0), XO ($3.0\times10^{-5}$ mol L$^{-1}$), and CTAB ($2.0\times10^{-5}$ mol L$^{-1}$) was transferred in a 10 mL conical-bottom polypropylene centrifuge tube. Then 1.5 mL ethanol (disperser solvent) containing 120 µL chloroform (extraction solvent) was injected rapidly into the sample solution using a syringe and a stable cloudy solution (water, ethanol and chloroform) was formed. In order to separate the phases, the cloudy solution was centrifuged for 5 min at 3000 rpm and the aqueous phase was removed with a transfer pipette. Afterwards, the sedimented phase was dissolved in 500 µL of pure ethanol and transferred to a quartz cell and then the absorbance was measured at 592 nm.

### 2.4. Analysis of the real samples

A 5 mL of tap water, well water, and mineral water samples were filtered through 0.45 µm membrane filter, adjusted to the optimum pH and subjected to the recommended procedure for the preconcentration and determination of metal ions. To 1.0 g of ceramic samples in a platinum crucible, 10 mL of HF, 1 mL of H$_2$SO$_4$, and 1 mL of HClO$_4$ were added and heated to 150 °C on a hot plate. The process was repeated three times. The residue was cooled and dissolved in 50 ml of 0.1 mol L$^{-1}$ HCl and made up to 100 mL. Suitable aliquots were taken and subjected to preconcentration and determination by the procedure described above.
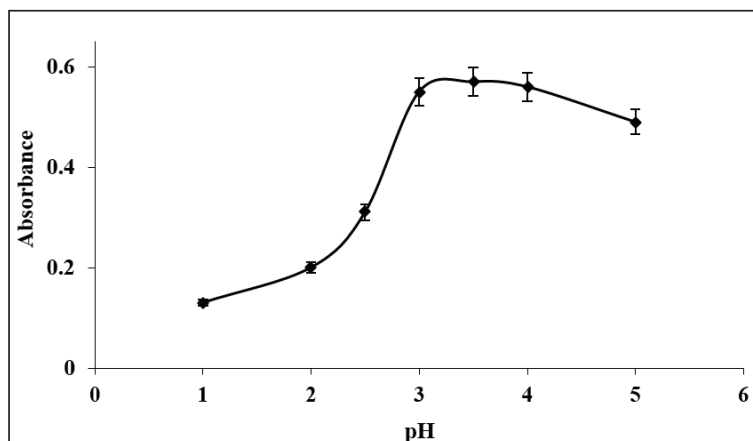
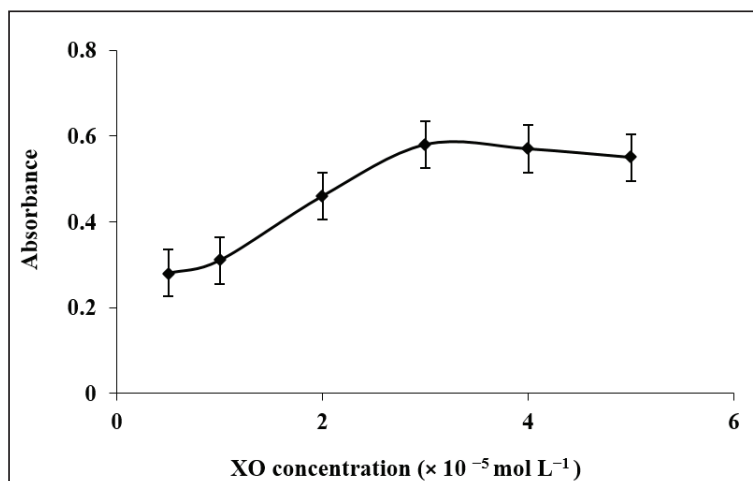**Fig. 1.** Effect of pH on the absorbance of
metal–xylenol orange complex.



**Fig. 2.** Effect of xylenol orange concentration on the absorbance of
metal–xylenol orange complex.

## 3. 3. Results and discussion
### 3.1. Effect of pH
The formation of metal chelate and its chemical stability are the two important influence factors for the extraction of metal ions, and the pH plays a unique role on metal chelate formation and subsequent extraction. The effect of pH on the complex formation and extraction of zirconium was studied in the range of 1.0–5.0 using hydrochloric acid or sodium hydroxide. As can be seen in **Fig. 1**, the highest signal intensity was obtained at pH 3.0–4.0. In more acidic or more alkaline solutions, absorbance decreased because of incomplete complex formation and hydrolysis of the complex. Therefore, pH 3.0 was selected for further study.

### 3.2. Effect of xylenol orange concentration
The effect of xylenol orange concentration on the absorbance was studied, and the results are shown in **Fig. 2.** We investigated xylenol orange concentration in the range of $5.0 \times 10^{-6}$ to $5.0 \times 10^{-5}$ mol $L^{-1}$. Maximum absorbance was obtained at a concentration of $3.0 \times 10^{-5}$ mol $L^{-1}$ of the ligand and after that, absorbance approximately stays constant.
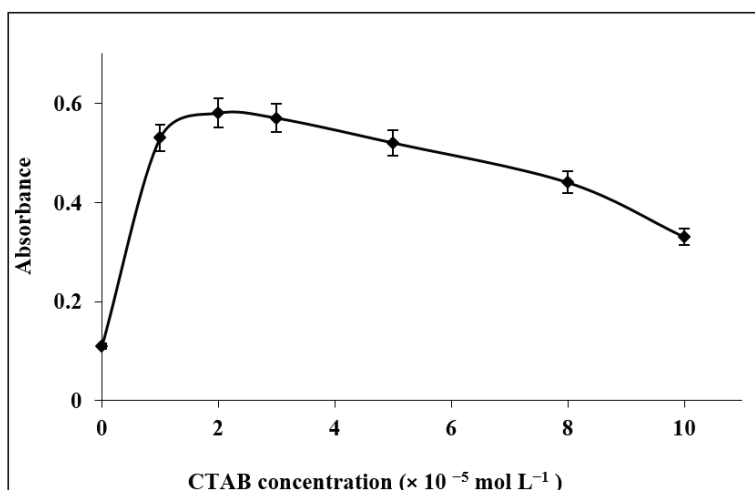
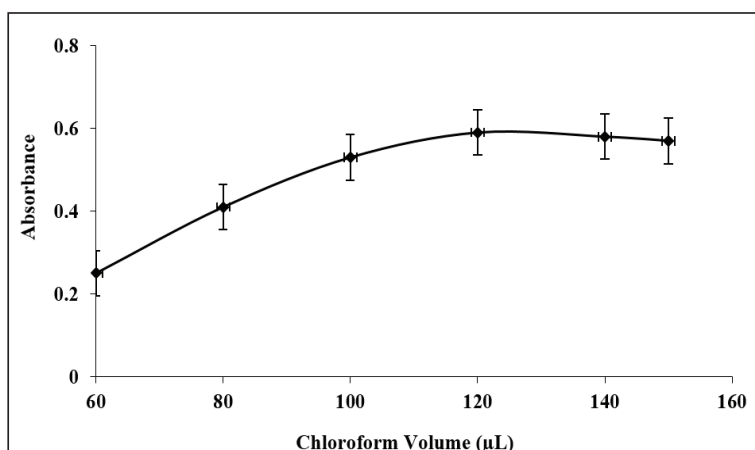**Fig. 3.** Effect of CTAB concentration on the absorbance of metal–xylenol orange.



**Fig. 4.** Effect of amount of chloroform on the absorbance of metal–xylenol orange.

### 3.3. Effect of CTAB concentration

Effect of CTAB concentration on the extraction and determination of zirconium was investigated in the range of 0 to $1.0 \times 10^{-4}$ mol $L^{-1}$. The results are shown in **Fig. 3.** The amount of the absorbance for sample increased by increasing CTAB concentration. The blank signal also increased by increasing CTAB concentration. This is due to more extraction of xylenol orange by increasing CTAB concentration, but the difference between the sample and blank signals increased by increasing CTAB concentration up to $2.0 \times 10^{-5}$

mol $L^{-1}$ and decreased at higher concentrations. Therefore, $2.0 \times 10^{-5}$ mol $L^{-1}$ CTAB was chosen as the optimum.

### 3.4. Effect of type and volume of the extraction solvent

Selecting the extraction solvent by paying attention to its characteristic properties is very important. Chloroform and carbon tetrachloride were compared in this extraction and obtained recoveries were higher for chloroform. To examine the effect of the extraction solvent volume, 1.5 mL of ethanol

containing different volumes of chloroform in the range of 60–150 μL were subjected to the same procedures. According to **Fig. 4**, increasing the volume of chloroform, initially increases the absorbance until at 120 μL it reaches the maximum amount. Thereby, the 120 μL of chloroform was employed to extract the zirconium from the aqueous samples.

### 3.5. Effect of type and volume of the disperser solvent

The main criterion for the selection of the disperser solvent is its miscibility in the extraction solvent and aqueous solution. In addition, the type of disperser directly influences the viscosity of the binary solvent. Thus, this solvent can control droplet production and extraction efficiency. To study this effect, two different solvents such as acetone and ethanol were tested. A series of sample solutions were studied using 1.5 mL of each disperser solvent with 120 μL of chloroform as the extraction solvent. The obtained enrichment factors for these two dispersers show no statistically significant differences between them; however we selected ethanol as the disperser because it was cheaper and more accessible than acetone. The effect of the volume of ethanol on the extraction recovery was also studied. The different volumes of ethanol (0.50, 1.00, 1.50, 2.00 and 2.50 mL) containing 120 μL chloroform were examined. For the first two tests, the droplets were big and the surface area was low, so the droplets rapidly settled at the bottom of the tube and low extraction efficiencies were obtained. Maximum extraction was observed when the disperser solvent volume was 1.5 mL. Thus 1.5 mL of ethanol was chosen as the proper amount.

### 3.6. Effect of diverse ions on the recovery

In order to assess the possible analytical applications of the recommended procedure, the effect of common coexisting ions in natural water samples on the preconcentration and determination of zirconium was studied. In these experiments, 5.0 mL solutions containing $0.10$ μg mL$^{-1}$ of zirconium and various amounts of interfering ions were treated according to the recommended procedure. Tolerable limit was defined as the highest amount of foreign ions that produced an error not exceeding $\pm5\%$ in the determination of investigated analyte. The results are summarized in **Table 1.** As it is seen, large numbers of ions used have no considerable effect on the determination of zirconium.

### 3.7. Analytical performance of the method

The linear working range of the method for determination of Zr(IV) was found to be $0.04-0.35$ μg mL$^{-1}$. The limit of detection (LOD) of the proposed methodology was calculated as three times the standard deviation of 8 blank solution readings over the slope of the calibration graph. The LOD for the determination of Zr(IV) was found to be 0.010 μg mL$^{-1}$. The relative standard deviation (R.S.D) for analysis of 0.10 μg mL$^{-1}$ Zr (IV) (n= 10) was 2.7 %.

### 3.8. Applications

The accuracy of the proposed method was tested by separation and determination of Zr(IV) ion in tap water, well water and mineral water samples. In order to validate the method, analytes were determined in spiked real samples. Also this method was applied to the determination of zirconium in ceramic materials. The results obtained are shown in **Tables 2 and 3**. The results demonstrated that the proposed method was suitable for the determination of Zr(IV) in real samples.

**Table 1.** Tolerance limits of some cations and anions on the determination of zirconium

| Ion | Tolerance limit (μg mL$^{-1}$) |
|---|---|
| $Li^+$, $Na^+$, $K^+$, $Cl^-$, $NO_3^-$ | 1000 |
| $Ca^{2+}$, $Mg^{2+}$, $Ba^{2+}$, $SO_4^{2-}$ | 50 |
| $Co^{2+}$, $Cr^{3+}$, $Zn^{2+}$, $Cd^{2+}$, $Ni^{2+}$, $Pb^{2+}$ | 5 |
| $Cu^{2+}$, $Hg^{2+}$, $La^{3+}$, $Ce^{3+}$, $UO_2^{2+}$ | 2 |
| $Fe^{3+}$ | 0.5 |

**Table 2.** Determination of zirconium in water samples (n= 3).

| Sample | Added ($\mu g\ L^{-1}$) | Found ($\mu g\ L^{-1}$) | Recovery (%) |
|---|---|---|---|
| | 0.0 | < LOD | – |
| Tap water | 50.0 | 45.8 ± 1.3[a] | 91.6 |
| | 100.0 | 93.2 ± 1.0 | 93.2 |
| | 0.0 | < LOD | – |
| Mineral water | 50.0 | 52.3 ± 0.45 | 104.6 |
| | 100.0 | 94.5 ± 1.5 | 94.5 |
| | 0.0 | < LOD | – |
| Well water | 50.0 | 54.1 ± 0.75 | 108.2 |
| | 100.0 | 93.7 ± 0.84 | 93.7 |

[a] Standard deviation.

**Table 3.** Determination of zirconium in the ceramic samples (n= 3)

| Sample | Proposed method  ($\mu g$) | ICP-OES ($\mu g$) |
|---|---|---|
| 1 | 456 ± 13.1[a] | 490 |
| 2 | 1098 ± 20.6 | 1140 |

[a] Standard deviation.

## 4. Conclusions

In the present study, a novel method for the preconcentration and spectrophotometric determination of zirconium in water samples is proposed. Dispersive liquid–liquid microextraction is a sensitive, efficient, and simple method for preconcentration and separation of trace metals with the use of low sample volumes. The proposed preconcentration and determination method gives a low limit of detection and good R.S.D. values. The method can be successfully applied to the separation and determination of zirconium in real samples.

## 5. References

[1]   CRC Handbook of Chemistry and Physics, 87th edition, 2006.

[2]   A. Abbaspour, L. Baramakeh, Simultaneous determination of zirconium and molybdenum by first-derivative spectrophotometry, Anal. Sci., 18 (2002) 1127–1130.

[3]   Agency for Toxic Substances and Disease Registry, U.S. Public Health Service, Chapman and Hall, New York, 2000.

[4]   H. Faghihian, M. Kabiri-Tadi, A novel solid-phase extraction method for separation and preconcentration of zirconium, Microchim. Acta, 168 (2010) 147-152.

[5]   A. Boveiri Monji, E. Zolfonoun, S.J. Ahmadi, Application of acidic extract of Platanus orientalis tree leaves as a green reagent for selective spectrophotometric determination of zirconium, Green Chem. Lett. Rev., 1 (2008) 107–112.

[6]   R. Purohit, S. Devi, Determination of nanogram levels of zirconium by chelating ion exchange and on-line preconcentration in flow injection UV—visible spectrophotometry, Talanta, 44 (1997) 319-326.

[7]   K. Saberyan, M. Shamsipur, E. Zolfonoun, M. Salavati-Niasari, Liquid-liquid distribution of the tetravalent zirconium, hafnium and thorium with a new tetradentate naphthol-derivative schiff base, Bull. Korean Chem. Soc., 29 (2008) 94–98.

[8]   K. Prasad, P. Gopikrishna, R. Kala, T.P. Rao, G.R.K. Naidu, Solid phase extraction vis-a`-vis coprecipitation preconcentration of cadmium and lead from soils onto 5,7-dibromoquinoline-8-ol embedded benzophenone and determination by FAAS, Talanta, 69 (2006) 938–945.

[9]   J. Ghasemi, E. Zolfonoun, Simultaneous spectrophotometric determination of trace amounts of uranium, thorium, and zirconium using the partial least squares method after their preconcentration by benzoin oxime modified Amberlite XAD-2000 resin, Talanta, 80 (2010) 1191–1197.

[10]  E. Zolfonoun, Solid phase extraction and determination of indium using multiwalled carbon nanotubes modified with magnetic nanoparticles, Anal. Method Environ. Chem. J., 1 (2008) 5–10.

[11]  S. Shariati, Y. Yamini, M. Khalili Zanjani, Simultaneous preconcentration and determination of U(VI), Th(IV), Zr(IV) and Hf(IV) ions in aqueous samples using micelle-mediated extraction coupled to inductively coupled plasma-optical emission spectrometry, J. Hazard. Mater., 156 (2008) 583–590.

[12]  S.Z. Mohammadi, D. Afzali, Y.M. Baghelani, Ligandless-dispersive liquid–liquid microextraction of trace amount of copper ions, Anal. Chim. Acta, 653 (2009) 173–177.

[13]  E. Zolfonoun, M. Salahinejad, Preconcentration procedure using vortex-assisted liquid–liquid microextraction for the fast determination of trace levels of thorium in water samples, J. Radioanal. Nucl. Chem., 298 (2013) 1801–1807.

[14]  P. Liang, H. Sang, Determination of trace lead in biological and water samples with dispersive liquid–liquid microextraction preconcentration, Anal. Biochem., 380 (2008) 21–25.

[15]  E.Z. Jahromi, A. Bidari, Y. Assadi, M.R. Milani Hosseini, M.R. Jamali, Dispersive liquid–liquid microextraction combined with graphite furnace atomic absorption spectrometry Ultra trace determination of cadmium in water samples, Anal. Chim. Acta, 585 (2007) 305–311.

[16]  P. Liang, E. Zhao, F. Li, Dispersive liquid–liquid microextraction preconcentration of palladium in water samples and determination by graphite furnace atomic absorption spectrometry, Talanta, 77 (2009) 1854–1857.

[17]  H. Ebrahimzadeh, Y. Yamini, F. Kamarei, Optimization of dispersive liquid–liquid microextraction combined with gas chromatography for the analysis of nitroaromatic compounds in water, Talanta, 79 (2009) 1472–1477.

[18]  M. Soylak, Y. Akkaya, Separation/preconcentration of xylenol orange metal complexes on Amberlite XAD-16 column for their determination by flame atomic absorption spectrometry, J. Trace Microprobe Tech., 21 (2005) 455–466.

[19]  J.F. Van Staden, S.S.I. Tlowana, On-line separation, simultaneous dilution and spectrophotometric determination of zinc in fertilisers with a sequential injection system and xylenol orange as complexing agent, Talanta, 58 (2002) 1115–1122.

[20]  S. Murakami, K. Ogura, T. Yoshino, Equilibria of complex formation between bivalent metal ions and 3,3′-Bis[N,N′-bis(carboxymethyl) aminomethyl]-o-cresolsulfonphthalein, Bull. Chem. Soc. Jpn., 53 (1980) 2228–2235.

# Magnetic bentonite nanocomposite for removal of amoxicillin from wastewater samples using response surface methodology before determination by high performance liquid chromatography

**Mohammad Reza Rezaei Kahkha [a,*], Ali Faghihi Zarandi[b] , Nahid Shafighi[a] , Saeedeh Kosari[a]**

**and Batool Rezaei Kahkha[a]**

[a] *Department of Environmental Health Engineering, Faculty of Health, Zabol University of Medical Sciences, Zabol.Iran.*
[b] *Department of Occupational Health Engineering, Faculty of Health, Kerman University of Medical Sciences, Kerman. Iran.*

**ABSTRACT**

In this study, feasibility of magnetic bentonite nanocomposite for removal of amoxicillin from wastewater samples was evaluated by high performance liquid chromatography (HPLC). Magnetic bentonite synthesized by co-precipitation of bentonite and $Fe_3O_4$ and used for removal of amoxicillin from water samples. Response surface methodology on central composition design (CCD) was applied for designing of experiment and building of model. Three factors including pH, adsorbent dose and temperature were studied and used for quadratic equation model to prediction of optimal points. By solving the equation and considering regression coefficient ($R^2$ =0.98). The optimal points of main parameters were obtained as a pH of 4.68, the adsorbent dosage of 1.50 g and the temperature of $48.9^0$ C. Results showed that three factor are significant on removal efficiency and experimental data are in good agreement with predicted data. Proposed methods were used to analysis of amoxicillin in three real samples.

## 1. Introduction

Nowadays, antibiotic residual is a serious concern for many of environmental researchers. Because of insufficient ability of conventional sewage treatment, some antibiotics such as ampicillin, erythromycin, tetracycline and penicillin are not even removed in sewage treatment processes and cause many environmental hazards [1]. Recent

studies have shown that some antibiotics have toxic effects on the life of microorganisms and, over the long term, have undesirable effects on ecological sustainability [2]. Amoxicillin ($C_{16}H_{19}N_3O_5S_3$) is a β- lactam antibiotic with a molecular weight of 365 gram per mole is used to treat bacterial infections [3]. The concentration of this type of antibiotics groups in surface waters is 48 ng $L^{-1}$ and in the hospital sewage between 28 -82 mg $L^{-1}$ have been reported. In many pharmaceutical effluent output higher concentration of these drugs can also be found. Several methods such as; the ozonation [4],

the Fenton process [5], electrochemical methods [6], the nano filtration [7] and the adsorption process [8] were applied for removal of antibiotics from aqueous environments samples. Absorption is one of the most effective methods to removal of antibiotics compounds from water and sewage even at low concentrations (less than 1 mg L$^{-1}$). Adsorption is very simple and low cost method in comparison to other techniques that applied for removal of common pollutants from aqueous samples [9]. Natural clay compounds are one of the best adsorbents to removal of contaminants from air and water samples. This ability obtained from their high surface area, the porous structure, the chemical stability, and their layered structure. Bentonite is a natural clay that used as an adsorbent to removal of pollutants from water and wastewater samples. Response surface methodology (RSM) is appropriate technique that used in many fields [10]. The main objective of RSM is to determine optimum operating conditions for the system or designated area of the practical satisfaction [11]. Experimental data points were obtained during our optimization and used to build a model for CCD which was ideal for sequential testing and allows the right amount of information to test the lack of fit a large number of unusual design points. In this study, removal of amoxicillin by nano-composite made of multi-walled carbon nanotubes and iron nanoparticles were studied. Design of Experiments were conducted using the RSM as well as factors affecting on absorption process of amoxicillin such as pH, amount of adsorbent, and the temperature were optimized. Finally, the data obtained from experiments compared with model output to optimize and predict the results. The concentration of amoxicillin determined by high performance liquid chromatography. HPLC is simple, accurate and precise technique that used for separation, identification and analysis of drugs. It can be successfully and efficiently adopted for routine quality control analysis of drugs in bulk and pharmaceutical dosage form. It can also be used in combination with other analytical methods to further elucidate the components of mixtures.

## 2. Material and methods

### 2.1. Apparatus and reagent

The measurement of amoxicillin was performed using high performance liquid chromatography accessory (CECIL Corporation, HPLC, England) equipped ACE C$_{18}$ column and UV-VIS detector at 230 nm. The mobile phase is ACN: water (60:40). Analytical grade of different reagents such as; HCl and NaOH were purchased from Merck (Darmstadt, Germany). The amoxicillin was prepared from Aldrich chemical Co. HPLC grade of acetonitrile and water purchased from Sharloa (Espain). Bentonite clay was purchased and from Merck (Darmstadt, Germany) and used for further work. The bentonite samples were powdered and sieved by 80-mesh sieve and washed with double distilled water (DDW) for 4 times before using by procedure.

### 2.2. Synthesize of adsorbent

Synthesize of magnetic bentonite are performed by co-precipitation methods by Hashem et al. First, 20 g of bentonite was added into 100 ml of distilled water containing FeCl$_2$ (0.02 mol L$^{-1}$) and FeCl$_3$ (0.04 mol L$^{-1}$). The pH of solution was set around 10 by adding NH$_4$OH buffer solution (1 mol L$^{-1}$) and stirred for 30 min at 300 rpm. Next, 40 ml of HNO$_3$ solution (2 M) was added with stirring for 5 minutes and then 60 ml of Fe(NO$_3$)$_3$ solution (0.35M ) was added to the previous solution and solution boiled for one hour. After settling suspension, the residual was filtered and solid of magnetic bentonite was separated by washing of DDW for 3-5 times. Finally, the product was heated in an oven at 80ºC for 24 h [12].

### 2.3. Removal Procedure

Experiments were performed with the central composite design (CCD) methodology. A standard solution of 1000 mg L$^{-1}$ amoxicillin was prepared by dissolving of 1 g of amoxicillin in 1 liter of deionized water. All standard working prepared from this solution. Experiments were performed at a batch reactor in 500 ml beaker that containing of 50 ml of amoxicillin concentration and the solution was shaked for the 30 minutes in incubation shaker at 200rpm by controlling of temperature. The pH

of the solution was adjusted by adding 0.1 M of NaOH and HCl. After completion of experiments, magnetic nanocomposite was removed by an external magnet and remaining amoxicillin was measured. The removal percentage of Amoxicillin (% removal) was calculated as Equation 1:

$$\%Removal = \frac{Ce - C0}{C0} * 100$$

**(Eq. 1)**

Where Ce and $C_0$ are initial and final Amoxicillin concentration (mg l$^{-1}$) in solution, respectively.

2.4. Experimental design

A central composition design (CCD) was carried out in this research for evaluate the variables for adsorption of amoxicillin from aqueous solution using in a batch reactor. The CCD method for three variables (pH, amount of nanocomposite and temperature), with two levels (the minimum and maximum) was used as experimental design model. In the experimental design model, the pH between

2-9, the adsorbent dosage from 0.5 g to 1.5 g and the temperature between 20-60º C were employed as the input variables. Percentage removal of amoxicillin was the response of the system. Table. 1 showed the experimental design matrix that obtained from CCD procedure. The amoxicillin concentration determined by HPLC. The quadratic equation model for predicting the optimal point of adsorption processes was expressed by Equation 2.

$$Y = \beta i + \sum_{i=1}^{k} \beta i x i + \sum_{i=1}^{k} \beta i i x i^2 + \sum_{i=0}^{k} \sum_{j=i+1}^{k} \beta x i x j + \epsilon$$

**(Eq.2)**

Where Y is the response of the system and $X_i$ and $X_J$ are the variables of action. $R^2$ is coefficient of determination of polynomial model . The statistical significance was verified with adequate precision ratio and by the F-test. Design expert (version 8) program was used for regression and graphical analysis. A total of 19 experiments were necessary to estimate of the full model **(Table 1)**

**Table 1.** Central composite design matrix with experimental and predicted values

| Run | pH | T(ºc) | adsorbent( g) | Actual Value (%) | Predicted Value(%) |
|-----|-------|--------|------|------|--------|
| 1 | 5.5 | 45 | 1 | 98 | 92.20 |
| 2 | 11.39 | 45.00 | 1.00 | 20 | 19.20 |
| 3 | 5.50 | 45.00 | 1.00 | 96 | 92.20 |
| 4 | 9.00 | 65.00 | .050 | 57 | 60.29 |
| 5 | 5.50 | 45.00 | 1.00 | 83 | 92.20 |
| 6 | 5.50 | 45.00 | 1.84 | 95 | 92.20 |
| 7 | 2.00 | 65.00 | 1.50 | 99 | 91.64 |
| 8 | 2.00 | 25.00 | 1.50 | 97 | 77.97 |
| 9 | 5.50 | 45.00 | 1.00 | 98 | 92.20 |
| 10 | 5.50 | 11.36 | 1.00 | 86 | 100 |
| 11 | 2.00 | 65.00 | 0.50 | 83 | 65.08 |
| 12 | 5.50 | 45.00 | 0.16 | 90 | 100 |
| 13 | 9.00 | 65 | 1.50 | 70 | 66.82 |
| 14 | 9.00 | 25.00 | 0.50 | 83 | 74.58 |
| 15 | 2.00 | 25.00 | 0.50 | 97 | 84.41 |
| 16 | 5.50 | 78.64 | 1.00 | 93 | 100 |
| 17 | 5.50 | 45.00 | 1.00 | 92 | 92.20 |
| 18 | 9.00 | 25.00 | 1.50 | 46 | 48.14 |
| 19 | 5.50 | 45.00 | 1.00 | 90 | 92.20 |

## 3. Result and discussion

### 3.1. Regression model and statistical analysis

The CCD method has been successfully used for optimizing affecting factor that influenced on the percentage of amoxicillin removal. For the best response of system, the experimental results were analyzed through RSM to obtain an empirical model. The regression model equations (second-order polynomial) relating the removal efficiency of amoxicillin and related parameters were developed as Equation 3:

$$\%Removal = +35.00926 + 7.71191 \times pH + 0.91252 \times T + 23.48479 \times Dose - 7.14286e^{-004} \times pH \times T + 0.38571 \times pH* \times Dose + 5.e^{-3} \times T \times Dose - 0.68596 \times pH^2 - 0.013048 \times T^2 - 8.99753 \times Dose^2$$

**(Eq. 3)**

The coefficients of Equation 3 are determined by using software Design-Expert 8. The optimal parameters are as follows: pH = 4.68, the adsorbent dosage = 1.5 g, and the temperature = 48.90° C.

The model prediction of the amoxicillin removal was obtained %99.48 while the experimental amount of removal efficiency achieved %99. These results confirmed that the RSM could be effectively applied to optimize the factors and parameters in complex processes. The term of encoded factor expressed relation between the independent variables and dependent response of system. Apart from the line are effects of the parameter for the amoxicillin removal, the RSM also gives an insight in to the quadratic and interaction effect of the parameters. Table 2 showed the results of regression analysis of obtained quadratic model. The F-values and p-values are related to significant of each coefficient **(Table 2)**. High magnitude of the F-values and small magnitude of the p-values indicated that corresponding coefficients was more significant. Also, Values of "probe> F" less than 0.0500 implied high significant regression at 95 percent confidence level. According to the F-value and p-values, the amount of adsorbent was found more effective on the adsorption process of amoxicillin. The "Lack of Fit F-value" of 0.26

**Table 2.** ANOVA analysis for removal of amoxicillin

| Source | sum of square | df | Mean Square | F Value | P-value Prob> F |
|---|---|---|---|---|---|
| Model | 3120.63835 | 14 | 222.902739 | 148.517383 | < 0.0001 |
| A-pH | 84.4231475 | 1 | 84.4231475 | 56.2501161 | < 0.0001 |
| B-adsorbent dose | 537.787036 | 1 | 537.787036 | 358.320959 | < 0.0001 |
| C-temperature | 0.66785645 | 1 | 0.66785645 | 0.44498463 | 0.5091 |
| D-time | 116.402257 | 1 | 116.402257 | 77.5574075 | < 0.0001 |
| AB | 0.01125 | 1 | 0.01125 | 0.00749574 | 0.9315 |
| AC | 25.56125 | 1 | 25.56125 | 17.0311499 | 0.0002 |
| AD | 4.5 | 1 | 4.5 | 2.99829525 | 0.0922 |
| BC | 15.40125 | 1 | 15.40125 | 10.2616655 | 0.0029 |
| BD | 29.645 | 1 | 29.645 | 19.7521028 | < 0.0001 |
| CD | 26.645 | 1 | 26.645 | 17.7532393 | 0.0002 |
| A^2 | 1107.54922 | 1 | 1107.54922 | 737.946571 | < 0.0001 |
| B^2 | 225.03502 | 1 | 225.03502 | 149.938096 | < 0.0001 |
| C^2 | 745.166816 | 1 | 745.166816 | 496.495584 | < 0.0001 |
| D^2 | 897.389678 | 1 | 897.389678 | 597.919825 | < 0.0001 |
| Residual | 52.52985 | 35 | 1.50085286 | | |
| Lack of Fit | 5.00385003 | 10 | 0.500385 | 0.26321645 | 0.9840 |
| Pure rror | 47.526 | 25 | 1.90104 | | |

indicated that the Lack of Fit is not significant.

The fitness of the model was expressed by the determination coefficient ($R^2$). The "Pred R-quared" of 0.9848 is in agreement with the "Adj R-Squared" of 0.9768. "Adeq Precision" expressed the value of signal to noise ratio. A ratio greater than 4 is favorable. In this case "Adeq Precision" of 30.63 indicates an adequate signal. Thus, as a result of the statistical analysis, quadratic model was found suitable for demonstrate the adsorption process and useful for developing empirical relationships. Removal efficiency of amoxicillin was sensitively depended to the amount of adsorbent. The removal efficiency was sharply increased when the amount of adsorbent increased from 0.5 g to 1.5 g. The increase in yield due to increase in adsorbent dosage was more dominated

than other significant factors. The pH of the solution was another factor that influenced the response of system. As can be seen on **Figure 1**, when the pH increased from 2 to 5, the removal efficiency of amoxicillin was increased. Temperature is a key factor which effect on adsorption process. In this study, effect of temperature on removal efficiency of amoxicillin was investigated. Results showed that by increasing of temperature, the removal efficiency of amoxicillin decreased and in 48°C the highest removal efficiency was obtained.

The parity plot are presented in **Figure 2**. As shown in **Fig. 2**, there was a satisfactory correlation between the observed and fitted values. In addition, a normal distribution of residual were observed in **Figure 2** which indicated the data points can be formed approximately straight line.
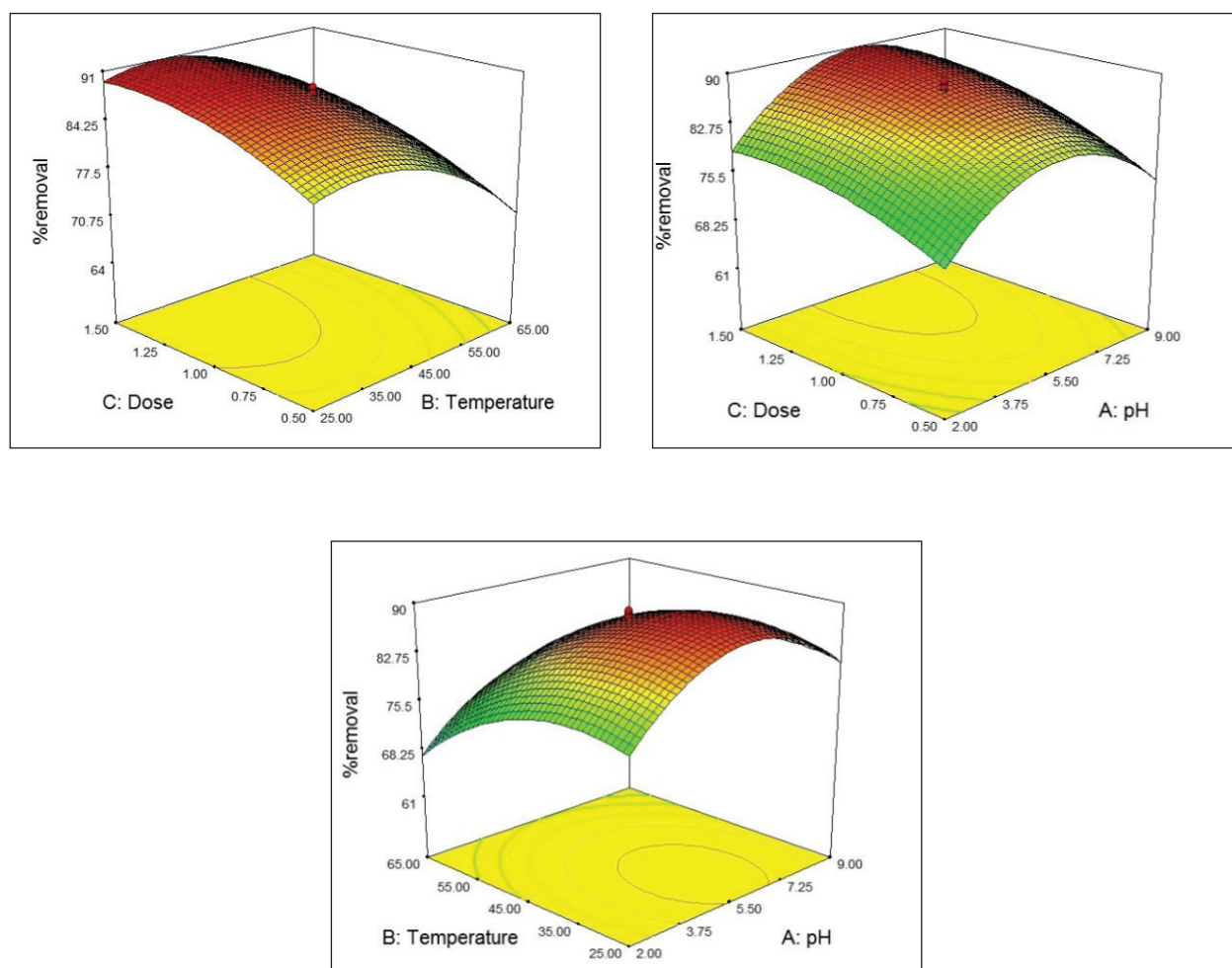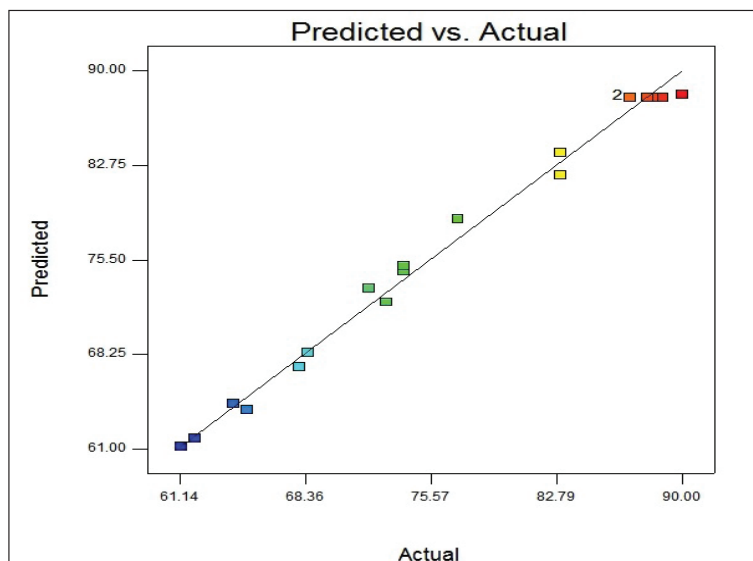


**Fig.1**. Response of surface by CCD method

**Fig. 2.** The normal probability plot of the residuals and parity plot show the
correlation between the observed and predicted values.

**Table 3.** Adsorption of amoxicillin in real samples based on magnetic bentonite nanocomposite
using response surface methodology

| Sample | Added (mg L$^{-1}$) | Initial Amount (mg L$^{-1}$) | Final Amount (mg L$^{-1}$) | Recovery (%) |
|---|---|---|---|---|
| **Sample 1** | --------- | --------- | 56.6 ± 2.1 | --------- |
| | 50 | --------- | 105.4 ± 4.7 | 97.6 |
| **Sample 2** | --------- | --------- | 66.3 ± 2.8 | --------- |
| | 50 | --------- | 117.1± 5.6 | 101.4 |
| **Sample 3** | --------- | --------- | 23.9 ± 0.9 | --------- |
| | 20 | --------- | 43.5 ± 1.7 | 98.0 |
| **CRM 1** | --------- | 23.4 | 22.2 ± 1.1 | 94.8 |
| | 20 | --------- | 41.6 ± 1.9 | 97.0 |
| **CRM 2** | --------- | 58.9 | 56.8 ± 2.3 | 96.4 |
| | 50 | --------- | 107.2 ± 5.1 | 100.8 |
| **CRM 3** | --------- | 102.5 | 98.7 ± 4.8 | 98.9 |
| | 100 | --------- | 96.9 ± 4.6 | 96.9 |
| **CRM 4** | --------- | 47.1 | 48.2 ± 1.7 | 102.3 |
| | 50 | --------- | 96.8 ± 1.7 | 97.2 |

Mean of three determinations ± standard deviation (P = 0.95, n = 5)
Sample 1: Wastewater Drug Factory
Sample 2: Wastewater Hospital
Sample 2: Wastewater Drug Razi
CRM 1, 2, 3 and 4 analysis with HPLC-MS with concentration of 23.4, 58.9, 102.5 and 47.1 respectively

### 3.2. Application of proposed methods to real sample

To verify the potential application of proposed method to real samples, three real wastewater samples were selected and used by proposed procedure. Different concentrations of amoxicillin include 100, 150 and 200 mg L$^{-1}$ were spiked to the samples and removal efficiency of amoxicillin was tested using proposed methods. Results are shown in **Table 3**. As expected, the magnetic bentonite nanocomposite has good recovery for adsorption of the spiked amoxicillin from all three real samples.

## 4. Conclusions

In this work, a magnetic bentonite nanocomposite was synthesized and applied for adsorption of amoxicillin from wastewater. A central composition design was applied for study of the effects of parameters such as; pH, temperature and amount of adsorbent which was influenced on the removal efficiency of amoxicillin. A quadratic model was solved and developed to correlate the independed variables and the response of system. Through the analysis of response surfaces, was found that amount of adsorbent was most significant variable on removal efficiency of amoxicillin by HPLC. Process optimization was performed and results showed that the experimental data were found to agree with the predicted values.

## 5. References

[1]    T.H. Le, C. Ng, Removal of antibiotic residues, antibiotic resistant bacteria and antibiotic resistance genes in municipal wastewater by membrane bioreactor systems, Water res., 145 (2018) 498-508.

[2]    W. Yan, Y. Xiao, W. Yan, The effect of bioelectrochemical systems on antibiotics removal and antibiotic resistance genes: a review, Chem. Eng. J., 358 (2019) 1421-1437.

[3]    S. Ren , C. Boo , N. Guo, Photocatalytic reactive ultrafiltration membrane for removal of antibiotic resistant bacteria and antibiotic resistance genes from wastewater effluent,

Environ. Sci. Technol., 52 (2018) 8666-8673.

[4]    Z. Cao, X. Liu, J. Xu, J. Zang, Removal of antibiotic florfenicol by sulfide-modified nanoscale zero-valent iron, Environ. Sci. Technol., 51 (2017) 11269-11277.

[5]    N. Li, G.-P. Sheng, Removal of antibiotic resistance genes from wastewater treatment plant effluent by coagulation, Water Res., 111 (2017) 204-212.

[6]    Y. Zhou, Q. Yang, D. Zhang, N. Gan, Q. Li, Detection and removal of antibiotic tetracycline in water with a highly stable luminescent MOF, Sensors and Actuators B: Chem., 262 (2018) 137-143.

[7]    Y. Hong, C. Li, G. Zhang, Efficient and stable Nb$_2$O$_5$ modified g-C3N4 photocatalyst for removal of antibiotic pollutant, Chem. Eng. J., 299 (2016) 74-84.

[8]    C. Guo, H$_2$O$_2$ and/or TiO$_2$ photocatalysis under UV irradiation for the removal of antibiotic resistant bacteria and their antibiotic resistance genes, J. Hazard. Mater., 323 (2017) 710-718.

[9]    C. Hong, P.-Y. Hong, Removal of antibiotic-resistant bacteria and antibiotic resistance genes affected by varying degrees of fouling on anaerobic microfiltration membranes, Environ. Sci. Technol., 51 (2017) 12200-12209.

[10]   B. Kayan, B. Gözmen, Degradation of Acid Red 274 using H2O2 in subcritical water: Application of response surface methodology, J. Hazard. Mater., 201 (2012) 100-106.

[11]   S. Tang, D. Yuan, Y. Rao, N. Li, Persulfate activation in gas phase surface discharge plasma for synergetic removal of antibiotic in water., Chem. Eng. J., 337 (2018) 446-454.

[12]   F.S. Hashem, Removal of methylene blue by magnetite covered bentonite nano-composite, Eur. Chem. Bull., 2 (2013) 524-529.
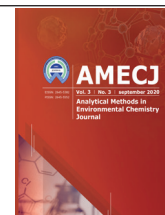
# Simultaneously determination of copper and zinc in human serum and urine samples based on amoxicillin drug by dispersive ionic liquid- liquid microextraction coupled to flame atomic absorption spectrometry

**Kian Azami [a,*] and Seyed Mojtaba Mostafavi [b]**

[a] *Department of Pharmacology and Toxicology, Pharmaceutical Sciences Research Center, Faculty of Pharmacy, Tehran University of Medical Sciences, P.O. Box 14155-6451, Tehran, Iran*
[b] *Department of Chemistry, Iranian-Australian Community of Science, Hobart, Tasmania, Australia*

**ABSTRACT**
In this work the effect of amoxicillin on copper and zinc (Cu and Zn) deficiency was evaluated by determining of Cu and Zn concentration in human serum and urine samples. By dispersive ionic liquid cloud point extraction procedure (DIL-CPE), 0.03 g of pure amoxicillin drug was added to mixture of 0.1 g of hydrophobic ionic liquid and 0.2 mL acetone which was injected to 2 mL of serum or urine samples which was diluted with DW up to 10 mL. The cloudy solution was shacked for 7 min and Cu and Zn ions was extracted based on sulfur group on amoxicillin ligand at pH of 7 by DIL-CPE. Then, the solution centrifuged and after back extraction with I mL of nitric acid (0.2 M), the remained solution was determined by flame atomic absorption spectrometry (F-AAS). The enrichment factor (EF), LOD and linear range (LR) for copper and zinc was obtained (9.92; 9.81), (28.5 µg L$^{-1}$; 15.2 µg L$^{-1}$) and (100 -505 µg L$^{-1}$; 41- 153 µg L$^{-1}$), respectively. The results showed us, the concentration of the Cu and Zn ions can be decreased by increasing amoxicillin drug dosage in human body. The mean value for serum copper/zinc ratio was obtained 1.11 ± 0.28. The DIL-LME method was validated by ICP-MS analysis and spike of real samples for Zn and Cu ions in serum and urine samples.

## 1. Introduction

Copper and zinc are essential ions for the human body. Copper has different forms such as CuS, CuS$_2$, CuFeS$_2$ and CuSO$_4$.5H$_2$O in environment. The high concentrations of Cu and Zn more than 2 ppm in human blood are toxic and the range between essentiality limit and toxicity form is very small. Copper and zinc has normal ranges between 0.8-1.6 mg L$^{-1}$ in different ages for the human serum and urine samples [1]. Zinc is used as cofactor for many enzymes in the human body. Zinc effect on cell structure of human body, the structure of protein, the gene expression, the immune system, and the growth in children. Zinc deficiency cause to many diseases such as, diarrhea, a compromised immune system, night blindness, hair loss, and the taste alterations [1-

2]. Total zinc is about 40 mg per day for adults over 20 years. Copper helps to transportation of iron, energy production, the pigmentation of skin, hair, and eyes. Copper acts as an antioxidant for defending of cell damage which was caused by free radicals. Copper deficiency cause to anemia, low white blood cell count, loss of myelin, multiple sclerosis (MS), the loss of pigmentation, the impaired growth and osteoporosis [3]. The copper intake from food/water or supplements has 10 mg per day and over limit accumulates in the liver. Based on previous studies, a ratio of 8-15 mg of zinc for every 1 mg of copper reported. However, this ratio seems to be more important for human bodies mechanism [1-4]. Zinc is absorbed in the small intestine by a carrier-mediated mechanism. Under normal physiologic conditions, transport processes of uptake are not saturated. The mean value for serum copper was normal range ($17.47 \pm 3.31$ µmol L$^{-1}$; 111.32 µg dL$^{-1}$), and the mean value for serum zinc was at the lower edge of the normal value ($12.24 \pm 1.04$ µmol L$^{-1}$; 80.01 µg dL$^{-1}$), while the mean value for serum copper/zinc ratio was $1.44 \pm 0.31$ ranging from 0.65 to 2.67 [5-7]. Copper and zinc concentration in liquid phase can be determined directly by inductively-coupled plasma atomic emission spectrometry (ICP-AES) [8] or electrothermal atomic absorption spectrometry (ET-AAS) [9] with low detection limit (LOD). The conventional flame atomic absorption spectrometry (F-AAS) [10] was used in many laboratories and had low interferences ions as compared to ICP-AES or ETAAS. As difficulty matrix in human blood or serum patients a sample preparation is require for preconcentration/separation/extraction of ions from samples before determination. Many procedures for metal determination in water and human matrix was used with different analytical techniques and reagents [11,12]. The Liquid–liquid extraction by using salophen as an complex reagents [13], the sandwich supported liquid membrane [14], the modified carbon based solid phase extraction [15], the solid-phase extraction on MWCNTs - D2EHPA-TOPO [16], dispersive liquid–liquid microextraction of copper (II) by oxinate chelate [17] and dispersive liquid-liquid microextraction-slotted quartz tube-flame atomic absorption spectrometry [18] are well-known procedures for preconcentration and separation of trace copper or zinc from different matrix.

In this work, the pure amoxicillin antibiotic drug was used as chelating agent for copper and zinc (Cu/Zn) extraction in human serum and urine samples by DIL-CPE procedure at optimized pH. The Cu and Zn deficiency was evaluated by determining its concentration in human serum/urine samples by F-AAS. The Cu and Zn ions can be separated from liquid phase by hydrophobic ionic liquid as green solvent.

## 2. Experimental
### 2.1. Apparatus and Reagents
A flame atomic absorption spectrometer model, with an air-acetylene flame, was used for copper (II) and zinc (II) determination in human serum and urine samples (Shimadzu, F-AAS, model 680, Tokyo, Japan).  Copper based on wavelength 324.7 nm, slit 0.5 nm and lamp current 3.0 mA (1-5 mg L$^{-1}$) were selected.  Zinc lamp with wavelength 213.9 nm, slit 0.5 nm and current 5.0 mA (0.4-1.5 mg L$^{-1}$) were used. A pH meter with glass electrode was adjusted the pH of human samples (Metrohm, E-632). For validation, the electrothermal atomic absorption spectrophotometer (ET-AAS, GBC 932) and ICP-MS in real samples as certified reference material (CRM) was used for determination of copper (II) and zinc (II) in serum and urine samples.  The calibration curve of copper (II) and zinc (II) with injecting 20 µL of standard solution to graphite tube were used. All the reagents with analytical grade were used. Deionized-distilled water (DW, Millipore, USA) was prepared for experimental run. The copper (II) and zinc (II) solutions were prepared by appropriate diluting a 1000 µg L$^{-1}$ of Cu and Zn solution (Merck) with DW. The pure amoxicillin **(Fig.1)**, acetone and ionic liquid purchased from Sigma Alderich (Switzerland) and Merck Company (Germany). Buffer solutions were prepared by standard methods. The pKa1 = 2.68 carboxyl, (pKa2 = 7.49 amine, and

pKa3 = 8.49) for amoxicillin (CAS N:26787-78-0) was considered. 1-Methyl-3-octylimidazolium hexafluorophosphate (CAS Number: 304680-36-2; $C_{12}H_{23}F_6N_2P$; [MOIM][PF$_6$]) was purchased from Sigma, Germany. The pH of the samples was adjusted up to 7 with a phosphate buffer (HPO$_4$/ H$_2$PO$_4$ 0.2 M).
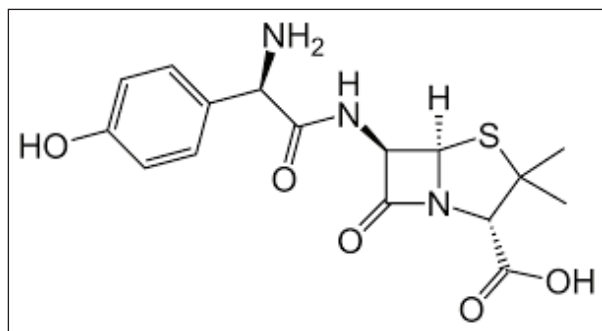


**Fig. 1.** The schema of amoxicillin

## 2.2. Characterizations

Amoxicillin, as organic compounds with the penicillin core structure was used as ligand in this study. Amoxicillin is structurally characterized by a penam ring (C$_5$H$_7$NOS) bearing two methyl groups and an amide group. Fourier transform infrared (FT-IR) spectra were recorded from KBr pellets using a spectrophotometer FTIR Shimadzu (Kyoto, Japan). For amoxicillin, the C-O stretching vibrations show intense IR absorptions, due to the considerable change in the molecular dipole moment produced by this vibration mode **(Fig. 2)**. Powder X-ray diffraction (XRD) was conducted on a X-ray diffractometer. X-ray diffraction analysis of pure amoxicillin and the optimized formulation was done by X-ray powder diffractometer (PW 3040/ 60 Xpert PRO, Panlytical, Netherlands). The X-ray diffraction patterns were recorded using Cu Kα radiations (λ=1.5405980Å), a current of 30 ma, and a voltage of 50 Kv. The samples were analyzed over 5–35 (2θ range) with a scan step size of 0.02s and 0.5s per step **(Fig. 3)**. Scanning electron microscopy (SEM) images were obtained using a Tescan Mira-3 Field Emission Scanning Electron Microscope (FE-SEM). The external and internal morphology

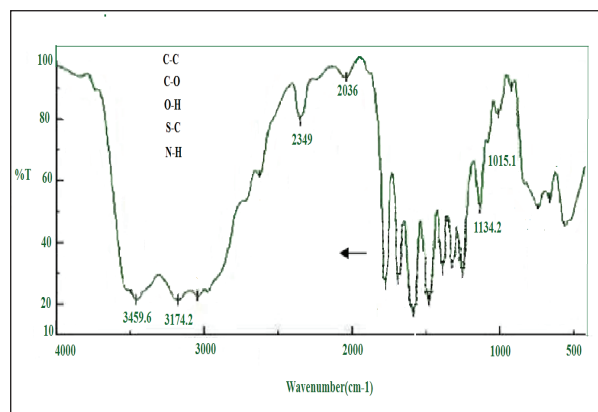of the amoxicillin was studied by scanning electron microscopy **(Fig. 4)**.



**Fig. 2.** FT-IR spectra of pure amoxicillin
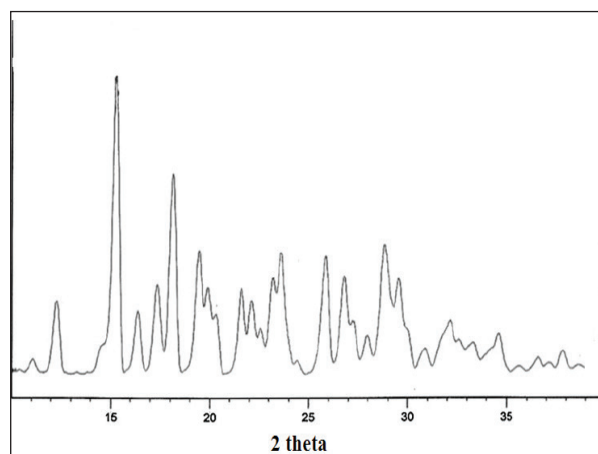


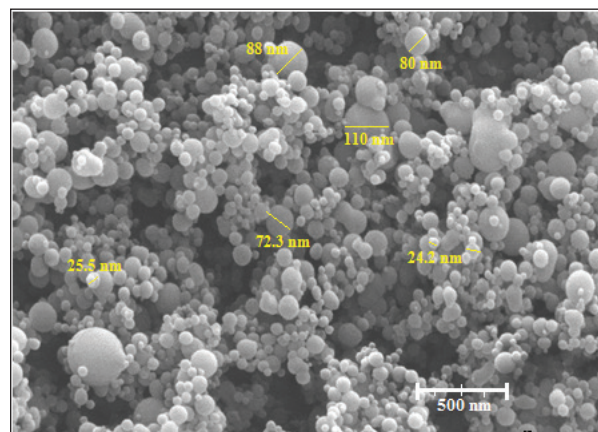**Fig. 3.** XRD spectra of pure amoxicillin



**Fig. 4.** FE-SEM for pure amoxicillin

## 2.3. Sample Preparation

Serum potentially contains elements and proteins which were produced in the human body. Sample preparation helps to reduce time, errors and interferences in analytical chemistry. The sample collection and handling have improved the sensitivity, selectivity, and reproducibility of Cu/Zn analysis in serum samples. For increasing accuracy and precision of results, the human serum samples were prepared. First, the glass laboratories placed in mixture of sulfuric acid and nitric acid (ultra pure grade; 0.5 molar: 0.5 molar) for 24 hours and washed for ten times with DW. The Cu and Zn concentrations in serum have an important limit concentration ($\sim$0.8-1.5 mg L$^{-1}$) and So, the human serum sampling, storage and analysis must be carefully done. In addition, 10 mL of the human serum were prepared from personnel of multiple Sclerosis patients in Iran (MS; 25 Men, 25 women, 25-55 age), based on the world medical association declaration of Helsinki (WMADH). Clean and sterilized syringes with plastic needles were purchased for Merck, Germany for serum blood sampling. The human biological samples were maintained frozen in refrigerator (below -4°C). For long-term storage of serum samples, we placed samples at −20, −80 °C or using liquid nitrogen. Urine samples were prepared and storage based on standard method in human samples.

## 2.4. Extraction Copper and Zinc Procedure

As shown in **Figure 5**, the copper and zinc were simultaneously extracted based on pure amoxicillin by DIL-CPE procedure. Firstly, 0.1 g of hydrophobic ionic liquid [MOIM][PF$_6$] and 0.2 mL acetone was mixed together and then 0.03 g of pure amoxicillin as a antibiotic drug was added. The mixture was injected to diluted serum or urine sample (2:10) by 2 mL of syringe with PVC needle. The cloudy solution was obtained and shacked for 7 min by shaker accessory. Then, the Cu or Zn ions was extracted from serum or urine samples based on sulfur bonding of amoxicillin at pH of 7 by DIL-CPE procedure (Cu─:S:─Zn). After centrifuging for 3 minute (3500 rpm), ionic liquid separated from serum sample in end of conical tube. The Cu or Zn ions were simply back extracted with 0.5 mL of nitric acid (0.2 M) and diluted with DW up to 1 mL. Finally, the remained solution was determined by flame atomic absorption spectrometry (F-AAS). The recovery of proposed method based on pure amoxicillin antibiotic drug was achieved for Cu and Zn extraction by the recovery equation (mean of RSD% < 2.2; more than 95%). The C$_p$ is the primary concentrations of Cu or Zn in sample and C$_F$ is the final concentration of Cu or Zn by DIL-CPE/F-AAS procedure (n=10, Eq. A).

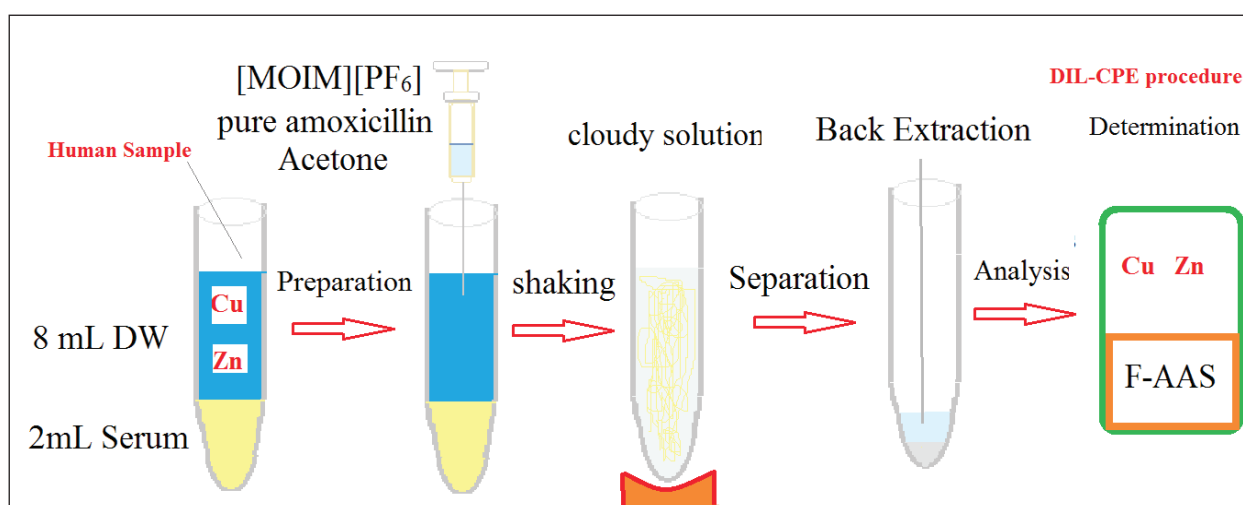$$\text{Recovery \%} = (C_p - C_F)/C_p \times 100$$

**(EQ.A)**



**Fig. 5.** Simultaneously extracted of Cu and Zn in serum and urine samples based on amoxicillin by DIL-CPE procedure

## 3. Results and Discussion

The DIL-CPE procedure provides novel and interesting approach based on amoxicillin drug for extraction of copper and zinc from human serum and urine samples. In order to obtain favorite separation and quantitative extraction of Cu and Zn ions with high sensitivity and precision, the analytical parameters of proposed DIL-CPE method must be optimized.

### 3.1. Optimization of pH

The pH of human serum or urine is main factor for efficient extraction of Cu and Zn ions by DIL-CPE procedure. The retention of Cu and Zn ions by amoxicillin ligand has been investigated at different pH from 2 to 11 with buffer solutions containing (100 µg $L^{-1}$, 500 µg $L^{-1}$) and ( 50 µg $L^{-1}$, 150 µg $L^{-1}$) for copper and zinc as LLOQ and ULOQ concentrations. It showed that amoxicillin ligand ($pH_{PZC}$ = 5.6), the extraction efficiencies of Cu (II) and Zn(II) were improved with the increase of pH values

more than 6 and the quantitative extraction were obtained at pH 6-8 and then the recoveries were reduced at pH more than 9. Consequently, the Cu and Zn ions quantitative extracted at pH 7 **(Fig.6)**. Due to serum pH, the extraction mechanism of Cu (II) and Zn(II) ions based on amoxicillin ligand is mainly depended on the electrostatic attractions of deprotonated sulfur groups of amoxicillin ligand with the positively charged $Cu^{2+}$ and $Zn^{2+}$ cations. At low pH (pH< $pH_{PZC}$), the amoxicillin ligand have positively charged ($SH_2^+$) as a protonation system. So, the extraction efficiency can be decreased due to the electrostatic repulsion between the $Cu^{2+}$ and $Zn^{2+}$ cations and positively charge of ligand. In addition, by increasing pH, the sulfur groups in amoxicillin ligand becomes negatively charged (R-S:$^{2-}$….Cu/Zn) and so the electrostatic attraction between negatively charged sulfur groups and positively charged $Cu^{2+}$ and $Zn^{2+}$ cations increased. In more pH (pH>9) the extraction were decreased due to the
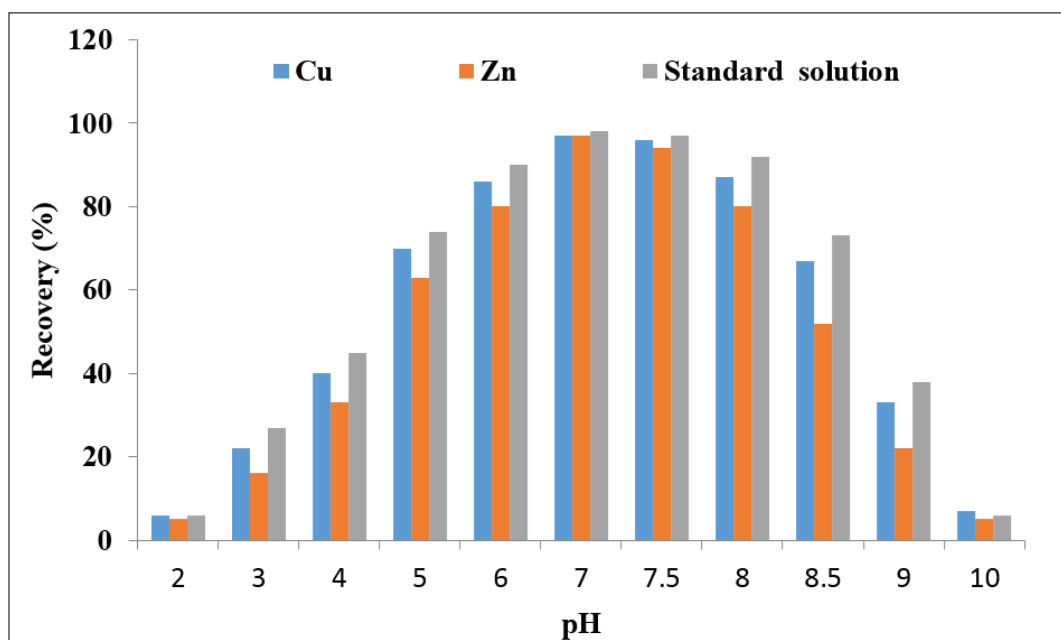


**Fig. 6.** The pH effect on simultaneously copper and zinc extraction with pure amoxicillin by DIL-CPE procedure

formation of hydroxyl complexes of Cu (II) and Zn(II) ions.

### 3.2. Effect of amoxicillin dose

Different amounts of amoxicillin ligand (AMOX-L) in the range of 5 to 50 mg were tested on the recoveries of Cu (II) and Zn(II) ions for the presented DIL-CPE procedure. The results were shown in **Figure 7**. It was found that 30 mg and 25 mg of AMOX-L was sufficient for quantitative recoveries of copper and zinc ions in serum and urine samples, respectively. So, 30 mg of AMOX-L was used as optimum amount of AMOX-L for further works. Higher amount of AMOX-L had no significant effect on the extraction of Cu (II) and Zn(II) ions. Due to capture of Cu (II) and Zn(II) on surface of AMOX-L and the metal concentration in solution, it came to equilibrium with each other. Eventually, 30 mg of AMOX-L was used as ligand for further work.

### 3.3. Effect of the IL amount

In the presented DIL-CPE method, 1-Methyl-3-octylimidazolium hexafluorophosphate ($C_{12}H_{23}F_6N_2P$; [MOIM][PF$_6$]) as hydrophobic ionic liquid was used as green extraction solvent in order to separate the Cu (II) and Zn(II) ions which was complex with AMOX-L as a coordination complex ions in the serum and urine samples.

The effect of [MOIM][PF$_6$] amounts on the extraction efficiencies of presented method was studied within the range of 0.05-0.25 g for 10 mL of standard solution, serum and urine samples containing 30 mg of AMOX-L, copper values (100 µg L$^{-1}$, 500 µg L$^{-1}$) and zinc values ( 50 µg L$^{-1}$, 150 µg L$^{-1}$) as LLOQ and ULOQ concentrations. The results showed that the quantitative recoveries were obtained with 0.08 g of [MOIM][PF$_6$]. Therefore, in order to achieve a suitable preconcentration, 0.1 g of IL was chosen as optimum leading to a final IL for serum and urine samples **(Fig.8)**. Moreover, the effect of IL for
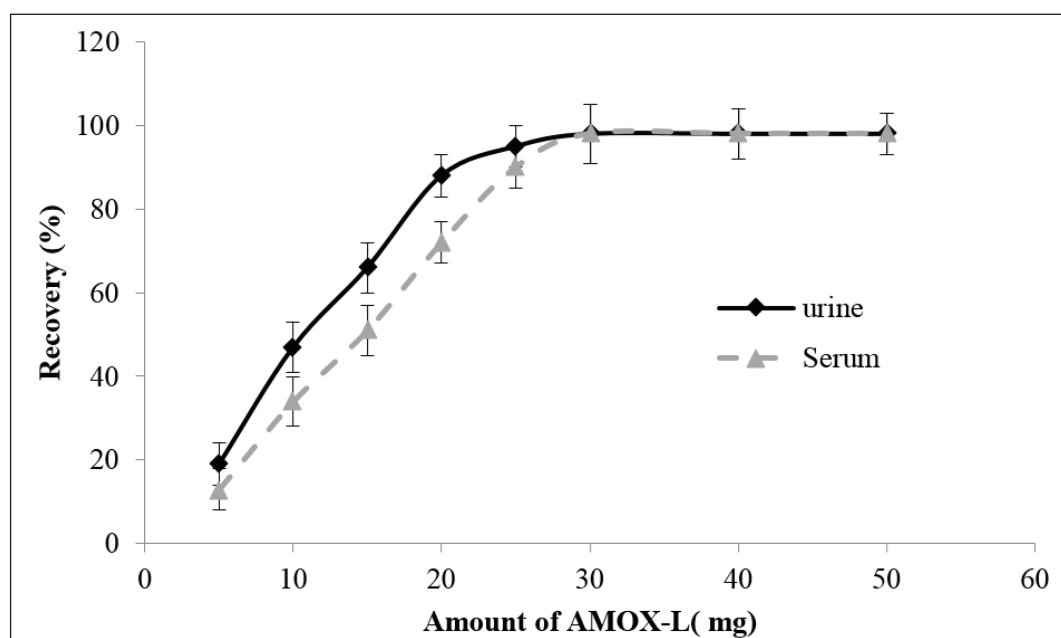


**Fig. 7.** The effect of AMOX-L on simultaneously copper and zinc extraction by DIL-CPE procedure
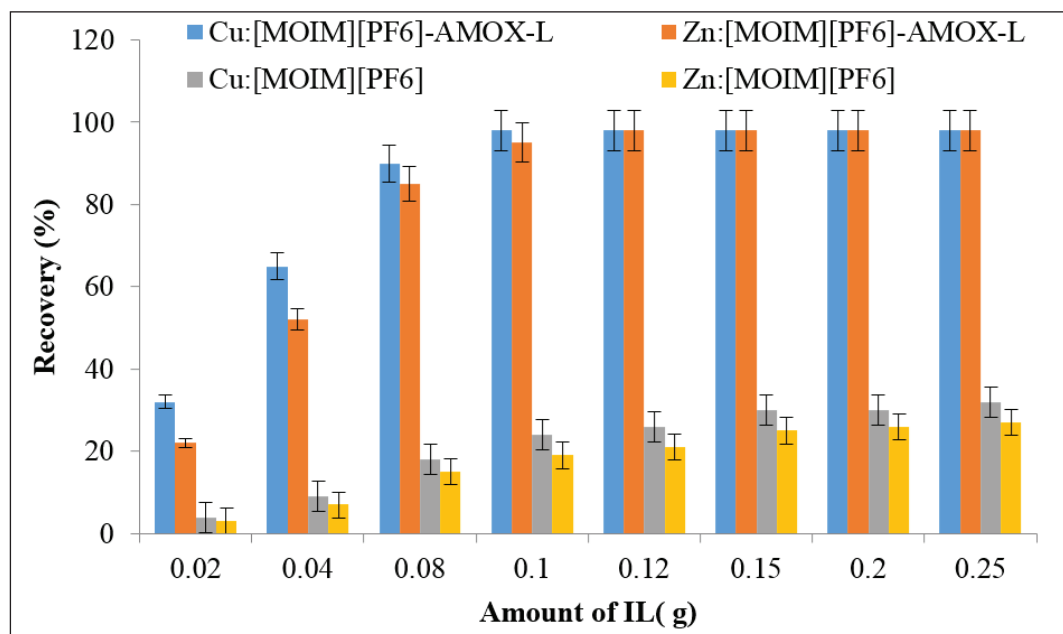
**Fig. 8.** The effect of [MOIM][PF$_6$] on simultaneously copper and zinc extraction
by DIL-CPE procedure

Cu and Zn extraction with the same experiments were evaluated without and AMOX-L. Based on results, the efficient extraction for Cu and Zn ions were obtained less than 24% and 19% for urine and serum as complexation Cu and Zn with amino acids such as cysteine (Cys) and proteins (Cu/ Zn….Pr /Cys). Therefore the IL had low effect on Cu and Zn extraction at optimum conditions. In addition, by increasing the ultrasonication time up to 60 min, the almost 27% and 31% of Cu and Zn ions extracted by 0.1 g of IL without any AMOX-L. These results confirm the critical role of AMOX-L as complex agent for Cu and Zn extraction.

### 3.4. Effect of eluents
The elution solutions were optimized in order to obtain the maximum back-extraction Cu and Zn ions from IL with the minimum concentration and volume of the elution solution. By DIL-CPE method, the different elution solutions were selected with high recovery. The coordination of Cu and Zn cations with AMOX-L was dissociated and ions released into the aqueous phase in acidic pH. For evaluation of the type, the concentration and the volume of acid

solutions for back extraction ions from ligand, 1000 μL of different mineral acids solutions such as HCl, H$_3$PO$_4$, HNO$_3$ and H$_2$SO$_4$ (0.1-0.5 mol L$^{-1}$) were examined by DIL-CPE procedure. The results showed that 0.2 mol L$^{-1}$ HNO$_3$ (0.5 mL) quantitatively back-extracted Cu and Zn from ligand/IL **(Fig. 9)**.

### 3.5. Effect of sample volume
As shown in **Figure 10**, the effect of sample volume on the extraction of copper and zinc in serum and urine samples were evaluated and optimized by different volumes from 1- 25 mL containing copper values (100 μg L$^{-1}$, 500 μg L$^{-1}$) and zinc values ( 50 μg L$^{-1}$, 150 μg L$^{-1}$) as LLOQ and ULOQ concentrations by DIL-CPE procedure. As shown in Fig. 10, satisfactory recoveries were obtained between 2-10 mL for urine and serum samples. In addition, the high sample volume caused to significantly decrease the extraction Cu and Zn in human samples. Therefore, 10 mL of human samples was used for further investigation.
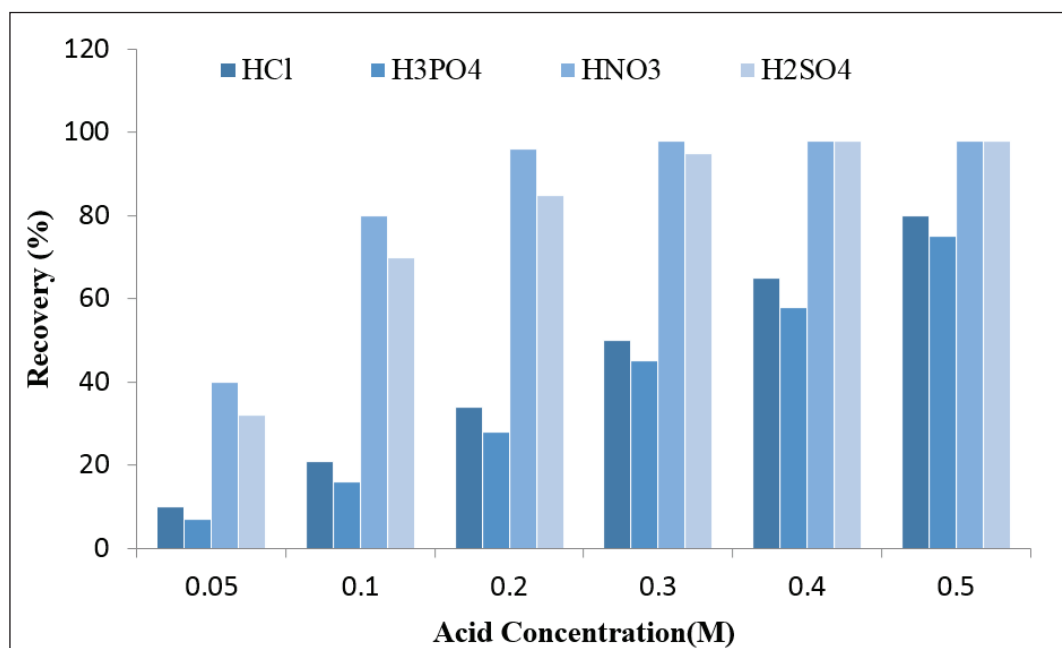
### 3.6. Effect of time

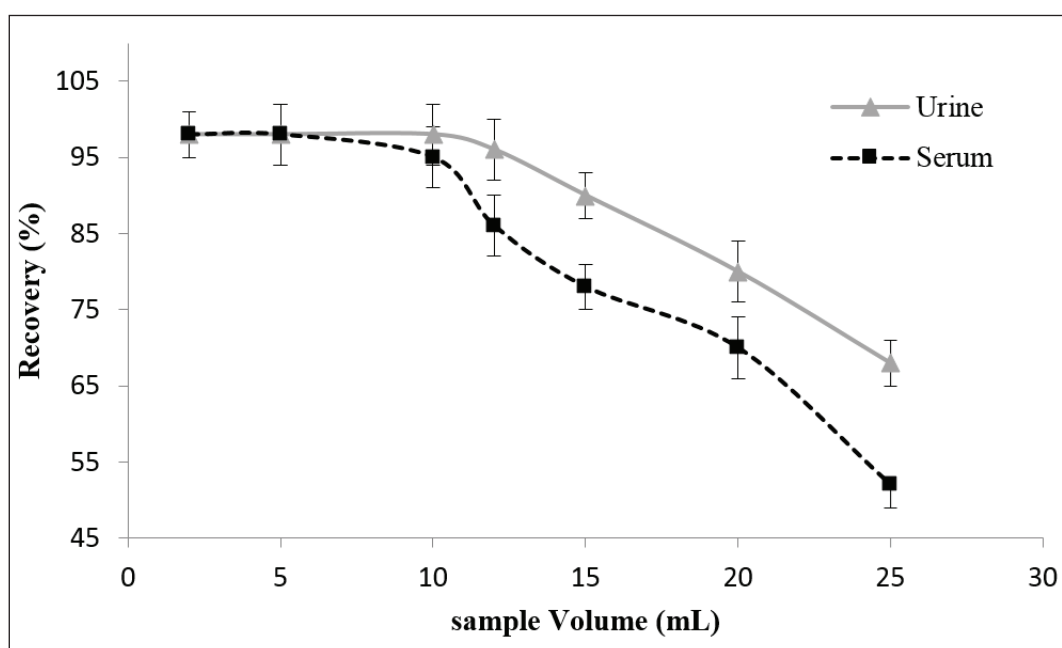**Fig. 9.** The effect of eluents on back-extraction of copper and zinc extraction by DIL-CPE procedure



**Fig. 10.** The effect of sample volume on extraction of copper and zinc by DIL-CPE procedure

Dispersion is main factors for DIL-CPE procedure and allows to perfectly contacting of the Cu and Zn cations with AMOX-L as complex agent. Due to the favorite dispersion of the ligand into the liquid phase, the recovery of extraction phase increased. The effect of the ultrasonication time on the DIL-CPE procedure based on AMOX-L was studied within the range of 1–10 min. The results showed, by increasing time up to 2.5 min, the relative extraction increased and after this time remained constant. So, the time of 2.5 min selected for Cu and Zn extraction for further studies. On the other hand, after complex ions with AMOX-L, the centrifugation was needed to accelerate the separation IL from liquid phase.

Therefore, different times for centrifuging were examined between 1-5 min at 3500 rpm. The result showed that 2.0 minutes is sufficient to perfect separation phase.

### 3.7. Interference study

For evaluating of the analytical application in real samples, the important interference of coexisting ions effected on copper and zinc extraction in serum and urine samples were studied by the DIL-CPE procedure. For this proposed, the different amounts of the interfering ions added to 10 mL of liquid solution containing 500 µg L$^{-1}$ of copper and 150 µg L$^{-1}$ of zinc. The results showed, the most of the coexisting cations and anions had no effect on

the extraction of Cu and Zn ions under optimum conditions (SD of recovery < ±5%). In fact, the tolerable concentration ratio of interference of coexisting ions (M) per Cu and Zn (M/Zn$^{2+}$ or M/Cu$^{2+}$) for Hg$^{2+}$, Ag$^+$ and Au$^{3+}$ was less than 50 and 30 for zinc and copper, respectively. This ratio was almost 100-200 for Ni$^{2+}$, Pb$^{2+}$ and Co$^{2+}$ ions. The results showed that the AMOX-L have favorite ligand for Cu and Zn extraction despite the high concentrations of the coexisting ions **(Table 1)**. .

### 3.8. Analytical figures of merit

The analytical characteristics for Cu and Zn extraction in human serum and urine samples were

**Table 1.** The effect of interferences ions on extraction of Cu(II) and Zn (II)  in serum samples by DIL-CPE procedure

| Interfering  Ions in serum (M) | Mean ratio ($C_M/C_{Cu(II)}$) | Recovery (%) |
|---|---|---|
| | Cu(II) | Cu(II) |
| V$^{3+}$, Fe$^{3+}$ | 800 | 97.2 |
| Cd$^{2+}$, Mn$^{2+}$ | 600 | 98.1 |
| I$^-$ , Br$^-$, F$^-$, Cl$^-$ | 1200 | 99.3 |
| Na$^+$, K$^+$ | 1000 | 98.4 |
| Ca$^{2+}$, Mg$^{2+}$ | 750 | 97.1 |
| CO$_3^{2-}$,  PO$_4^{3-}$, NO$_3^-$ | 900 | 97.7 |
| Ni$^{2+}$,  Co$^{2+}$ | 100 | 96.9 |
| Pb$^{2+}$ | 700 | 98.2 |
| Hg$^{2+}$,  Ag$^+$,  Au$^{3+}$ | 30 | 97.3 |

| Interfering  Ions in serum (M) | Mean ratio ($C_M/C_{Zn(II)}$) | Recovery (%) |
|---|---|---|
| | Zn(II) | Zn(II) |
| V$^{3+}$, Fe$^{3+}$ | 900 | 98.7 |
| Cd$^{2+}$, Mn$^{2+}$ | 750 | 97.6 |
| I$^-$ , Br$^-$, F$^-$, Cl$^-$ | 1100 | 98.8 |
| Na$^+$, K$^+$ | 900 | 98.2 |
| Ca$^{2+}$, Mg$^{2+}$ | 950 | 96.6 |
| CO$_3^{2-}$,  PO$_4^{3-}$, NO$_3^-$ | 1100 | 98.7 |
| Ni$^{2+}$,  Co$^{2+}$ | 200 | 97.5 |
| Pb$^{2+}$ | 800 | 96.7 |
| Hg$^{2+}$,  Ag$^+$,  Au$^{3+}$ | 50 | 98.0 |

studied by the purposed DIL-CPE procedure. The intra-day analytical performance was shown in **Table 2** for the multiple sclerosis patients (50) and healthy peoples (50). Under the optimal conditions, the linearity for the Cu (II) and Zn(II) concentration ranges between 100 -505 μg $L^{-1}$ and 41- 153 μg $L^{-1}$, respectively as a lower limit of quantification (LLOQ) and upper limit of quantification (ULOQ) with mean correlation coefficient of $R^2$=0.9997 for Intra-day analysis. The LOD and LOQ are as an analytical signal three times higher than the background noise and three times higher than LOD, respectively. The precision of the AMOX-L/DIL-CPE procedure showed by the relative standard deviation (RSD %) for ten replicate determination containing 100 μg $L^{-1}$ of Cu and Zn concentration which was obtained lower than

2.2%. The enrichment factor was calculated based on calibration curve and curve fitting rule (tga=$m_1$/$m_2$). According to proposed method, a favorite linear ranges and satisfactory EF were achieved for determination of Cu(II) and Zn (II) ions in human samples. The mean value for serum copper/zinc ratio in MS patients was obtained $1.11 \pm 0.28$ which was lower than normal range as $1.44 \pm 0.31$.

### 3.9. Analysis of real and certified samples

The DIL-CPE procedure was used for determination of copper and zinc in serum and urine samples by AMOX-L ligand. The validation of method was obtained based on spiking samples by known concentration of Cu (II), and Zn(II). The efficient recovery was achieved by spiking samples, which confirms the accuracy of the

**Table 2.** Determination of copper and zinc in serum by DIL-CPE procedure (Mean intra-day and inter –day analysis for 50 MS and 50 healthy peoples (HP); μg$L^{-1}$)

| Serum Sample | [a] Mean of MS (n=50) | | [a] Mean of HP (n=50) | | + Data Subject | |
|---|---|---|---|---|---|---|
| | Intra-day | Inter day | Intra-day | Inter day | r | P value |
| Copper | $965.4 \pm 51.6$ | $972.1 \pm 58.7$ | $1154.5 \pm 62.6$ | $1168.7 \pm 71.4$ | 0.107 | <0.001 |
| Zinc | $658.4 \pm 29.5$ | $666.2 \pm 33.8$ | $875.3 \pm 44.6$ | $861.9 \pm 48.8$ | 0.123 | <0.001 |

＊Mean of three determinations of samples $\pm$ confidence interval (P = 0.95, n =10)

✚Correlations are based on Pearson coefficients (r). Statistical significance will be observed if P < 0.001

**Table 3.** Validation of developed the DIL-CPE procedure based on AMOX-L for Cu and Zn determination by spiking real samples (μg$L^{-1}$)

| Sample | Added Cu | Added Zn | Found Cu* | Found Zn* | Recovery(%)Cu | Recovery(%)Zn |
|---|---|---|---|---|---|---|
| **Serum** | ------ | ------ | $235.5 \pm 11.2$ | $189.6 \pm 9.3$ | ------ | ------ |
| | 200 | 200 | $429.6 \pm 20.8$ | $380.4 \pm 18.7$ | 97.1 | 95.4 |
| **Urine** | ------ | ------ | $197.3 \pm 10.1$ | $201.2 \pm 9.4$ | ------ | ------ |
| | 200 | 200 | $394.8 \pm 17.6$ | $404.7 \pm 18.9$ | 98.7 | 101.7 |
| **Serum** | ------ | ------ | $252.7 \pm 11.2$ | $168.8 \pm 8.3$ | ------ | ------ |
| | 250 | 150 | $499.8 \pm 23.6$ | $315.5 \pm 14.7$ | 98.8 | 97.8 |
| **Urine** | ------ | ------ | $171.4 \pm 8.1$ | $142.3 \pm 6.6$ | ------ | ------ |
| | 150 | 150 | $324.2 \pm 13.5$ | $288.7 \pm 14.2$ | 101.8 | 97.6 |

* Mean of three determinations of samples $\pm$ confidence interval (P = 0.95, n =10)

All samples (2 mL) diluted with DW up to 10 mL( Dilution factor: DF=5)

**Table 4.** Validation of methodology based on ICP-MS analysis in real samples
and compared to the DIL-CPE procedure ($\mu gL^{-1}$)

| Sample | Added($\mu gL^{-1}$) | *Found(ICP-MS) | *Found(DIL-CPE) | Recovery |
|--------|-----------|----------------|-----------------|----------|
| Serum(Cu) | ------ | 302.2 ± 7.2 | 297.5 ± 14.2 | 98.4 |
|  | 200 | ------ | 492.8 ± 22.4 | 97.6 |
| Serum (Zn) | ------ | 182.3± 4.2 | 178.9 ± 8.2 | 98.1 |
|  | 150 | ------ | 334.2 ± 15.4 | 103.5 |
| Urine (Cu) | ------ | 261.5 ± 6.8 | 257.2 ± 11.7 | 98.3 |
|  | 250 | ------ | 497.9 ± 24.6 | 96.3 |
| Urine (Zn) | ------ | 192.3 ± 4.5 | 200.6 ± 9.5 | 104.3 |
|  | 200 | ------ | 399.8 ± 17.4 | 99.6 |

* Mean of three determinations of samples ± confidence interval (P = 0.95, n =10)
All samples (2 mL) diluted with DW up to 10 mL( DF=5)

DIL-CPE procedure **(Table 3)**. The recoveries of spiked samples for Cu and Zn were ranged from 96 to 105%, which demonstrated that the DIL-CPE procedure was satisfactory for determination copper and zinc in urine and serum samples. On the other hand, the certified standard reference materials (CRM) were prepared in serum and urine sample by ICP-MS and used for the validation methodology **(Table 4)**.

## 4. Conclusions

A simple, rapid, reliable and sensitive method was developed for separation and extraction of Cu (II) and Zn(II) in serum and urine samples based on AMOX-L by the DIL-CPE procedure. The [MOIM][PF$_6$] ionic liquid as a trapping phase was used for separating of Cu/Zn-loaded AMOX-L from liquid phase. IL helps to reducing the sample preparation and separation time for extraction process. Using a small amount of AMOX-L with high extraction recovery, good precision, minimal acid elution (500 μL) and green solvent caused to make the efficient e xtraction b ased on environmentally friendly for determining of Cu and Zn in urine and serum samples. Also, the low LOD and RSD% values as well as the quantitative recoveries (more than 95%) were obtained in optimized conditions. Therefore, the developed method based on AMOX-L can be used as favorite sample preparation in human biological samples in short time. As obtained results, the amoxicillin can be affected on copper and zinc deficiency in human body at human pH when the patients used it by over dosage for many times.

## 6. References

[1] Zinc, Institute of Medicine, Dietary Reference Intakes: The essential guide to nutrient requirements, The National Academies Press, Washington D.C., pp. 402-413, 2006.

[2] R. K Gupta, S.S. Gangoliya, N.K. Singh, Reduction of phytic acid and enhancement of bioavailable micronutrients in food grains, J. Food Sci. Technol., 52 (2015) 676-684.

[3] Copper, Institute of Medicine. Dietary Reference Intakes: The Essential Guide to Nutrient Requirements, The National Academies Press, Washington D.C., pp. 304-311, 2006.

[4] J. Osredkar, N. Sustar. Copper and zinc, biological role and significant of copper/zinc imbalance, J. Clinic. Toxicol., S3 (2011) 001. http://doi: 10.4172/2161-0495. S3-001

[5]  E. Kouremenou-Dona, A. Dona, J. Papoutsis, C. Spiliopoulou, Copper and zinc concentrations in the serum of healthy Greek adults, Sci. Total Environ., 359 (2006)76–81.

[6]  V. rvanitidou, I. Voskaki, G. Tripsianis, S. Flippidis, K. Schulpis, I. Androulakis, Serum copper and zinc concentrations in healthy children aged 3–14 years in Greece, Biol. Trace Elem. Res., 115 (2007) 1–12

[7]  Z. L.-L. Zhang, L. Lu, Y.-J. Pan, Baseline Blood Levels of Manganese, Lead, Cadmium, Copper, and Zinc in Residents of Beijing Suburb, Environ. Res., 2015 140 (2015) 10–17.

[8]  Y. M. Park, J. Y. Choi, E. Y. Nho, Ch. M. Lee, I. M. Hwang, N. Khan, Determination of macro and trace elements in canned marine products by inductively coupled plasma—optical emission spectrometry (ICP-OES) and ICP—mass spectrometry (ICP-MS), J. Anal. Lett., 52 (2019)1018-1030.

[9]  Y. Wang, J. Xie, Y. Wu, X. Hu, A magnetic metal-organic framework as a new sorbent for solid-phase extraction of copper(II), and its determination by electrothermal AAS, Microchim. Acta, 2014, 181, 949–956.

[10]  S. Hamida, L. Ouabdesslam, A. F. Ladjel, M. Escudero, J. Anzano, Determination of Cadmium, Copper, Lead, and Zinc in Pilchard Sardines from the Bay of Boumerdés by Atomic Absorption Spectrometry, J. Anal. Lett., 51 (2018) 2501-2508.

[11]  T. Sahraeian, H. Sereshti, A. Rohanifar, A. Simultaneous determination of bismuth, lead, and iron in water samples by optimization of USAEME and ICP–OES via experimental design. J. Anal. Test., 2 (2018) 98–105.

[12]  H. Sereshti, A.R. Far, S. Samadi, Optimized ultrasound-assisted emulsification-microextraction followed by ICP-OES for simultaneous determination of lanthanum and cerium in urine and water samples, Anal. Lett., 45 (2012) 1426–1439.

[13]  G.Bagherian, M. A. Chamjangali, H. S. Evari, M. Ashrafi, Determination of copper (II) by flame atomic absorption spectrometry after its perconcentration by a highly selective and environmentally friendly dispersive liquid–liquid microextraction technique, J. Anal. Sci. Technol., 10 (2019) 3.

[14]  H. Duan, Z. Wang, X. Yuan, S. Wang, H. Guo, X. Yang, A novel sandwich supported liquid membrane system for simultaneous separation of copper, nickel and cobalt in ammoniacal solution, Sep. Purif. Technol., 173 (2017) 323–329.

[15]  B. Ebrahimi, S. Mohammadiazar, S. Ardalan, New modified carbon based solid phase extraction sorbent prepared from wild cherry stone as natural raw material for the pre-concentration and determination of trace amounts of copper in food samples, Microchem. J. 147 (2019) 666–673.

[16]  S. Vellaichamy, K. Palanivelu, Preconcentration and separation of copper, nickel and zinc in aqueous samples by flame atomic absorption spectrometry after column solid-phase extraction onto MWCNTs impregnated with D2EHPA-TOPO mixture,. J. Hazard. Mater., 185 (2011) 1131–1139

[17]  M.A. Farajzadeh, M. Bahram, B.G. Mehr, J.A. Jönsson, Optimization of dispersive liquid–liquid microextraction of copper (II) by atomic absorption spectrometry as its oxinate chelate: application to determination of copper in different water samples, Talanta, 75 (2008) 832–40.

[18]  G. Özzeybek, S. Erarpat, D.S. Chormey, M. Fırat, Büyükpınar Ç, Turak F, Bakırdere S. Sensitive determination of copper in water samples using dispersive liquid-liquid microextraction-slotted quartz tube-flame atomic absorption spectrometry. Microchem J., 132 (2017) 406–10.
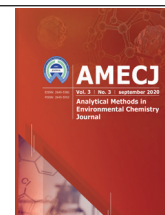
# Removal of Metronidazole residues from aqueous solutions based on magnetic multiwalled carbon nanotubes by response surface methodology and isotherm study

**Mohammad Reza Rezaei Kahkha [*,a], Gholamreza Ebrahimzadeh [a] and Ahmad Salarifar [b]**

[a]Department of Environmental Health Engineering, Faculty of Health, Zabol University Of Medical Sciences,Zabol.Iran
[b] Environmental Engineering, Faculty of Natural Resources, Islamic Azad University, Bandar Abbas Branch, Bandar Abbas, Iran

**ABSTRACT**

Antibiotics and pharmaceutical products cannot remove by conventional sewage treatment. In this work, an effective adsorbent magnetic multiwalled carbon nanotube ($Fe_3O_4$@MWCNTs; MMWCNTs) was synthesized by co-precipitation of MWCNTs with $Fe_3O_4$ and used for removal of Metronidazole from aqueous solutions. Response surface methodology on central composition design (CCD) was applied for designing of experiments and building of models for Metronidazole removal before determination by HPLC. Four factors including pH, the adsorbent dose, time, and temperature were studied and used for the quadratic equation model to the prediction of optimal points. By solvent the equation and considering the regression coefficient ($R^2 = 0.9997$), the optimal points obtained as follows: pH =2.98; adsorbent dosage =2.16 g; time =22 min and temperature = 37.9 ℃. The isotherm study of adsorption showed that the metronidazole adsorption on $Fe_3O_4$@MWCNTs follows the Langmuir model. The maximum adsorption capacity (AC) is 215 mg g$^{-1}$ obtained from Langmuir isotherm. The results showed that three factors including pH, amount of adsorbent, and temperature are significant on removal efficiency and an experimental point was found to agree satisfactorily with the predicted values. The proposed methods coupled to HPLC were used to analysis of metronidazole in six real samples. The results showed the best removal efficiency was obtained at optimal points. Moreover, the reusability of adsorbent showed that the $Fe_3O_4$@MWCNTs can be efficiently removed the Metronidazole from aqueous solutions as compared to other adsorbents.

## 1. Introduction

Antibiotic residual in environmental ecosystems is a serious concern for human's health. The conventional sewage treatment cannot remove antibiotics and pharmaceutical products and hence, a serious ecological risk that occurs by discharging of these effluent in environmental ecosystems and aquatic [1, 2]. Metronidazole ($C_6H_9N_3O_3$) is an antibiotic that used to treat a wide variety bacterial infections [3]. Recently, researchers reported that average concentration of metronidazole in river water and wastewater was approximately about 0.5

and 1.3 ng $L^{-1}$, respectively [4]. In addition, many pharmaceutical industries discharge this antibiotic in environmental water by higher dosage [5]. Several methods such as fenton process, filtration and adsorption were used for removal of metronidazole from different matrix and determined with HPLC [6]. Due to cost and simplicity methods, the adsorption techniques are favorite method for removal of metronidazole in water and biological samples. Many techniques based on metal nanoparticles, the polymer structures, the nanosheets, MWCNTs modified with  and neural network-genetic algorithm were used and developed for separation and determination metronidazole and other drug in different matrixes [7]. Adsorption is simple, effective and economic way with high recovery, easy operation and low cost technique for removal of contaminants such as antibiotic within water or wastewater even at large concentration. The type and size of adsorbent is a key factor for adsorption process that influences on removal efficiency of pollutant [8]. Carbon nanotubes (SWCNTs and MWCNTs) and functionalized of CNTs are widely used as an adsorbent in the removal, extraction and preconcentration of many contaminants including medicinal compounds, pesticides, and other molecules [9]. High surface area, high permeability, good mechanical and thermal stability and repeatability are some of the unique properties of nanotubes. Also, the absorption capacity is could be increased by modifying the surface of CNTs by $NH_2$, COO, SH, $C_6H_5$ groups and adsorption of contaminants would be more specific [10]. Response surface methodology (RSM) is a most applicable method used in many fields such as antibiotics and pharmaceutical products [11]. RSM is a technique that used for statistical analysis of complicated processes and can be utilized for investigating of relative significance of important factors even in the presence of complex interactions [12]. High performance liquid chromatography (HPLC) is a suitable method for isolation, identification and measurement of many drugs. Combining liquid chromatography with mass spectrometer(LC-MS, HPLC-MS) is the most appropriate method for

identifying different species of organic compounds in complex matrixes. Examples of these compound are amino acids, proteins, nucleic acids, hydrocarbons, carbohydrates, drugs, terpenoids and pesticides, antibiotics, steroids, any organic or inorganic metal and a group of various materials.

Experimental data points were obtained during optimization based on $Fe_3O_4$@MWCNTs and a model for central composition design (CCD). It is good method for the consecutive experimentation and illustrate accurate information for testing several parameters while not involving an unusually large number of data points. The adsorption Metronidazole  based on $Fe_3O_4$@MWCNTs was determination by HPLC instrument.

## 2. Experimental
### 2.1. Reagent and material
All reagent and solutions were analytical grade and purchased from Merck (Darmstadt, Germany). Metronidazole (CASN: 443-48-1) was obtained from Aldrich chemical Co. (Germany). HPLC grade of acetonitrile (ACN) and DW purchased from Sharloa (Spain). Carbon nanotubes with outer diameter of 3–20 nm, length between 1–10 nm, number of walls 3–15 and surface area of around 350 $m^2$ $g^{-1}$ were prepared from Plasma Chem. GmbH (Berlin, Germany). Also, The pristine MWCNTs (308068, 98% carbon base, O.D= 10 nm, L=5-20 μm) was purchased from Sigma Aldrich. A standard solution of 1000 mg $L^{-1}$ metronidazole prepared by dissolving of 1 gr metronidazole in 1liter deionized water. All standard working solutions prepared daily by dilution of DW. ) The shacking and centrifuging of blood samples were used based on 300 rpm and 3500 rpm speeds by vortex mixer (Thermo, USA) and Falcon centrifuge (20 mL of polypropylene conical tubes, Thermo, USA), respectively. The pH was adjusted pH by 0.25 mol $L^{-1}$ of sodium phosphate buffer solution (Merck, Germany) for pH of 5.5 to 8.2 ($Na_2HPO_4$/$NaH_2PO_4$).

### 2.2. Synthesis of MMWCNTs
Synthesis of magnetic carbon nanotube was

performed by co-precipitation methods that reported previously [13]. Briefly, 10 mg of pristine MWCNTs were added to 2 ml solution composed of 4.33 mmol $Fe^{+2}$ and 8.66 mmol $Fe^{+3}$ solution was stirred in ultrasonic bath for 10 min at 50°C while 10 ml concentrated ammonia (8 M) was added drop by drop to the solution. The pH of final solution should be alkaline in order to deposition of $Fe_3O_4$ on multi-walled carbon nanotubes. The adsorbent was washed for 7 times with distilled water and separated by a permanent magnet.

### 2.3. Metronidazole removal by MMWCNTs

Batch adsorption experiments were carried out as per the design developed with the central composite design methodology. Experiments were performed at a batch reactor in 500 ml beaker that containing 50 ml of given concentration of metronidazole. Beakers were shaken during that shaked for the specified time period in a temperature controlled incubation shaker at 200 rpm. The pH was adjusted by addition of 0.1 M NaOH or HCl. After completion of experiments adsorbent was removed by an external magnet and remaining metronidazole was measured. The measurement of metronidazole was performed using Cecil HPLC (CECIL Corporation, England) equipped ACE $C_{18}$ column and UV-VIS detector at 230 nm. The mobile phase is ACN: WATER (60:40). The removal percentage of Metronidazole (%removal) was calculated as follow by **equation 1**:

$$\%Removal = \frac{Cf - C0}{C0} * 100$$

**(Eq.1)**

Where $C_f$ and $C_0$ are initial and final metronidazole concentration (mg $L^{-1}$) of solution, respectively.

### 2.4. Experimental design

CCD was applied in this work to investigation of variables for adsorption of metronidazole on to MMWCNTs. The CCD for four variables (pH, adsorbent dosage, time and the temperature), with two levels (minimum and maximum), was used for experimental design model. In the experimental design model, pH (2-10), adsorbent dosage (0.5-2.5 g), time (5-30 min) and temperature (20-60° C) were taken as input variables. Percentage removal of (30 mg $L^{-1}$) of metronidazole was selected as response of the system. The quadratic equation model for prediction of optimal point was expressed by **Equation 2**.

$$Y = \beta0 + \sum_{i=1}^{k} \beta ixi + \sum_{i=1}^{k} \beta iixi^2 + \sum_{i=0}^{k} \sum_{j=i+1}^{k} \beta xixj + \epsilon$$

**(Eq. 2)**

Where Y is the response of the system and $X_i$ and $X_J$ are the variables of action, $\beta_0$, $\beta_i$, $\beta_{ii}$, $\beta_{ij}$ are constant coefficient, linear effects, quadratic effects and interaction effects, respectively. The coefficient of determination, namely, $R^2$ and Adj-$R^2$ were used for the explanation of quality of the model. The statistical significance was expressed with adequate precision ratio and the F-test. Design expert (version 8) program was used for regression and graphical analysis. A total of 31 experiments were necessary to estimate of the full model **(Table 1)**

## 3. Result and discussion

In this work, removal of metronidazole by a nano-composite made of multi-walled carbon nanotubes and iron nanoparticles were studied. Design of Experiments were conducted using the RSM as well as factors affecting on absorption process of metronidazole such as pH, adsorbent dosage, time, and the temperature were optimized. Finally, the data obtained from experiments compared with model output to optimize and predict the results.

### 3.1. Regression model and statistical analysis

The CCD has been successfully used for optimizing conditions of Metronidazole removal. A second-order polynomial regression model equations relating the removal efficiency and process variables are given in **Equation 3**.

**Table 1.** Central composite design matrix with experimental and predicted values

| Column1 | Factor 1 | Factor 2 | Factor 3 | Factor 4 | Actual | Predicted |
|---|---|---|---|---|---|---|
| Run | A:pH | B:adsorbent dose | C:temperature | D:time | Actual Value | Predicted Value |
| 1 | 2 | 2.5 | 60 | 5 | 65 | 65.79284266 |
| 2 | 6 | 1.5 | 40 | 10 | 59 | 60.50063264 |
| 3 | 6 | 1.5 | 40 | 10 | 74 | 72.34013804 |
| 4 | 10 | 0.5 | 60 | 5 | 66 | 66.97292803 |
| 5 | 2 | 0.5 | 60 | 15 | 67 | 68.94958105 |
| 6 | 2 | 0.5 | 60 | 5 | 68.7 | 66.96949568 |
| 7 | 2 | 2.5 | 20 | 15 | 70.8 | 70.74179107 |
| 8 | 10 | 2.5 | 20 | 15 | 70 | 68.94958105 |
| 9 | 2 | 2.5 | 60 | 15 | 69.1 | 68.22151495 |
| 10 | 6 | 1.5 | 40 | 10 | 65 | 64.42930494 |
| 11 | 2 | 0.5 | 20 | 5 | 73 | 74.75160032 |
| 12 | 10 | 2.5 | 60 | 15 | 63 | 65.53095796 |
| 13 | 2 | 0.5 | 20 | 15 | 74 | 73.37046337 |
| 14 | 2 | 0.5 | 60 | 5 | 73 | 73.07825335 |
| 15 | 10 | 2.5 | 60 | 5 | 67 | 65.74816798 |
| 16 | 10 | 2.5 | 20 | 15 | 74 | 73.07825335 |
| 17 | 6 | 1.5 | 40 | 15 | 63 | 63.19805057 |
| 18 | 6 | 1.5 | 40 | 15 | 80.5 | 79.9594382 |
| 19 | 10 | 0.5 | 60 | 15 | 81 | 82.86325088 |
| 20 | 10 | 2.5 | 60 | 15 | 83.4 | 82.86325088 |
| 21 | 2 | 2.5 | 60 | 5 | 63 | 62.62408038 |
| 22 | 2 | 2.5 | 20 | 5 | 62 | 62.0334084 |
| 23 | 10 | 0.5 | 60 | 15 | 56 | 56.42972396 |
| 24 | 6 | 1.5 | 40 | 10 | 65 | 64.22776481 |
| 25 | 10 | 2.5 | 60 | 5 | 83.5 | 82.86325088 |
| 26 | 2 | 2.5 | 60 | 5 | 83.2 | 82.86325088 |
| 27 | 10 | 0.5 | 20 | 5 | 82.9 | 82.86325088 |
| 28 | 10 | 0.5 | 20 | 15 | 82.4 | 82.86325088 |
| 29 | 2 | 0.5 | 60 | 15 | 83.1 | 82.86325088 |
| 30 | 2 | 2.5 | 20 | 15 | 83.2 | 82.86325088 |
| 31 | 6 | 1.5 | 40 | 10 | 83 | 82.86325088 |

%Removal=+41.66308+2.39902 (pH)+9.57629 (adsorbent dose)+0.7686 (temperature)+1.00897 (time)-4.68750× $10^{-3}$ (pH.×adsorbent dose)+0.011172 (pH× temperature)+7. 5×$10^{-3}$( pH×time) -0.034687 (adsorbent×temperature)+0.077000 ( adsorbent ×time) -3.65×$10^{-3}$ (temperature×time)-0.27659 (pH$^2$)-1.99484(adsorbent$^2$)-9.07506× $10^{-3}$ (temperature$^2$)-0.025495(time$^2$)

**(Eq.3)**

Design-Expert 8 software was applied for determination of the coefficients in **Equation 3**. The optimal points were as follows: pH = 2.98; adsorbent dosage = 2.16 g; time = 22.2 min and temperature = 37.88 ºC. The model prediction of the metronidazole removal recovery is 82.8% while the experimental amount of removal efficiency is 83.4%. These results confirmed that RSM effectively used for the investigation of parameters in complex process could be utilized to optimize the process parameters.

The mathematical expressions of relationship between the independent parameters and response of system are given in terms of encoded factors. The results of regression analysis on quadratic model are given in **Table 3**. The significance of each coefficient was expressed by F-values and p-values **(Table 2)**. The larger of the F-values and the smaller of the p-values, indicated more significant of the corresponding coefficients. Values of "prob > F" less than 0.0500 also indicated high significant regression at 95 percent confidence level. According to the F- and p-values, temperature, time and adsorbent dose were found more effective on the adsorption process. The "Lack of Fit F-value" of 0.26 implies the Lack of Fit is not significant relative to the pure error. There is a 98.40% chance that a "Lack of Fit F-value" this large could occur dueto noise. The fit of the model was checked by the determination coefficient (R$^2$).The "Pred R-quared" of 0.9660 is in satisfactory accordance

with the "Adj R-Squared" of 0.9768."Adeq Precision" measures the signal to noise ratio. A ratio greater than 4 is desirable. In this case "Adeq Precision" of 42.257 indicates an adequate signal. Thus, as a result of the statistical analysis, quadratic model was found satisfactory for describing the process and useful for developing empirical relation. Metronidazole removal showed to be very sensitive to changes in the adsorbent dosage and time of adsorption. Magnitude of F-value in **Table 2** was expressed in comparison of these two factors adsorbent dosage was more effective on removal efficiency of metronidazole than time of experiments. **Figure 1** showed 3D plots of interaction effects of all parameters on removal efficiency. As can be seen in **Figure 1** when the pH increased from 2 to 6, the removal efficiency increased about 4%. Also **(Figure 1)**, the results of the study showed that removal efficiency decreased in alkaline solutions. Adsorption time has more effect than pH on metronidazole

**Table 2.** ANOVA analysis for removal of metronidazole

| Source | Sum of square | Df | Mean Square | F-Value | P-value Prob > F |
|---|---|---|---|---|---|
| Model | 3120.63835 | 14 | 222.902739 | 148.517383 | < 0.0001 |
| A-pH | 84.4231475 | 1 | 84.4231475 | 56.2501161 | < 0.0001 |
| B-adsorbent dose | 537.787036 | 1 | 537.787036 | 358.320959 | < 0.0001 |
| C-temperature | 0.66785645 | 1 | 0.66785645 | 0.44498463 | 0.5091 |
| D-time | 116.402257 | 1 | 116.402257 | 77.5574075 | < 0.0001 |
| AB | 0.01125 | 1 | 0.01125 | 0.00749574 | 0.9315 |
| AC | 25.56125 | 1 | 25.56125 | 17.0311499 | 0.0002 |
| AD | 4.5 | 1 | 4.5 | 2.99829525 | 0.0922 |
| BC | 15.40125 | 1 | 15.40125 | 10.2616655 | 0.0029 |
| BD | 29.645 | 1 | 29.645 | 19.7521028 | < 0.0001 |
| CD | 26.645 | 1 | 26.645 | 17.7532393 | 0.0002 |
| A^2 | 1107.54922 | 1 | 1107.54922 | 737.946571 | < 0.0001 |
| B^2 | 225.03502 | 1 | 225.03502 | 149.938096 | < 0.0001 |
| C^2 | 745.166816 | 1 | 745.166816 | 496.495584 | < 0.0001 |
| D^2 | 897.389678 | 1 | 897.389678 | 597.919825 | < 0.0001 |
| Residual | 52.52985 | 35 | 1.50085286 | | |
| Lack of Fit | 5.00385003 | 10 | 0.500385 | 0.26321645 | 0.9840 |
| Pure Error | 47.526 | 25 | 1.90104 | | |

removal in this investigation. It was found that nearly 22.2minute was enough to obtain highest yield.

In addition, **Figuer 2** showed the parity plot of obtained results and predicted results that explains a satisfactory correlation between the observed results and fitted values. In this work, the plotted

residuals indicate normal distribution; the data points form an approximately straight line. The data points farther from the line, expressed departure from normality [14, 15]. In this study, the residuals are approximately plotted along straight line for response, indicating no evidence of non-normality or unidentified variables.
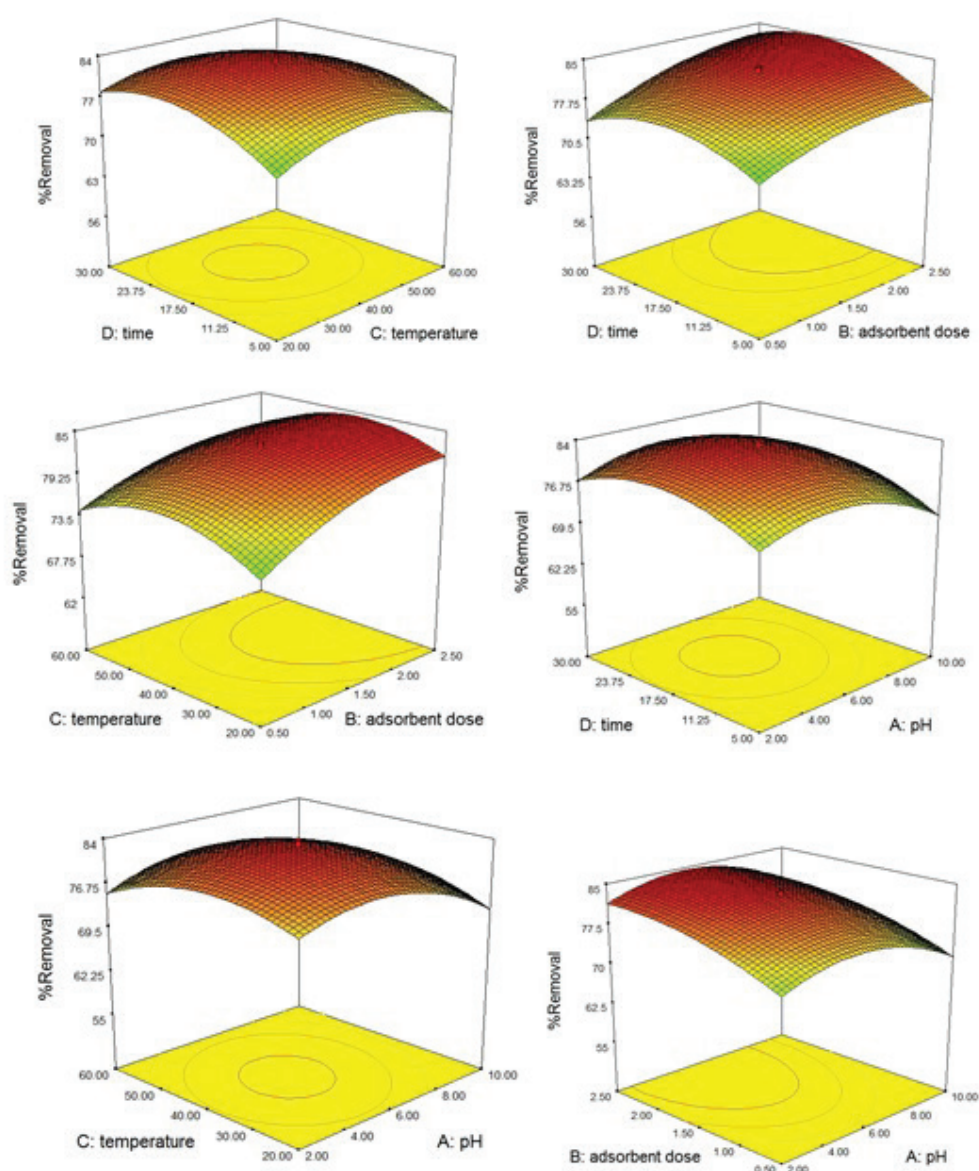


**Fig.1.** Response surface modeling obtained by CCD.
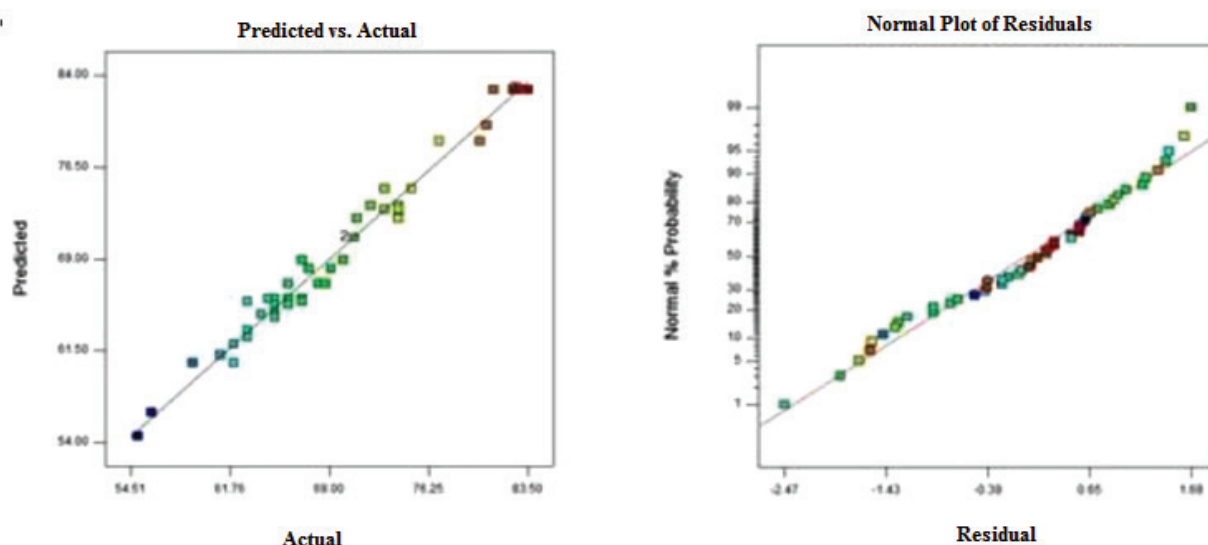
**Fig.2** The normal probability plot of the residuals and parity plot show the correlation between the observed and predicted values

### 3.2. Isotherm study

The adsorption isotherms for metronidazole adsorption on MMWCNTs were obtained with different metronidazole concentrations (1–30 mg L$^{-1}$). The Freundlich and the Langmuir adsorption isotherm models were used for evaluation experimental data. The Langmuir model and Freundlich model are given in **Equation 4 and 5** as follows:

$$\text{Langmuir:} \quad \frac{Cf}{qf} = \frac{1}{bqm} + \frac{Cf}{qm}$$

**(Eq. 4)**

$$\text{Freundlich:} \quad \log qf = \log Kf + \frac{1}{n}\log Cf$$

**(Eq. 5)**

Where C$_f$ (mg L$^{-1}$) is the equilibrium concentration

of metronidazole, q$_f$ (mg g$^{-1}$) is adsorption capacity at equilibrium, q$_m$ (mg g$^{-1}$) is the maximum adsorption capacity, b (L mg$^{-1}$) is a constant related to the adsorption energy, K$_f$ and n are Freundlich constants which characterize a particular adsorption isotherm. All the constants obtained according to the slope and intercept of the related lines and they are listed in **Table 3**. As shown in Table 3, the Langmuir isotherm plot fits better to the experimental adsorption data with higher correlation coefficient (R$^2$ = 0.9994), which expressed that the adsorption of metronidazole ions onto MMWCNTs follows the Langmuir model **(Fig. 3)**.

The q$_m$ and b calculated from the slope and intercept of the regression line are 215.4 mg g$^{-1}$ and 0.52 L mg$^{-1}$, respectively **(Table 3)**. Langmuir model depends on the acceptation of homogeneous distribution of metronidazole molecules on to surface of adsorbent.

**Table 3.** Adsorption isotherm parameters of Langmuir and Freundlich models for adsorption of the metronidazole on the MMWCNTs

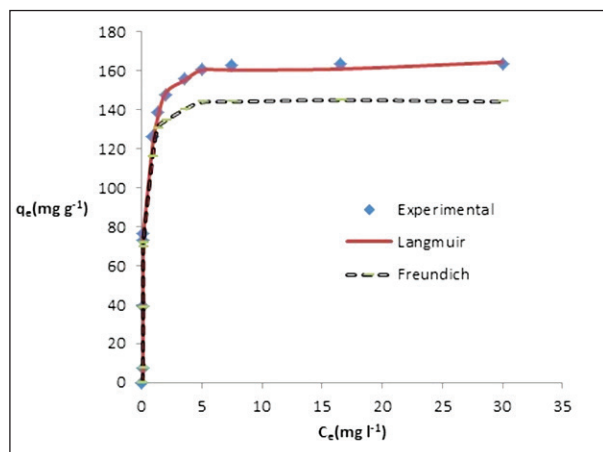| Langmuir isotherm | | | Ferundlich isotherm | | |
|---|---|---|---|---|---|
| q$_m$(mg g$^{-1}$) | b(L mg$^{-1}$) | R$^2$ | K$_f$(l g$^{-1}$) | n | R$^2$ |
| 215.14 | 0.52 | 0.991 | 65.815 | 2.063 | 0.879 |

**Fig.3.** Fitting results of Langmuir and Ferundlich models with experimental data for adsorption of the metronidazole on the MMWCNTs

### 3.3. Desorption and reusability study
Desorption studies of metronidazole were carried out by using different volume of methanol containing NaOH 1% as eluent solvent. For desorption studies, when adsorption of metronidazole was completed, the adsorbent was magnetically separated and washed with deionized water. Then, (0.5-5) mL of the eluent was added to the adsorbent. After 30 min samples were collected to evaluate the metronidazole recoveries. Based on results, the best volume of eluent with high recovery of metronidazole was obtained by 2 mL. To assess the reusability and stability of the adsorbent, the adsorption–desorption experiment with eluent (methanol containing NaOH 1%) was

repeated with 30 mg $L^{-1}$ metronidazole several cycles. After 15 cycles, the adsorption capacity of the MMWCNTs decreases from 163 to 87 mg $g^{-1}$. This result shows that the adsorbent can be applied effectively in a real process such as pharmaceutical industries wastewater treatment. Moreover, in order to investigate the inter-day validation of the results, the method was used for the determination of metronidazole (30.0 mg $l^{-1}$) in three consecutive days by HPLC, and the Relative Standard Deviation percent was found to be 4.1%. These results indicate that MMWCNTs are usable and stable for the extraction of metronidazole and the method has high reproducibility and repeatability for the determination and extraction of the antibiotics by HPLC.

### 3.4. Application of proposed methods to real sample
To verify the potential application of proposed method to real samples, the adsorption performance within real wastewater that spiked with different amount of metronidazole in optimum condition that obtained from model is also provided in **Table 4**. As expected, magnetic carbon nanotubes therefore show high removal efficiency (95-102 %) for the tested concentrations. It must be noted; the adsorbent cannot completely removed the metronidazole due to the competition between other substances which is also present in the wastewater.

**Table 4.** Adsorption of metronidazole in wastewater samples
by spiking of metronidazole at different concentration by HPLC (mg $L^{-1}$)

| Sample | Added | Initial concentration | *Found | %Removal Efficiency |
|--------|-------|----------------------|--------|---------------------|
| **Sample A** | ----- | 100 | 3.7 ± 0.2 | 96.3 |
| | 50 | 150 | 5.2 ± 0.3 | 96.5 |
| **Sample B** | | 200 | 10.8 ± 0.5 | 94.6 |
| | 100 | 300 | 14.2 ± 0.7 | 95.3 |
| **Sample C** | | 30 | 0.5 ± 0.03 | 98.3 |
| | 30 | 60 | 1.9 ± 0.9 | 96.8 |

*Mean of three determinations of samples ± confidence interval (P = 0.95, n =8)

## 4. Conclusions

In this study, a central composition design (CCD) was used for evaluation of four variables of adsorption (time, temperature, initial ion concentration and amount of adsorbent) for Metronidazole by $Fe_3O_4@$ MWCNTs. Quadratic model was developed to correlate the variables to the response. Through the analysis of response surfaces, adsorbent dose, pH and adsorption time were found to have significant effects on removal efficiency, whereas adsorbent dose showed that most significant. All removal analysis of Metronidazole were done based on $Fe_3O_4@$MWCNTs by HPLC in water and wastewater samples. Optimization was carried out and the experimental values were found to agree satisfactorily with the predicted values. Isotherm study of process showed maximum adsorption capacity of $Fe_3O_4@$MWCNTs for removal of metronidazole (215 mg $g^{-1}$). Also, application of proposed method for real wastewater sample showed high removal efficiency of proposed sorbent.

## 5. Acknowledgement

## 6. References

[1] W.Yan, Y. Xiao, W. Yan, The effect of bioelectrochemical systems on antibiotics removal and antibiotic resistance genes: a review, Chem. Eng. J. 358 (2019) 1421-1437.

[2] J. Xu, Z. Cao, Y. Wang, Y. Zhang, X. Gao, Distributing sulfidized nanoscale zerovalent iron onto phosphorus-functionalized biochar for enhanced removal of antibiotic florfenicol, Chem. Eng. J., 359 (2019) 713-722.

[3] T. D. Pham, T. Ngan Vu, H. L. Nguyen, Adsorptive removal of antibiotic ciprofloxacin from aqueous solution using protein-modified nanosilica, Polymers, 12 (2020) 57.

[4] N. Hanna, P. Sun, Q. Sun, Presence of antibiotic residues in various environmental compartments of Shandong province in eastern China: its potential for resistance development and ecological and human risk, Environ. Int., 114 (2018) 131-142.

[5] R. Pallares-Vega, Determinants of presence and removal of antibiotic resistance genes during WWTP treatment: a cross-sectional study, Water Res., 161 (2019) 319-328.

[6] T. Ariyanto, R. Aprillia G. Sarwendah, Y. Maulana, Modifying nanoporous carbon through hydrogen peroxide oxidation for removal of metronidazole antibiotics from simulated wastewater, Processes, 7 (2019) 835.

[7] M. L. Tran, C.-C. Fu, R.-S. Juang, Removal of metronidazole and amoxicillin mixtures by UV/TiO 2 photocatalysis: an insight into degradation pathways and performance improvement, Environ. Sci. Pollut. Res., 26 (2019) 11846-11855.

[8] Y. Zhou, T. Wang, D. Zhi, Applications of nanoscale zero-valent iron and its composites to the removal of antibiotics: a review, J. Mater. Sci., (2019) 1-18.

[9] Zhang, Shuai, et al. "A review of bioelectrochemical systems for antibiotic removal: Efficient antibiotic removal and dissemination of antibiotic resistance genes, J. Water Process Eng., 37 (2020) 101421.

[10] S.Talwar, A. K. Verma, V. K. Sangal, U. L. Štangar, Once through continuous flow removal of metronidazole by dual effect of photo-Fenton and photocatalysis in a compound parabolic concentrator at pilot plant scale, Chem. Eng. J. 388(2020) 124184.

[11] B. Davoud, A. Dokht Khatibi, K. Chandrika, Antibiotics removal from aqueous Solution and pharmaceutical wastewater by adsorption process: A review, Int. J. Pharm. Investigate., 10 (2020) 106-111.

[12] H. Cai, T. Zhao, Z. Ma, J. Liu, Efficient Removal of Metronidazole by the Photo-

Fenton Process with a Magnetic Fe3O4@ PBC Composite, J. Environ. Eng., 146 (2020) 04020056.

[13] K. Hasani, A. Peyghami, A. Moharrami, The efficacy of sono-electro-Fenton process for removal of Cefixime antibiotic from aqueous solutions by response surface methodology (RSM) and evaluation of toxicity of effluent by microorganisms, Arab. J. Chem. 13 (2020) 6122-6139.

[14] M. Galedari, M. Mehdipour Ghazi, S. R. Mirmasoomi, Photocatalytic process for the tetracycline removal under visible light: Presenting a degradation model and optimization using response surface methodology (RSM), Chem. Eng. Res. Design, 145 (2019) 323-333.

[15] S. Gholamiyan, M. Hamzehloo, F. Abdolhadi, RSM optimized adsorptive removal of erythromycin using magnetic activated carbon: Adsorption isotherm, kinetic modeling and thermodynamic studies, Sustain. Chem. Pharm., 17 (2020) 100309.
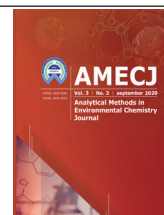
# In-vitro speciation of molybdenum (II, VI) in human biological samples based on thiol-functionalized mesoporous silica nanoparticles and hexyl-methylimidazolium tris-pentafluoroethyl-trifluorophosphate

**Roya Ashouri [a,b] and Seyed Alireza Hajiseyed Mirzahosseini [b,*]**

[a]*Department of Environmental science, Science and Research Branch, Islamic Azad University, Tehran, Iran*
[b]*Department of Environmental Engineering, Faculty of Natural Resources and Environment, Science and Research Branch, Islamic Azad University, Tehran, Iran*

**ABSTRACT**

Molybdenum (Mo) ions enter to human body from the diet or drinking waters and have a potentially toxic effect on human. The thiol-functionalized mesoporous silica nanoparticles (HS-MSNPs) was used for determination and speciation of Mo (II, VI) in human biological samples by dispersive ionic liquid-micro-solid phase extraction (DIL-μ-SPE) coupled to electrothermal atomic absorption spectrometry (ET-AAS). Firstly, the mixture of HS-MSNPs (15 mg), the hydrophobic ionic liquid (1-Hexyl-3-methylimidazolium tris(pentafluoroethyl) trifluorophosphate; [HMIM][T(PFE)PF$_3$]) and acetone injected to 10 mL of human blood and serum samples. After shaking for 5 min, the Mo(II) and Mo(VI) ions were extracted with thiol group of MSNPs at pH 6 and 2, respectively and collected through IL in bottom of conical tube by centrifuging. Then, the Mo(II,VI) ions were back-extracted from HS-MSNPs with elent based on changing pH, and remained solutions were determined by ET-AAS after dilution with DW up to 0.5 mL, separately. So, the total of Mo(T-Mo) was simply calculated by the summation of Mo(II) and Mo(VI) content. In optimized conditions, the linear range (LR), the limit of detection and enrichment factor (EF) for Mo(II) and Mo(VI) were obtained (0.41-3.82 μg L$^{-1}$; 0.48–4.55 μg L$^{-1}$), (0.1 μg L$^{-1}$; 0.12 μg L$^{-1}$) and (19.6; 16.5) for 10 mL of human blood samples, respectively (Mean of RSD%=3.3). At optimized pH, the adsorption capacities of the HS-MSNPs for Mo(II) and Mo(VI) was obtained 68.7 mg g$^{-1}$ and 55.8 mg g$^{-1}$, respectively. In purposed study, a new analytical method for rapid speciation and determination of trace amount of Mo (II, VI) was used in human blood and serum samples. The developed method was successfully validated by ICP-MS analysis.

## 1. Introduction

Molybdenum as inorganic material belongs to transition metal. Molybdenum (Mo) exists in environment with different oxidation numbers and complex compounds. The high concentration of Mo has toxic effects in humans and cause to many diseases in human body like central nervous system,

Corresponding Author: Alireza Hajiseyed Mirzahosseini
Email: mirzahosseini@gmail.com
https://doi.org/10.24200/amecj.v3.i03.115

liver and renal disorder. Molybdenum has low concentration in seawater and high concentrations in kidney, liver, and adrenals of human [1]. In human body, the concentration of Mo in serum is almost 0.6 μg $L^{-1}$ and depends on dietary intake. Normal serum concentrations are between 0.3-2.0 μg$L^{-1}$. Normal whole blood concentrations are between 0.6-4.0 μg $L^{-1}$ in unexposed peoples and 1.2-4.8 μg $L^{-1}$ in exposed peoples [2]. The, molybdate can be chemically adsorbed onto positively charged iron, aluminium or manganese oxides [3]. Therefore, high molybdenum intake causes a secondary copper deficiency and is called molybdenosis or hypocuprosis [4]. Molybdenum toxicity caused to diarrhea, anorexia, graying of hair, anemia and these symptoms are readily reversed by copper supplementation. The tetrathiomolybdates interact with copper and caused to the treatment of copper disorders such as Wilson's disease [5]. The intracellular pool of cysteine is relatively small as compared to the glutathione (GSH) [6]. By oxidizing, cysteine is oxidized to cystine and so, the cysteine in plasma has low concentration between 10–25 μM as compared to cystine concentration from 50 to 150 μM [7]. The cells have different transport for cysteine (Cys) and cystine by different membrane carriers and both of them can be reaction with Mo and complex with Mo as R-Mo [8]. Molybdenum cofactor deficiency (Moco) is a metabolic disorder and cause to defects in the biosynthesis of Moco leading to loss of activity of Mo enzymes [9]. Molybdenum has seen in brain and can be measured in urine, blood, and cerebrospinal fluid (CSF). Mo(II) locates in the mitochondria and cytoplasm of cells. Mo helps to involve the metabolism pathway of sulfate and sulfite oxide deficiency. Mo(VI) as $MoO_4^{2-}$ or $MoO_3$ binds strongly to amino acids, enzymes (aldehyde Oxidase, sulfite oxidase and xanthine oxidase), metallothionein (MT), molybdenum cofactor (Mo(VI), molybdopterin), cysteine (Cys), proteins (Pr) and metabolized in the brain and other tissues. So, the organic Mo(R-Mo) is important in human body and must be determined [10-12]. Many developed methods included,

flame atomic absorption spectrometry (F-AAS) [13], the stripping voltammetry [14], the UV visible spectrophotometer [15-17] were used for determination Mo in different matrixes such as water and human biological samples. As difficulty matrix in human blood samples, we have to use the extraction techniques for preparation of human blood samples. The ionic liquids (ILs) as an organic salts have the various advantages such as thermal stability, high viscosity and good solvent for separation phase. The ILs as a green solvent were used for extraction or separation ions from liquid phases. Recently, the sample preparation such as liquid-liquid microextraction (LLME) [15, 17], flow injection chemiluminescence method combined with controlled potential electrolysis technique [18] and solid phase extraction based on inductively coupled plasma-optical emission spectrometry (ICP-OES (SPE) [19-21] reported for extraction Mo from samples.

In this study, the speciation of Mo(II) and Mo(VI) in human blood samples was obtained based on HS-MSNPs nanostructure by DIL-μ-SPE procedure. The concentration of Mo was determined by ET-AAS and hydrophobic Ionic liquid (1-Hexyl-3-methylimidazolium tris (pentafluoroethyl) trifluorophosphate; $[HMIM][T(PFE)PF_3])$ can be used for separating and collecting of HS-MSNPs adsorbent from liquid phase. In optimized conditions, a simple, fast and sensitive procedure was demonstrated for speciation and determination of trace Mo(II) and Mo(VI) in human biological samples.

## 2. Experimental
### 2.1. Instruments
Determination of Mo was performed with a GBC atomic absorption spectrometer (GBC 932–HG3000- Australia) equipped with a graphite furnace module (GF-AAS) and deuterium-lamp background corrector. A hollow cathode lamp of Mo with wavelength of 313.3 nm (7 mA, and 0.2 nm slit) was used. The temperature programming adjusted as the ash and atomize points of 1200°C and 2700°C, respectively. Argon is the preferred as

a carrier gas for Mo with flowrate of 0.4 ng mL$^{-1}$. The concentration of standard solutions of Mo (20 µL, 30 µg L$^{-1}$) has a 0.3 absorption (Abs) by ET-AAS. The pH values of the solutions were measured by a digital pH meter (PeakTech, model P5310, China, CAS No: 9027802000). A refrigerated centrifuge, from 1.5 per 2 mL microtubes was used for separation IL from solution. Long and short blood collection tubes for 15 mL and 50 mL of tubes were used with RCF of 2.6×g (4000rpm, model S300TR, Japan). The ultrasonic bath with heating system has been designed for performance, control, durability and reliability to disperse nanoparticles in liquid phase. (Branson, Tomas Scientific, Swedesboro, U.S.A.). The crystal structure studies of the solids were carried out by X-ray diffractions (PW 1840, Phillips X-ray diffractmeter, Netherland) with Cu-K$_\alpha$ radiation source.

## 2.2. Reagents

All reagents with high purity and analytical grade were purchased from Merck (Darmstadt, Germany). The ethanol, acetone and toluene all were purchased from Merck, Germany. All aqueous solutions were prepared in ultra-pure deionized water from water purification system (Millipore, Bedford, MA, USA). The powder standard of MoO$_3$ (VI) (CAS: 1313-27-5) was purchased from Sigma, Aldrich, Germany (1 g of powder dissolved in one liter of DW as 1000 mg L$^{-1}$ in 1% nitric acid). The Molybdenum (II) acetate dimer as di-molybdenum tetraacetate (CAS: 14221-06-8) was purchased from Merck, Germany. The general procedure for synthesis of thiol-functionalized bimodal mesoporous silica nanoparticles (HS-MSNPs) was done in RIPI, Iran. The reagents; HCl, CH$_3$COOH, tetraethyl ortho-silicate (TEOS, CAS: 8006580025), cetyltrimethylammonium bromide (CTAB, CAS: 57-09-0), and 3-mercaptopropyltriethoxysilane was purchased from Sigma Aldrich (Darmstadt, Germany).1-Hexyl-3-methylimidazolium hexafluorophosphate ([HMIM][PF6]; CAS No.: 304680-35-1),1-Hexyl-methylimidazolium tris(pentafluoroethyl) trifluorophosphate ([HMIM]

[T(PFE)PF$_3$]; CAS No: 713512-19-7) and 1-Butyl-3-methylimidazolium hexafluorophosphate ([BMIM][PF6]; CAS No: 174501-64-5) purchased from Sigma, Germany.

## 2.3. Synthesis of thiol functionalized MSNPs

The general procedure for synthesis of MSNPs is the atrane route, in which the presence of the polyalcohol is the key to balancing the hydrolysis and condensation reaction rates [22]. After preparation MSNPs, 1.4 g of 3-Mercaptopropyltriethoxysilane (C$_9$H$_{22}$SO$_3$Si) and 1.5 g of pure MSNPs were added to appropriate volume of toluene and then the mixture was refluxed for two days and followed by filtering and washing of product with ethanol and water for many times. The thiol functionalized MSNPs (HS$_-$MSNPs$_)$ was created after drying at 80ºC for 8-10 h.

## 2.4. Characterization

Functional groups of SH on MSNPs were analyzed by Fourier transform infrared spectrophotometer (FTIR, IFS 88, Bruker Optik GmbH, Germany) using KBr pelleting method in the 4000–300 cm$^{-1}$. The scanning/ transmission electron microscopy was obtained in this study. Scanning electron microscopy (SEM, Phillips, PW3710, Netherland) was used for morphology and surface image analysis of the sorbents. The nanoparticles size for HS$_-$MSNPs was examined by transmission electron microscopy (TEM, CM30, Philips, Netherland). The X-ray diffraction (XRD) patterns continued with the Shimadzu XRD which are designed with the concept of provide solution to XRD analysis by ease of use and versatility. Basic system with high precision goniometer can be varied with optional items to adapt to the purpose (MAXima-X XRD-7000).

## 2.5. DIL-µ-SPE Procedure

The DIL-µ-SPE Procedure was performed with 10 mL of human blood and serum samples. For adjusting of the parameters, the standard aqueous solution containing Mo(II) and Mo(VI) with concentration in the range of 0.5-3.0 µg L$^{-1}$

was used in optimum pH of 6 and 2 with buffer solution, respectively before moved to centrifuge conical tube. After adjusting pH, the HS MSNPs (15 mg), 0.15 g of [HMIM][T(PFE)PF$_3$] and 200 μL of acetone were mixed and rapidly injected by a syringe into the sample solution. Then, the sample was dispersed in solution by ultrasonic bath for 7 min at room temperature (50 kHz, 100 W). Mo(II) and Mo(VI) species were extracted and preconcentrated by HS-MSNPs at pH of 6 and 2, separately. The loaded sorbent (Mo—HS-MSNPs) was collected with IL by centrifuging at 4000 rpm for 5 min. The adsorbed Mo(II) and Mo(VI) on HS-MSNPs/IL was back-extracted in different pH (acidic pH=2.5 for Mo$^{2+}$ and pH=7.5 for Mo$^{6+}$) and concentration of Mo(II) and Mo(VI)

ions determined by ET-AAS ( Fig. 1). lso, the total Mo was calculated by the summation of Mo(II) and Mo(VI) content [Mo(II)+ Mo(VI)]. By DIL-μ-SPE Procedure, the matrix effect in human blood and serum samples were achieved by ratio of extracted Mo(II) or Mo(VI) in human blood sample to standard solution as a matrix-free solution which was shown in below equation. Matrix Effect (%) = (Signal of the Mo extraction in blood / signal of Standard solution)×100

## 3. Results and discussion
### 3.1. The XRD and FT-IR analysis
The XRD patterns of calcined HS-MSNPs and MSNPs are shown in Figure 2. There are three resolved diffraction peaks in XRD patterns,
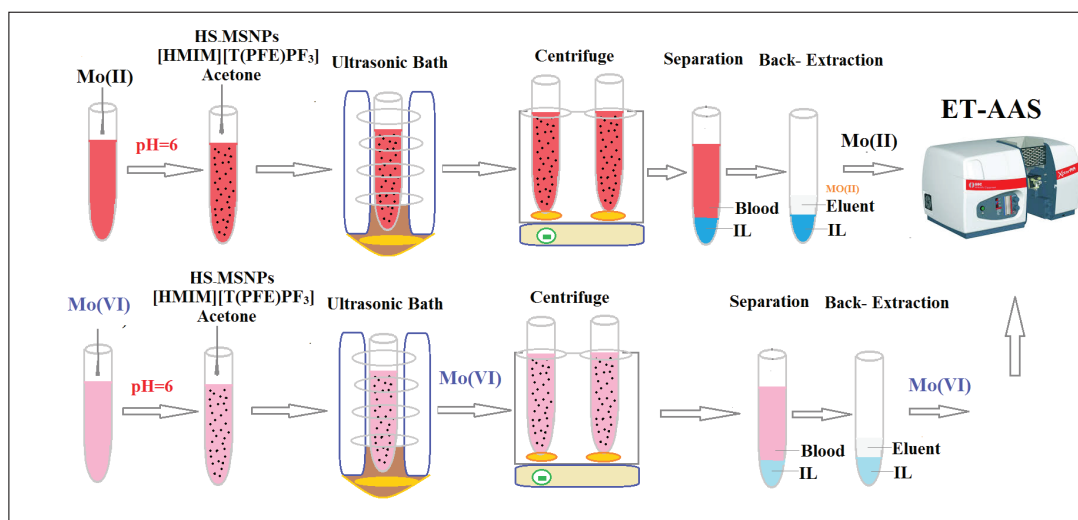


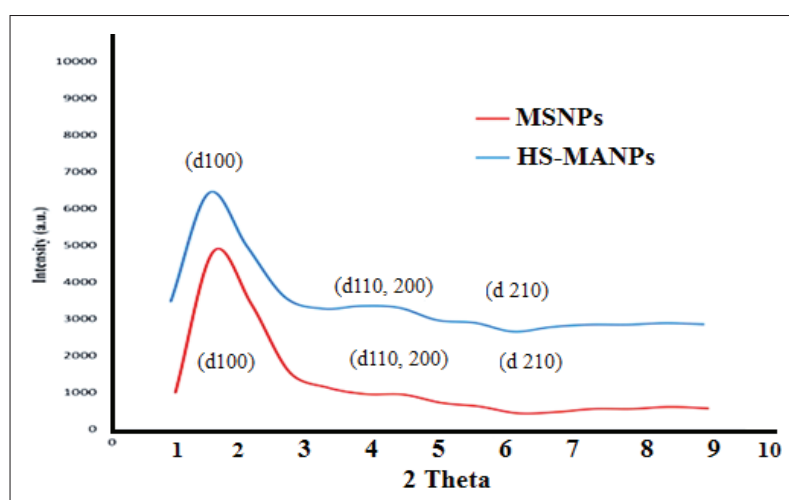**Fig. 1.** The speciation of Mo(II) and Mo(VI) based on HS-MSNPs by DIL-μ-SPE Procedure



**Fig.2.** The XRD patterns of of MSNPs and HS- MSNPs

which can be indexed as the (100), (110), (200) and (210) reflections associated with hexagonal symmetry (d110 and d200 were overlapped with each other). After the attachment of HS on the silica wall of MSNPs, the main three diffraction peaks are still clear and similar which means that functionalization of HS on MSNPs did not had worth effect on the structural order of MSNPs (Fig. 2). The FTIR spectra patterns of MSNPs and HS- MSNPs was shown in Figure 3. A peak of absorption about 3550 $cm^{-1}$ and 1640 $cm^{-1}$ related to OH bonding, the peak at 1100 $cm^{-1}$ showed silicon dioxide ($SiO_2$) and peak at 2565

$cm^{-1}$ was confirmed the SH group on the walls of MSNPs.

### 3.2. SEM and TEM imaging

The SEM was performed to illustrate the morphology and particle size distribution of the calcined HS-MSNPs. As shown in Fig. 4a, HS-MSNPs has a highly porous morphology and the mesoporous silica particles are in nanometer range (40 nm). Moreover, functionalization of HS did not lead to bulky silica nanoparticles. TEM image also illustrates the size and pore structure of HS-MSNPs. As shown in Fig. 4b, the mesoporous
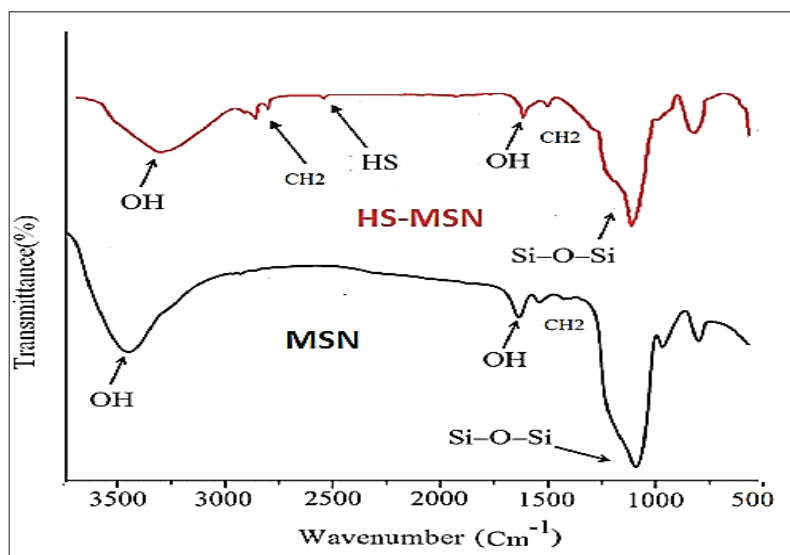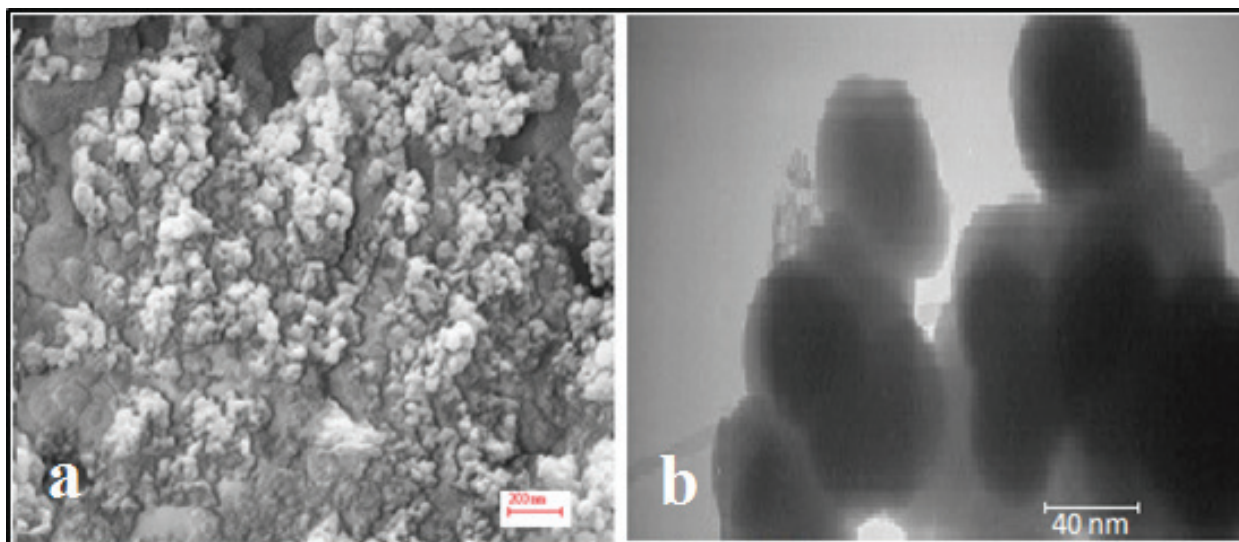


**Fig. 3.** The FT-IR spectra patterns of MSN and HS- MSN
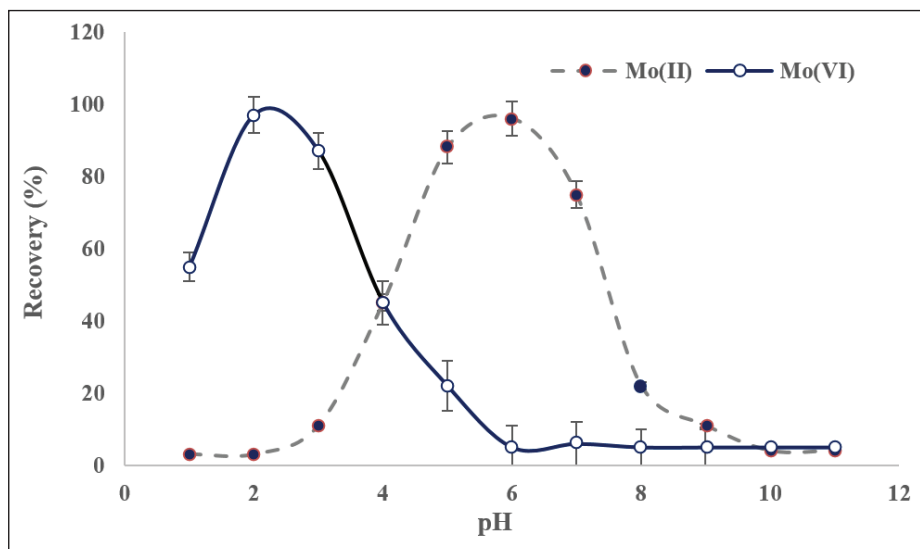


**Fig. 4.** The SEM (a) and TEM (b) of HS-MSNPs

**Fig. 5.** The effect of pH on speciation of Mo(II) and Mo(VI) ions by HS-MSNPs adsorbent

are clearly visible in the silica nanoparticles and particle size of the samples is in nanometer range around 25 to 50 nm.

### 3.3. The pH and sample volume optimizations
By DIL-μ-SPE technique for determination and speciation of Mo in human blood samples, the pH must be studied and optimized. The pH effect on quantitative recoveries of Mo(II) and Mo(VI) ions by changing of the surface charge of the thiol group on HS-MSNPs adsorbent as the negative or positive charges which can attract with Mo(II) and Mo(VI) ions. So, the influence of sample pH on the extraction efficiency of Mo(II) and Mo(VI) ions was investigated in pH ranges from 1 to 11 by using favorite buffered solutions and containing 0.4-3.0 μg L$^{-1}$ of Mo(II) and Mo(VI). The results showed us, the Mo(II) and Mo(VI) ions were efficiently extracted at pH of 5-7 and pH of 1-3. Therefore, the pH 2 and 6 was used as optimum pH for extraction of Mo(II) and Mo(VI) ions from blood samples by HS-MSNPs adsorbent (Fig. 5). Also, the effect of blood sample volume for extraction of Mo(II) and Mo(VI) ions based on HS-MSNPs adsorbent was studied from 2-25 mL. The results of extraction showed us, the best recovery was obtained for 12 mL of blood samples. So, 10 mL of blood samples was used for further study.

### 3.4. Speciation mechanism
The thiol functionalized mesoporous silica nanoparticles (HS-MSNPS) can be adsorbed Mo(II) and Mo(VI) ions from blood samples. The thiol groups can be deprotonated (SH$^-$) more than pH=5 and Mo(II) can be absorbed as a rule of opposite charge at optimized pH. So, the interaction of HS groups of sorbent with cationic form of Mo$^{2+}$ was occurred at pH 5-7. In addition, the positive charge of thiol (SH2$^+$) was obtained at acidic pH (1-3) and so, Mo(VI) anions adsorbed on HS-MSNPS by positive charged of thiol group in human blood samples. Therefore, the pH of 2 and 6 was selected as optimum pH for extraction and speciation Mo(II) and Mo(VI) ions from blood samples by DIL-μ-SPE procedure.

### 3.5. Effect of the amount of adsorbent and ILs
In this work, the effect of HS-MSNPs mass on the recoveries of Mo(II) and Mo(VI) ions was investigated. So, the various amounts of HS-MSNPs in the ranges of 2 to 20 mg of adsorbent were studied and optimized. The results showed us, the extraction efficiency for speciation of Mo(II) and M0(VI) ions were obtained more than 14 mg of HS-MSNPs. By same conditions, the recovery of extraction for MSNPs was obtained less than 28% and 23% for Mo(II) and Mo(VI) ions, respectively. So, 15 mg of HS-MSNPs were used or further works (Fig. 6).
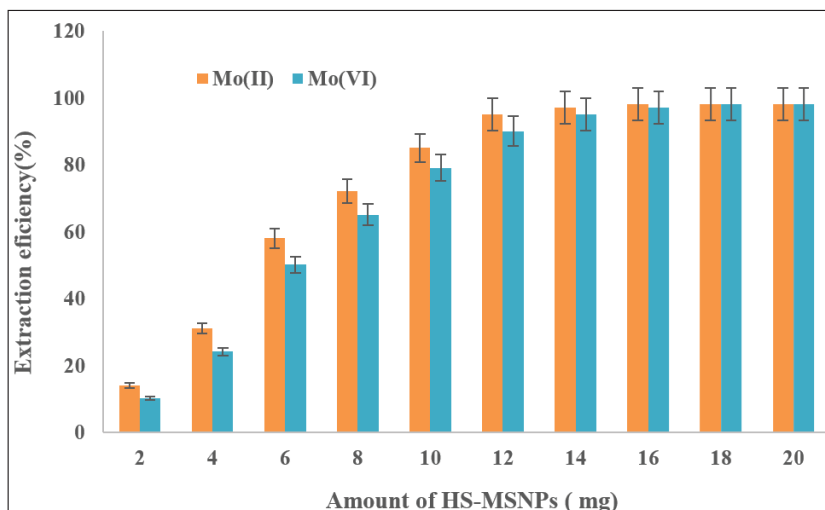
**Fig. 6.** The effect HS-MSNPs adsorbent on speciation of Mo(II) and Mo(VI) ions by DIL-µ-SPE Procedure
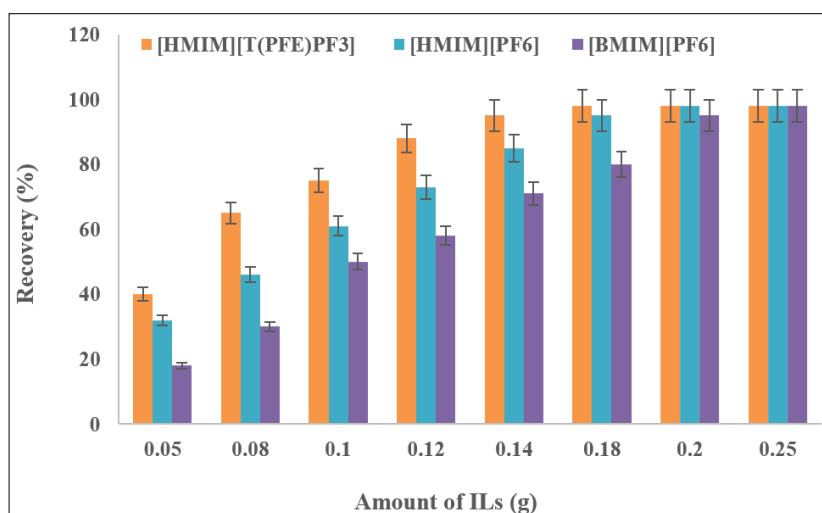


**Fig. 7.** The effect of ILs on speciation of Mo(II) and Mo(VI) ions by DIL-µ-SPE Procedure

Moreover, the effect of kind and amount of ILs were studied by proposed procedure. So, the different amount of hydrophobic ionic liquids such as; 1-Hexyl-3-methylimidazolium hexafluorophosphate; [HMIM][PF6], Hexyl-methylimidazoliumtris(pentafluoroethyl) trifluorophosphate; [HMIM][T(PFE)PF$_3$] and Butyl 3- methyl imidazolium hexafluorophosphate; [BMIM][PF6] were studied between 0.05-0.25 g. The results showed, 0.15 g of [HMIM][T(PFE)PF$_3$] had the favorite recovery more than 95% as compared to others. The recovery for extraction Mo(II) and Mo(VI) ions for 1-Hexyl-3-methylimidazolium hexafluorophosphate and 1-Butyl-3-methylimidazolium hexafluorophosphate

were obtained 79% and 74%, respectively. Therefore, 0.15 g of [HMIM][T(PFE)PF$_3$] was selected as optimum amount of IL for this work **(Fig. 7)**.

### 3.6. Effect of matrix

The effect of interference ions concentration for extraction of Mo(II) and Mo(VI) ions must be studied by DIL-µ-SPE Procedure. So, the effect of some interfering ions for the determination of Mo(II) and Mo(VI) ions were investigated. The procedure was done for 10 ml of sample containing 3.5 µgL$^{-1}$ of Mo(II) and Mo(VI) ions with different concentration of interference ions between 0.5-2 mg L$^{-1}$. Based on results, the interference ions in blood samples such

as $Cu^{2+}$, $Mn^{2+}$, $Mg^{2+}$, $Zn^{2+}$, $CO_3^{2-}$, $PO_4^{3-}$ and $HCO3^-$ do not interfere for extraction of Mo(II)/ Mo(VI) ions under optimized conditions **(Table 1)**.

### 3.7. Validation in real samples

The DIL-µ-SPE method was used to determine Mo(II) and Mo(VI) ions in 10 mL of human blood samples.

For validation in real samples, the serum and blood samples were spiked to demonstrate the accuracy and precision of the method for determination of Mo(II) and Mo(VI) ions. The spiked samples is satisfactorily recoveries between 95-102% and was confirmed using addition method **(Table 2)**.

By procedure, the calibration curve for Mo(II) and

**Table 1.** The effect of interferences ions on extraction of Mo(II) and Mo(VI) ions in blood samples by DIL-µ-SPE Procedure

| Blood Interfering ions (BII) | Mean ratio ($C_{BII}$ /$C_{Mo}$) | | Recovery (%) | |
| --- | --- | --- | --- | --- |
| | Mo(II) | Mo(VI) | Mo(II) | Mo(VI) |
| $Mn^{2+}$, $Cd^{2+}$, | 800 | 650 | 97.7 | 98.2 |
| $Cr^{3+}$, $Al^{3+}$, | 700 | 700 | 98.8 | 96.5 |
| $V^{3+}$ | 850 | 500 | 97.1 | 97.6 |
| $Ca^{2+}$, $Mg^{2+}$ | 900 | 1000 | 98.9 | 99.2 |
| $Na^+$, $K^+$, | 1100 | 1100 | 98.2 | 98.5 |
| $Zn^{2+}$, $Cu^{2+}$ | 750 | 600 | 97.5 | 96.4 |
| $I^-$, $Br^-$, $F^-$, $Cl^-$ | 1200 | 1100 | 99.4 | 98.3 |
| $CO_3^{2-}$, $SO_3^{2-}$ | 900 | 1000 | 97.5 | 98.6 |
| $HCO_3^-$, $PO_4^{3-}$ | 800 | 700 | 97.0 | 96.4 |
| $Ni^{2+}$, $Co^{2+}$ | 450 | 600 | 95.7 | 97.2 |
| $Pb^{2+}$ | 350 | 500 | 98.1 | 98.4 |
| $Hg^{2+}$ | 50 | 80 | 96.3 | 97.2 |

**Table 2.** Validation of methodology based on HS-MSNPs adsorbent for speciation of Mo(II) and Mo(VI) ions in serum and blood samples by spiking to real samples

| Sample | Added (µg $L^{-1}$) | | Found (µg $L^{-1}$) | | | Recovery (%) | |
| --- | --- | --- | --- | --- | --- | --- | --- |
| | Mo (II) | Mo(VI) | Mo (II) | Mo(VI) | T-Mo | Mo (II) | Mo(VI) |
| Blood A | ----- | ----- | 0.72 ± 0.04 | 0.56 ± 0.03 | 1.28 ± 0.06 | ----- | ----- |
| | 0.5 | ----- | 1.20 ± 0.05 | 0.54 ± 0.02 | 1.74 ± 0.08 | 96.0 | ----- |
| | ----- | 0.5 | 0.69 ± 0.04 | 1.07 ± 0.04 | 1.76 ± 0.09 | ----- | 102 |
| Blood B | ----- | ----- | 1.74 ± 0.03 | 0.83 ± 0.03 | 2.57 ± 0.12 | ----- | ----- |
| | 1.5 | ----- | 3.19 ± 0.16 | 0.80 ± 0.04 | 3.99 ± 0.19 | 96.6 | ----- |
| | | 1.0 | 1.76 ± 0.04 | 1.81 ± 0.05 | 3.57 ± 0.17 | ----- | 98 |
| Serum C | ----- | ----- | 0.92 ± 0.05 | 2.05 ± 0.11 | 2.97 ± 0.16 | ----- | ----- |
| | 1.0 | ----- | 1.89 ± 0.09 | 1.99 ± 0.09 | 3.88 ± 0.21 | 97.0 | ----- |
| | | 2.0 | 0.89 ± 0.04 | 3.98 ± 0.22 | 4.87 ± 0.25 | ----- | 96.5 |
| Serum D | ----- | ----- | 2.12 ± 0.11 | 1.33 ± 0.06 | 3.45 ± 0.18 | ----- | ----- |
| | 1.5 | ----- | 3.60 ± 0.17 | 1.29 ± 0.05 | 4.89 ± ·,24 | 98.6 | ----- |
| | | 1.5 | 2.16 ± 0.12 | 2.76 ± 0.15 | 4.92 ±.0.25 | ----- | 95.3 |

[a] Mean of three determinations ± SD (P= 0.95, n=5)

**Table 3.** Validation of results for determination of Mo(II) and Mo(VI) ions in standard solutions by ICP-MS analysis and compared to DIL-μ-SPE method

| Sample | CRM (μg L$^{-1}$) | | Found [a] (μg L$^{-1}$) | | Recovery (%) | |
|---|---|---|---|---|---|---|
| | Mo (II) | Mo(VI) | Mo (II) | Mo(VI) | Mo (II) | Mo(VI) |
| Standard | 1.56 ± 0.01 | 2.07 ± 0.04 | 1.51± 0.08 | 1.97 ± 0.12 | 96.8 | 95.2 |
| Standard | 3.25 ± 0.02 | 1.84 ± 0.03 | 3.27± 0.14 | 1.79 ± 0.09 | 100.6 | 97.3 |

[a] Mean of three determinations ± SD (P= 0.95, n=5)

**Table 4.** Validation of results for determination of total Mo(T-Mo) ions in blood and serum samples by ICP-MS analysis and compared to DIL-μ-SPE method

| Sample | ICP-MS (μg L$^{-1}$) T-Mo | | [a]DIL-μ-SPE (μg L$^{-1}$) T-Mo | | Recovery (%) T-Mo | |
|---|---|---|---|---|---|---|
| | Blood | Serum | Blood | Serum | Blood | Serum |
| Sample A | 2.43 ± 0.03 | 2.72 ± 0.05 | 2.33± 0.11 | 2.75 ± 0.14 | 95.8 | 101.1 |
| Sample B | 1.17 ± 0.02 | 1.29 ± 0.03 | 1.15 ± 0.05 | 1.24 ± 0.07 | 98.3 | 96.1 |
| Sample C | 3.36 ± 0.07 | 3.71 ± 0.08 | 3.25 ± 0.14 | 3.62 ± 0.16 | 96.7 | 97.6 |

[a] Mean of three determinations ± SD (P= 0.95, n=5)

Mo(VI) ions was linear between 0.41-3.82 μg L$^{-1}$ and 0.48–4.55 μg L$^{-1}$ , respectively. In addition, the ICP-MS analysis was used for speciation of Mo(II) and Mo(VI) ions in standard solutions **(Table 3)**. Also, the ICP-MS analysis was used for determination of total Mo(T-Mo) in human blood and serum samples as certified reference material (CRM) which compared to DIL-μ-SPE method. The ICP-MS analysis confirmed the accuracy and precision of proposed procedure for determination and speciation of Mo(II) and Mo(VI) ions in human blood samples **(Table 4)**.

## 4. Conclusions

In this research, a simple, sensitive, accurate and precise method was used to demonstrate the separation /speciation and determination of trace Mo(II) and Mo(VI) ions in human blood samples. By DIL-μ-SPE procedure, the effect of main factors on extraction process such as pH and amount of adsorbent and IL were optimized. The mean of enrichment factor and recovery was obtained 18.05 and 98.6 %, respectively. The mean of LOD and LR was achieved 0.11 μg L$^{-1}$ and between 0.445-4.19 μg

L$^{-1}$, respectively in optimized pH. Based on Table 4, the results of DIL-μ-SPE method for determination of total Mo in blood and serum samples were comparable to ICP-MS technique. The adsorption capacities of the HS-MSNPs and MSNPs for total Mo was obtained 62.3 mg g$^{-1}$ and 18.2 mg g$^{-1}$, respectively. Also, the relative standard deviation (RSD%) for speciation and determination of trace Mo(II) and Mo(VI) ions in human blood samples was obtained 2.3 and 2.8, respectively. The validation of the methodology was confirmed by spiking to real samples and ICP-MS analysis in standard solution or human blood samples.

## 5. Acknowledgment

## 6. References

[1] J. L. Burguera, M. Burguera, Molybdenum in human whole blood of adult residents of the Merida State (Venezuela), J. Trace Elem. Med. Biol., 21 (2007) 178–183.

[2] J. Oh, S. H. Shin, R. Choi, S. Kim, H. D. Park, S. Y. Kim, S. A. Han, W. J. Koh, and S. Y. Lee, Assessment of 7 trace elements in serum of patients wif nontuberculous mycobacterial lung disease, J. Trace Elem. Med. Biol., 53 (2019) 84-90.

[3] J. R. Turnlund, W. R. Keyes, Plasma molybdenum reflects dietary molybdenum intake, J. Nutr. Biochem., 15 (2004) 90–95.

[4] G. N. George, I. J. Pickering, H. H. Harris, J. Gailer, D. Klein, J. Lichtmannegger, K. H. Summer, Tetrathiomolybdate Causes Formation of Hepatic Copper−Molybdenum Clusters in an Animal Model of Wilson's Disease, J. Am. Chem. Soc., 125 (2003) 1704–1705.

[5] G. J. Brewer, The use of copper-lowering therapy with tetrathiomolybdate in medicine Expert Opin. Investig. Drugs, 18 (2009) 89–97.

[6] C. Picó, F. Serra, Biomarkers of Nutrition and Health: New Tools for New Approaches, J. Nutr., 11 (2019) 1092.

[7] G. Wu, Y. Z. Fang, S. Yang, J. R. Lupton, N. D. Turner, Glutathione metabolism and its implications for health, J. Nutr., 134 (2004) 489–492.

[8] Y. Xiong, Y. Xiong, Y. Wang, Z. Wang, A Zhang, Inhibition of Glutathione Synthesis via Decreased Glucose Metabolism in Stored RBCs, Cell Physiol. Biochem., 51(2018) 2172–2184.

[9] J.L. Johnson M. Duran, Molybdenum cofactor deficiency and isolated sulfite oxidase deficiency, 8th ed. McGraw-Hill, New York, pp. 3163–3177, 2001.

[10] G. Schwarz, A. Ali Belaidi, Molybdenum in human health and disease, Metal Ions Life Sci., 13 (2013) 415-450.

[11] K. Pytlakowska, K. Kocot, M. Pilch, M. Zubko, Ultrasound-assisted dispersive micro-solid phase extraction using molybdenum disulfide supported on reduced graphene oxide for energy dispersive X-ray fluorescence spectrometric determination of chromium species in water, Microchim. Acta,

187 (2020) 542.

[12] G. R.Helz, T. P.Vorlicek, Precipitation of molybdenum from euxinic waters and the role of organic matter, Chem. Geo., 509 (2019) 178-193.

[13] M. Sanchez, D. Gazquez, P. Garcia, Determination of molybdenum by atomic-absorption spectrometry after separation by 5,5'-methylenedisalicylohydroxamic acid extraction and further reaction wif thiocyanate and tin (II), Talanta, 38 (1991) 747-52.

[14] V. Arancibi, C. R. R. Margarit, E. Aliag, E. Stegmann, Fast and highly sensitive method for molybdenum(VI) determination by catalytic adsorptive stripping voltammetry Sensors Actuators B: Chem., 258 ( 2018) 612-620.

[15] M. B. Febrian, T. S. Mulyati, A. Suherman, Spectrophotometic determination of Mo content in 99mTc solution Via Mo-TGA-KSCN complexes formation, Indonesian J. Nucl. Sci. Technol., 19 ( 2018) 71-80.

[16] B. Spasova, C. Kuesters, B. Stengel, Pectrophotometric determination of molybdenum-containing compounds in aqueous glucose solutions, Chem. Eng. Technol., 41(2018) 1776-1782.

[17] S. Bhardwaj, L.R. Kakkar, A highly sensitive and selective spectrophotometeric determination of molybdenum using o -Phenanthroline in presence of thiocyanate, Der Chem Sin., 4 (2013) 32–43.

[18] J. X. Du, J. J. Li, L. J. Yang, J. R. Lu, Sensitive and selective determination of molybdenum by flow injection chemiluminescence method combined with controlled potential electrolysis technique, Anal. Chim. Acta, 481 (2003) 239–244.

[19] S. Hassanpour, M. Taghizadeh, Rapid and Selective Separation of Molybdenum Ions using a novel magnetic Mo(VI) ion imprinted polymer: a study of the adsorption properties, RSC Adv., 6 (2016) 100248–100261.

[20] F. Ardestani, M. H. Hosseini, M. Taghizadeh,

M. R. Pourjavid, M. Rezaee, Synthesis and characterization of nanopore MoVI-imprinted polymer and its application as solid phase for extraction, separation and preconcentration of molybdenum ions from water samples, J. Braz. Chem. Soc., 27 (2016) 1279–1289.

[21] A. Bagheri, M. Behbahani, M. M. Amini, O. Sadeghi, A. Tootoonchi, Z. Dahaghin, Preconcentration and separation of ultra-trace palladium ion using pyridinefunctionalized

magnetic nanoparticles, Microchim. Acta, 178 (2012) 261–268.

[22] H. Shirkhanloo, A. Khaligh, H.Z. Mousavi, A. Rashidi, Ultrasound assisted-dispersive-micro-solid phase extraction based on bulky amino bimodal mesoporous silica nanoparticles for speciation of trace manganese (II)/(VII) ions in water samples. Microchem. J., 124 (2016) 637-645.

# Speciation of chromium in blood samples based on dithioglycerol immobilized on carbon nanotube by dispersive micro solid phase bioextraction

**Nafiseh Esmaeili [a], Eskandar Kolvari [a] and Jamshid Rakhtshah[b,*]**

[a,*] *Department of chemistry, Faculty of Science, Semnan University, Semnan, Iran*
[b,*] *Department of Inorganic Chemistry, Faculty of Chemistry, University of Tabriz, Tabriz, Iran*

**ABSTRACT**

A novel method based on the synthesis of dithioglycerol immobilized on carbon nanotubes (CNTs@DTG) was used for speciation of chromium ($Cr_{III}$ and $Cr_{VI}$) in human blood samples by dispersive micro solid-phase bioextraction (D-μ-SPBE). By procedure, a mixture containing acetone and 1-octyl-3-methylimidazolium hexafluorophosphate ([OMIM][$PF_6$]) and CNTs@DTG were injected into 5 mL of standard and blood sample containing 1.0 μg $L^{-1}$ of $Cr_{III}$ and $Cr_{VI}$ which was diluted with DW up to 10 mL at optimized pH. The Cr (VI) anions and Cr (III) cations were efficiently extracted by HS of CNTs@DTG at pH 2 and 6, respectively (HS.....Cr) and trapped into IL phase at the bottom of the conical tube. Then, Cr (III) and Cr(VI) ions were back-extracted from the IL/ CNTs@DTG to the aqueous phase by changing pH for each of them before determined by electrothermal atomic absorption spectrometry (ETAAS). Total chromium was calculated by summarizing $Cr_{III}$ and $Cr_{VI}$ content. The enrichment factor (EF), linear range and limit of detection (LOD) were obtained 9.85, 0.12-3.88 μg $L^{-1}$ and 30 ng $L^{-1}$, respectively. Validation of the methodology was confirmed with standard addition to real samples and ICP-Ms analysis.

## 1. Introduction

Heavy metals accumulate in different human tissues as non biodegradability property. Many of them enter to the human body from foods and waters and absorb them by the gastrointestinal system. Moreover, even with low concentration in the human biological matrix have a toxicological effect in human body and cause chromosomal aberration, cancer, and changes in DNA. The main source of chromium pollutants in the environment is chemical factories, steelworks and industrial electroplating. [1, 2]. The chromium has two species ($Cr_{III}$ and $Cr_{VI}$) in the environment with different toxicity and physiological effects in humans. The metabolism of glucose, protein and lipids in the human body depend on Cr (III) compounds in humans [3-5]. But the Cr (VI) is toxic and causes cancer in humans. Due to the high oxidation of Cr (VI), it can be simply entered cells and damage the proteins and DNA of the nucleolus. Also, the Cr (VI) is harmful to different organs such as the lungs, liver and kidneys [6, 7]. The World Health Organization (WHO) reported the concentration chromium in water less than 2

Corresponding Author: Jamshid Rakhtshah

Email:jamshid_rakhtshah@yahoo.com

https://doi.org/10.24200/amecj.v3.i03.114

μg L$^{-1}$ and 50 μg L$^{-1}$ as normal range and toxicity in waters [8]. Also, the national health company announced that the value of 0.1-1.7 μg L$^{-1}$ and 0.24-1.8 μg L$^{-1}$ for normal chromium in blood and urine samples [9, 10]. So, as different toxicity and exposure, the favorite and efficient procedure must be used for chromium speciation. Many efficient techniques such as inductively coupled plasma mass spectrometry [11], flame atomic absorption spectrometry (F-AAS) [12], inductively coupled plasma optical emission spectrometry (ICP-OES) [13], inductively coupled plasma-mass spectrometry (ICP-MS) [14], energy dispersive X-ray fluorescence spectrometry [15] and electrothermal atomic absorption spectrometry (ETAAS) [16] were used for chromium determination and speciation. However, the high cost of instrumental and difficulty matrix in human samples caused to use of these techniques with sample preparation methods. Recently, green analytical chemistry based on ionic liquids (ILs) as a simplification and authors reported miniaturization of the sample preparation with green solvent. Therefore, some of sample preparation procedures such as the liquid-liquid microextraction (LLME) [17], the solid-phase extraction (SPE) [18], the dispersive micro solid phase extraction [19] and the magnetic solid-phase extraction (MSPE) [20] applied as sample preparation. The ILs as an organic salt has various advantages such as low vapor pressure, thermal stability about 200-350 ℃, large viscosity, good extractability and separation phase [21]. The different adsorbents such as multi-walled carbon nanotubes (MWCNTs) [22], silica nanoparticles [23], MIL-101(Fe) and dithiocarbamate-modified magnetite nanoparticles [24], and fabrication of magnetic particles imprinted cellulose based biocomposites [25] were used for extraction and separation of chromium ions in a different matrix.

In this study, the D-μ-SPBE procedure was used to develop a new procedure based on CNTs@DTG adsorbent for the speciation of trace amount of Cr (III) and Cr (VI) in human blood samples. Experimental parameters were optimized for chromium speciation, and the performance of the proposed method was evaluated by ET-AAS. As a high efficient recovery, the [OMIM][PF$_6$] was used for collecting and separation nanoparticles of CNTs@DTG from blood samples.

## 2. Experimental
### 2.1. Apparatus
Chromium determination was done based on a spectra electrothermal atomic absorption spectrometer (ET-AAS, GBC 932, Aus.) by a graphite furnace accessory. All operating parameters were set based on manufacturer book of GBC. A multi hollow cathode lamp (MHCL) with a current of 6 mA, wavelength of 357.9 nm with 0.2 nm slit was adjusted. All volumes from 20 to 100 μL were injected to furnace tubes by auto-sampler 3000. The instrumental and extraction conditions are listed in **Table 1.** The temperature programming for chromium was shown in **Table 2.** The pH of the solutions and human samples were tuned by a digital pH meter (Metrohm 744). Microwave digestions were carried out with a multi-wave 3000 (Anton Paar, 100 mL, 20 bar; Austria). The ICP-MS (Perkin Elmer, USA) as ultra-trace analysis with high sensitivity was used for determining of chromium ions in human blood samples (1200 W; 1.0 L min$^{-1}$; 2.0 sec per mass; auxiliary gas 1.2 L min$^{-1}$). An ultrasonic bath for molecular biology such as blood samples with temperature controlling in real-time was prepared (Thomas, HB120 LED digital dry bath, USA).

**Table 1.** Instrumental conditions for chromium by ET-AAS

| Parameters | Values |
|---|---|
| Wavelength | 357.9 nm |
| Slit | 0.2 nm |
| Lamp current | 6 mA |
| Injection mode | Automatic |
| Volume Injection | 20 μL |
| Mode | Peak Area |

**Table 2.** The temperature program for chromium determination by ET-AAS

| Step | Temperature (°C) | Ramp time (s) | Hold time (s) | Ar flow rate (mL min$^{-1}$) |
|---|---|---|---|---|
| Dry | 120 | 15 | 15 | 300 |
| Ash | 1150 | 30 | 15 | 300 |
| Atomize | 2500 | 1 | 2 | 0.0 |
| Clean | 2600 | 1 | 2 | 300 |

## 2.2. Reagents and materials

All reagents with ultra-trace analytical grade purchased from Merck, Germany. Cr(III) and Cr(VI) stock solution were prepared from an appropriate amount of the nitrate salt of this analytes as 1000 mg L$^{-1}$ solution in 0.02 mol L$^{-1}$ HNO$_3$ (Merck). Standard solutions were prepared daily by dilution of the stock solution. The dithioglycerol material (DTG, CAS. N: 59-52-9) was purchased from Sigma Aldrich, Germany. The buffer solution was 0.3 mol L$^{-1}$ CH$_3$COOH adjusted to pH 5.5-6.0 with 0.14 mol L$^{-1}$ of NaOH solutions (Merck). The pH was adjusted to 0.2 molL$^{-1}$ of sodium phosphate buffer solution from the pH of 5.5 to 8.2 (Na$_2$HPO$_4$/NaH$_2$PO$_4$). TX-100 as the anti-sticking agent, HNO$_3$, HCl, and acetone were purchased from Merck. Ultrapure water (18 MΩ.cm) was prepared from Millipore Water System (Bedford, USA), and 1-octyl-3-methylimidazolium hexafluorophosphate ([OMIM][PF$_6$]) was prepared from Sigma Aldrich (Germany).
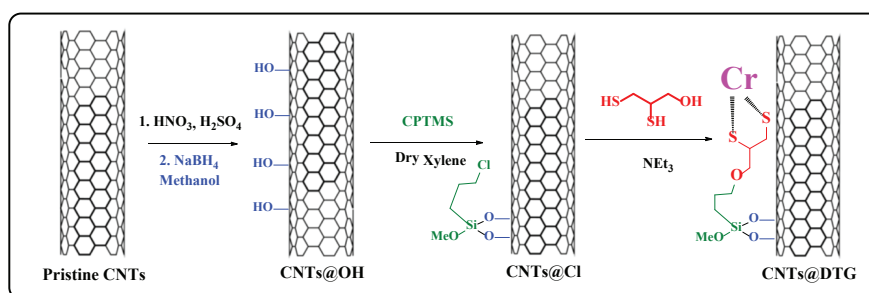
## 2.3. Sample preparation of human blood

For sampling, all glass tubes were washed with a 1.0 mol L$^{-1}$ HNO$_3$ solution for one day and thoroughly rinsed for 6 times with DW. As chromium, concentrations in human blood are very low, even minor contamination at any step of sampling, storage and analysis has the potential to affect on the accuracy of the results. For analysis in human blood samples, 20 μL of pure heparin (not chromium) was added to a 5 mL blood sample. The human blood sample was maintained at -20 °C in a PVC tube. The world medical association declaration of Helsinki (WMADH) in human blood samples was considered for sampling and analysis with permit form for all patients.

## 2.4. Synthesis of CNTs@DTG

First, the CNTs@COOH was prepared according to the acid oxidation method [26] and the CNTs@COOH convert to CNTs@OH by Sodium borohydride. Then, the 0.5 g of CNTs@OH and 40 mL of dry xylene were sonicated for 15 minutes in a 100 mL round-bottomed flask (RBF). Then, the 3 mL of (3-chloropropyl) trimethoxysilane (CPTMS) was added to the mixture. After sonicating, the resulting mixture was refluxed at 60 °C under N$_2$ atmosphere to remove the produced HCl. The product of CNTs@Cl was cooled down to room temperature, and then filtered and washed with ethanol. In a 100 mL RBF, 1 g of CNTs@Cl and 1 mL of DTG were mixed in 60 mL ethanol using an ultrasonic bath. Then, a few drops of triethylamine were added to the above slurry, and the mixture was refluxed at 60 °C for 3 h. The product was separated from the reaction mixture by a PTFE membrane filter and washed with ethanol three times and finally dried under vacuum at 100 °C **(Fig. 1)**.



**Fig. 1.** Representation of the formation of CNTs@DTG.

## 2.5. The extraction procedure

By D-μ-SPBE method, 5 mL of human blood samples were used for speciation and determination of Cr (III) and Cr (VI) at optimized pH. By procedure, the mixture of 25 mg of CNTs@DTG adsorbent, [OMIM][$PF_6$] as hydrophobic IL and acetone added to standard and human blood samples with Cr (III) and Cr (VI) concentration between 0.05-1.8 µg $L^{-1}$ at pH=6 and 2, respectively. After sonication for 3.0 min, the Cr (III) and Cr (VI) ions were extracted with the HS group of CNTs@DTG (as a dative covalent bond) in optimized pH (pH=6; CrIII$^+$→:(SH-SH)@CNTs) (pH=2; CrVI$^-$→$^+$:($SH_2$-$SH_2$)@CNTs). After extraction, the nanoparticles of CNTs@DTG were trapped in [OMIM][$PF_6$] in the bottom of the conical tube by centrifuging samples for 5 min. The upper phase was removed and then, the Cr (III) and Cr (VI) ions back-extracted from adsorbent in acidic pH ($HNO_3$, 1M, 0.1 mL) for Cr (III) and basic pH (NaOH, 0.5M, 0.1 mL) for Cr (VI), respectively. Finally, the remained solution determined by ET-AAS after diluted with DW up to 0.2 mL. The total chromium (T-Cr) was simply calculated by summarizing Cr (III) and Cr (VI) content **(Table 3)**. The procedure used for a 10 blank solutions by D-μ-SPBE method. The enrichment factor (EF) calculated by curve fitting of calibration curves before and after preconcentration process (tga=$m_1$/$m_2$). Validation of method followed by ICP-MS and CRM for chromium in real samples.

**Table 3**. Extraction conditions based on CNTs@DTG by D-μ-SPBE procedure

| Fathers | Values |
|---|---|
| Working pH of Cr(III) | 6.0 |
| Working pH of Cr (VI) | 2.0 |
| Sample volume of D-μ-SPBE | 5 mL |
| Linear range of D-μ-SPBE | 0.12-3.88 µg $L^{-1}$ |
| Correlation coefficient | R = 0.9996 |
| Volume of Triton X-100 | 30 µL |
| Volume of back-extraction (eluent) | 0.5 mL |
| Concentration of back-extraction ($HNO_3$, NaOH) | 1 and 0.5 mol $L^{-1}$ |
| Amount of IL | 100 µL, 0.1 g |
| Volume of dispersant solvent (Acetone) | 500 µL |
| Shaking time | 3 min |
| Centrifugation time | 5min |
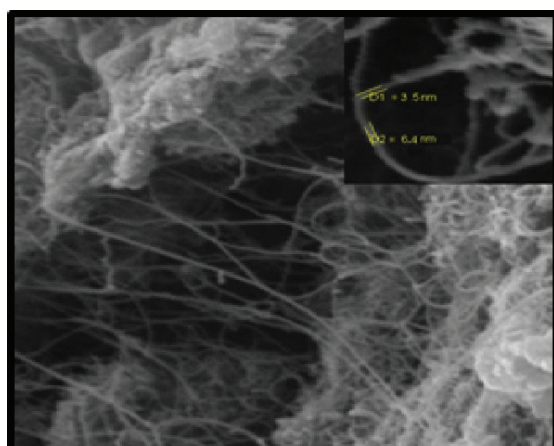


**Fig.2.** The SEM of CNTs@DTG adsorbent
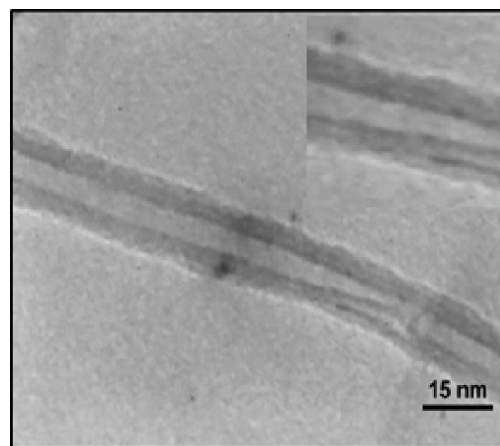


**Fig.3.** The TEM of CNTs@DTG adsorbent

# 3. Results and discussion

## 3.1. Characterizations

The hydroxyl-functionalized CNTs are used for the synthesis of CNTs@DTG adsorbent. The SEM and TEM of CNTs@DTG showed low nanoparticles size about 80 nm, that was showed in Figures 2 and 3, respectively.

The FT-IR spectrum of CNTs@DTG shows an absorption band corresponding to the C=C bond at 1570 cm$^{-1}$. The C=O stretching vibration band of the OH-functionalized CNTs was seen at 1722 cm$^{-1}$, corresponding to the primary COOH group of the CNTs. Figure 4 saw the absorption band of the O-Si-O in adsorbent seen at 1110 cm$^{-1}$. Moreover, the absorption bands at the range of 2500-3000 cm$^{-1}$ related to C–H bond, which indicates the successful functionalization of CNTs with Cl-alkylsilane material. The appearance of a band at 2625 cm$^{-1}$ confirms the presence of HS groups in the CNTs@DTG adsorbent.

## 3.2. Effect of ETAAS conditions

For increasing accuracy and repeatability of the procedure, the triton X-100 was used in human blood samples. First, we selected a drying time of 30 s for water evaporation with 40s of ramp time. Then, the effect of pyrolysis temperature on Abs was studied within a range of 600-1400 ℃. The maximum Abs was obtained from 1000 to 1200 ℃. So, 1150 ℃ was selected as the optimum point. Also, the effect of atomization on chromium determination was examined between 2000–3000 ℃, and the maximum signal was obtained at 2.500 ℃. Cleaning time and temperature were ordered at 3 s and 2.600 ℃, respectively with Ar flow rate of 300 mL min$^{-1}$.

## 3.3. Effect of pH on the extraction

The influence of pH on adsorption of Cr (III) and Cr (VI) ions on CNTs@DTG was investigated in different pH between 2-11 for 1.0 μg L$^{-1}$ of chromium concentration. The chemical and physical adsorption was strongly conditioned by the pH of solutions. The results show that the highest extraction efficiency for Cr (VI) was achieved in pH ranges from 1 to 3, but the recovery values for Cr (III) were below 5% in this pH. On the other hand, the efficient extraction for Cr (III) was achieved in pH ranges from 5 to 7, but the recovery values for Cr (VI) were below 5%. Thus, the procedure was applied to the speciation of two forms of chromium at pH 2 and 6 as optimum points for Cr (VI) and Cr (III) extraction, respectively, by D-μ-SPBE procedure (Fig. 5).
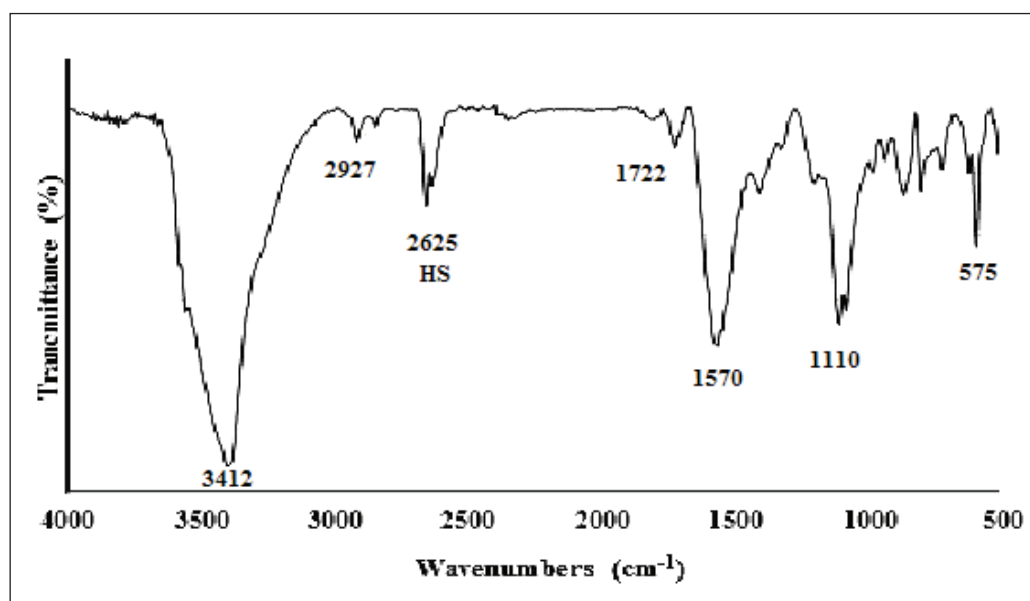


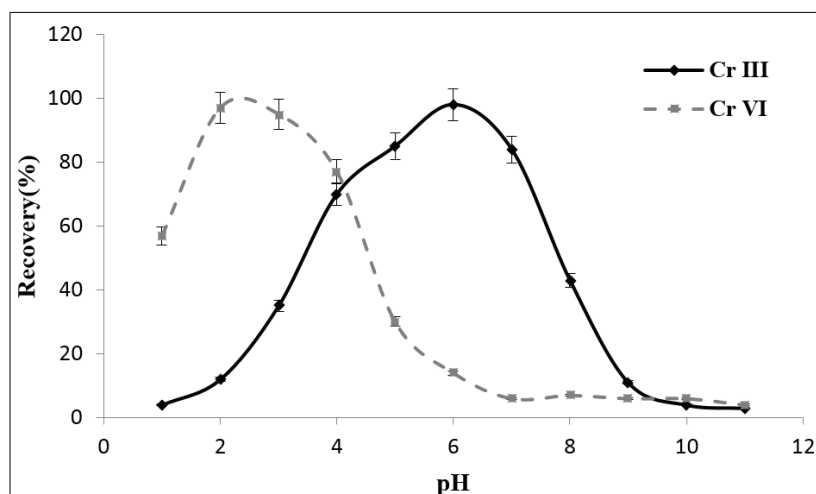**Fig.4.** The FTIR of CNTs@DTG adsorbent

**Fig. 5.** The effect of pH on extraction and speciation of Cr (III)
and Cr (VI) based on CNTs@DTG adsorbent by the D-μ-SPBE procedure

### 3.4. Effect of sample volume and amount of ionic liquid

Sample volume is one of the most important parameters to be studied. The effect of sample volume between 2-20 mL was studied for 1.0 μg L⁻¹ of Cr (III) and Cr (VI) ions. Quantitative extraction was observed between 2 ml and 10 ml. The recovery was decreased by more than 10 mL of blood samples. Moreover, in high sample volumes, the ionic liquid is partially solubilized in the liquid phase and leads to non-reproducible results. Therefore, a sample volume of 5 mL was selected for further works by D-μ-SPBE procedure **(Fig. 6)**. On the other hand, the extraction efficiency of

the procedure was remarkably dependent on the ionic liquid amount as a separating phase. So, the amount of [OMIM][PF$_6$], [HMIM][PF6] and [EMIM][PF6] as hydrophobic ILs was studied between 0.05-0.2 g. The results showed us, and the quantitative extraction was obtained more than 0.08 g of [OMIM][PF$_6$]. Therefore, the amount of 0.1 g was selected as optimum mass for ionic liquid for collecting and separating CNTs@DTG from the liquid phase **(Fig. 7)**.

### 3.5. Effect of CNTs@DTG mass

By procedure, the amount of CNTs@DTG adsorbent studied and optimized. Therefore, the amounts of
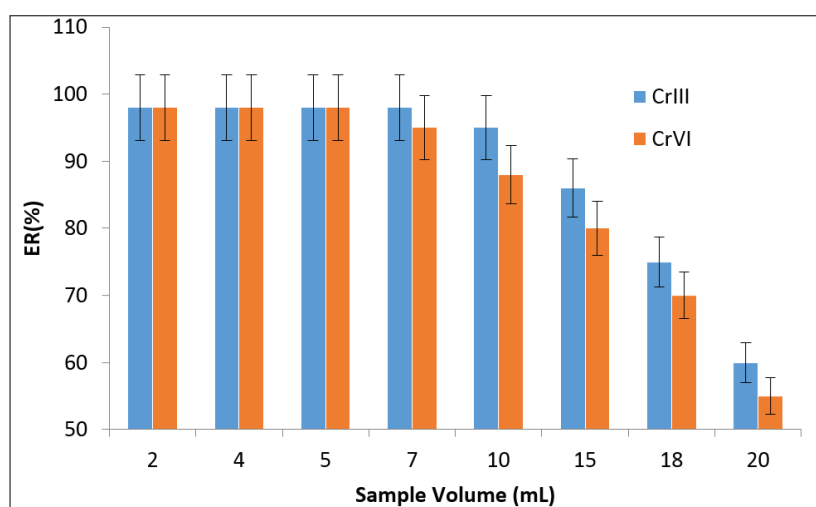


**Fig. 6.** The effect of sample volume on extraction and speciation of
Cr (III) and Cr (VI) based on CNTs@DTG adsorbent by the D-μ-SPBE procedure
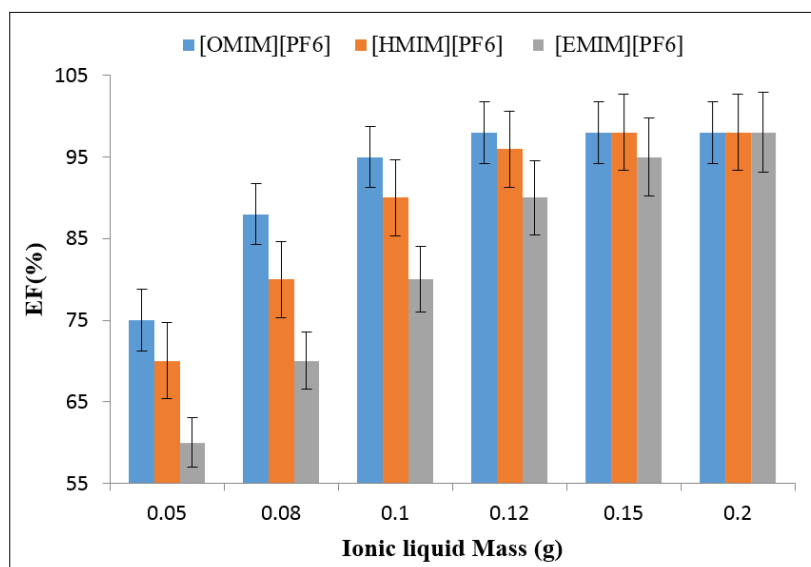
**Fig. 7.** The effect of ionic liquids mass on extraction and speciation of
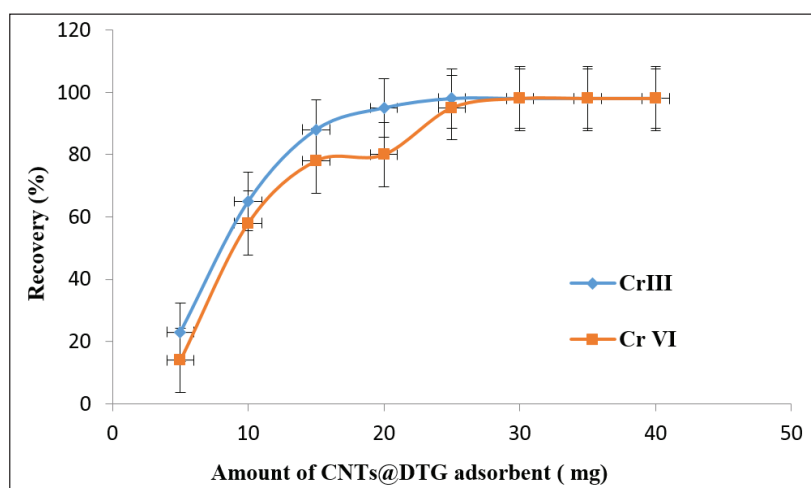Cr (III) and Cr (VI) based on CNTs@DTG adsorbent by the D-µ-SPBE procedure



**Fig. 8.** The effect of CNTs@DTG mass on extraction and speciation of
Cr (III) and Cr (VI) by the D-µ-SPBE procedure

CNTs@DTG adsorbent between 5-35 mg were examined for Cr (III) and Cr (VI) extraction by the D-µ-SPBE procedure. Based on results, the quantitative recoveries in human blood samples were obtained with 20 mg and 25 of CNTs@DTG for Cr (III) and Cr (VI) extraction, respectively. So, 25 mg of CNTs@DTG was used as an optimum mass for D-µ-SPBE procedure **(Fig. 8)**.

### 3.6. Effect of eluent on recovery
The Cr (III) and Cr (VI) were back-extracted from CNTs@DTG sorbent based on changing pH by D-µ-SPBE procedure. By decreasing and increasing the

pH, the covalence bonding in Cr (III) and Cr (VI) dissociate and release into the liquid phase. Different mineral reagents such as NaOH, HCl, $HNO_3$, $H_2SO_4$ were selected for investigating of chromium back-extraction from the CNTs@DTG /IL phase. The research showed that 1 mol $L^{-1}$ of $HNO_3$ and 0.5 mol $L^{-1}$ of NaOH quantitatively extracted Cr (III) and Cr (VI) from the CNTs@DTG /IL phase.

### 3.7. Effect of interference ions on extraction
By procedure, the interference ions can be affected by the extraction chromium in blood samples. Due to human blood samples, the most probable

**Table 4.** The effect of matrix ions on the determination of Cr (III)
and Cr (VI) by D-μ-SPBE procedure

| Ions | Maximum tolerance ratio (matrix ion conc./Cr conc.) | | Recovery (%) | |
|---|---|---|---|---|
| | Cr (VI) | Cr (III) | Cr (VI) | Cr (III) |
| $K^+$, $Na^+$, $Li^+$, $Ca^{2+}$, $Mg^{2+}$ | 1100 | 900 | 97.4 | 98.3 |
| $Mn^{2+}$, $Cu^{+2}$, $Zn^{2+}$ | 850 | 700 | 98.2 | 96.5 |
| $Cd^{2+}$, $Pb^{2+}$ | 500 | 600 | 99.2 | 97.7 |
| $Cl^-$, $F^-$, $I^-$, $NO_3^-$, $CH3COO^-$ | 1200 | 1000 | 98.1 | 96.8 |
| $PO_4^{3-}$, $CO_3^{2-}$, $SO_4^{2-}$ | 900 | 750 | 97.5 | 98.2 |
| $Ag^+$, $Ni^{2+}$, $Hg^{2+}$ | 200 | 250 | 95.3 | 97.6 |
| $Fe^{3+}$, $V^{3+}$ | 500 | 650 | 96.8 | 98.9 |

metal ions in blood were selected for evaluating of potential interfering ions on the extraction of chromium. So, the 5 ml of the sample containing 3.5 μgL$^{-1}$ of Cr (III) and Cr (VI) and 1-2 mg L$^{-1}$ of different ions in the matrix were used. The tolerate amounts of each ion had less than 5% of the absorbance alteration. The results showed interference ions do not decrease the extraction of chromium in optimized conditions. The results are shown in **Table 4**.

### 3.8. Validation of D-μ-SPBE procedure
The D-μ-SPBE method was applied to determine Cr (VI) and Cr (III) in 10 mL of human blood samples at pH of 2 and 6, respectively. Since no standard reference material (CRM) for Cr (III) and Cr (VI) are currently available, So, ICP Ms analysis in blood samples as CRM was used to spike real samples **(Table 5)**. Also, the spiked samples have demonstrated the

reliability, precision and accuracy of the method for determination of Cr (III) and Cr (VI) in human blood samples by D-μ-SPBE procedure **(Table 6)**. The extraction efficiency of spiked samples is satisfactorily reasonable and was confirmed using the addition method, which indicates the capability of the system in the determination of Cr (VI) and Cr (III) in human blood samples. The calibration curve of the D-μ-SPBE method was linear between 0.12-3.88 μg L$^{-1}$ after the preconcentration process. The Cr (VI) enters to the cytoplasm of red blood cells (RBC) and is reduced to Cr(III) by Cys and ascorbic acid. So, the concentration of chromium in the red blood cells related to exposure of Cr (VI). Thus, the total concentration of Cr in blood was calculated by summarizing of Cr (VI) and Cr (III) which was determined by ET-AAS. Therefore, The Cr (VI) has a low concentration in serum or plasma samples as compared to blood samples.

**Table 5.** Method validation for chromium in human blood samples by ICP-MS
and compared to the D-μ-SPBE method (n=5)

| [a] Sample | Added (μg L$^{-1}$) | *ICP-MS (μg L$^{-1}$) | *Found (μg L$^{-1}$)[a] | Recovery (%) |
|---|---|---|---|---|
| A | ------ | 1.22 ± 0.02 | 1.19 ± 0.06 | 97.5 |
| | 1.0 | ------ | 2.15 ± 0.07 | 96.0 |
| B | ------ | 1.51 ± 0.03 | 1.54 ± 0.08 | 101.9 |
| | 1.5 | ------ | 2.97 ± 0.14 | 95.3 |
| C | ------ | 2.04 ± 0.05 | 1.98 ± 0.11 | 97.1 |
| | 1.5 | ------ | 3.43 ± 0.16 | 96.6 |
| D | ------ | 0.55 ± 0.01 | 0.58 ± 0.02 | 105.4 |
| | 0.5 | ------ | 1.06 ± 0.05 | 96.0 |

*Mean of three determinations ± confidence interval (P = 0.95, n =5)
[a] A,B,C,D are real blood samples which analysis with ICP-MS as CRM of total chromium

**Table 6.** Validation of chromium speciation based on CNTs@DTG in human serum and blood samples by D-μ-SPBE method

| Sample | Added (μg L⁻¹) | | Found (μg L⁻¹)[a] | | Total[a] | Recovery (%) | |
|---|---|---|---|---|---|---|---|
| | Cr (III) | Cr (VI) | Cr (III) | Cr (VI) | | Cr (III) | Cr (V) |
| **Blood** | --- | --- | 1.45 ± 0.08 | 0.26 ± 0.02 | 1.71 ± 0.09 | --- | --- |
| | 1.5 | --- | 2.93 ± 0.15 | 0.24 ± 0.01 | 3.17 ± 0.29 | 98.6 | --- |
| | --- | 0.2 | 1.47 ± 0.09 | 0.45 ± 0.02 | 1.92 ± 0.11 | --- | 95.0 |
| **Blood** | --- | --- | 1.61 ± 0.11 | 0.76 ± 0.03 | 2.37 ± 0.12 | --- | --- |
| | 1.5 | --- | 3.09 ± 0.14 | 0.73 ± 0.04 | 3.82 ± 0.20 | 98.7 | --- |
| | --- | 1.0 | 1.59 ± 0.10 | 1.78 ± 0.08 | 3.36 ± 0.18 | --- | 102 |
| **Serum** | --- | --- | 1.92 ± 0.09 | 0.14 ± 0.01 | 2.06 ± 0.12 | --- | --- |
| | 1.5 | --- | 3.38 ± ٠,١9 | 0.16 ± 0.01 | 3.56 ± 0.16 | 97.3 | --- |
| | --- | 0.2 | 1.89 ± ٠,10 | 0.33 ± 0.01 | 2.22 ± 0.11 | --- | 95 |

[a]Mean of three determinations ± confidence interval (P = 0.95, n = 5)

## 4. Conclusion

In this work, the D-μ-SPBE procedure combined with ET-AAS to develop a new procedure for the speciation and determination of trace amount of Cr (III) and Cr (VI) in blood samples. Moreover, the factors influencing the D-μ-SPBE procedure such as; the sorbent mass, the sample volume, the amount of IL and pH were studied and optimized. The [OMIM][PF6] as hydrophobic ionic liquid helps to provide a reliable and efficient extraction for speciation of Cr (III) and Cr (VI) in blood samples as an environmentally friendly solvent for collecting of CNTs@DTG adsorbent from the liquid phase. The enrichment factor and recovery was 9.8 and 95-105%, respectively. The limit of detections (LOD) of 32 ng L⁻¹ and 28 ng L⁻¹ for Cr (III) and Cr (VI) were achieved at pH 6 and 2, respectively. In this study, a simple, efficient extraction and sensitive procedure were used for speciation of Cr (III) and Cr (VI) in human blood samples in a short time as compared to other methods. The mean of PF, reusability, RSD%, and LOD were obtained 9.85, 24 times, 2.53 and 30 ng L⁻¹ for 5.0 mL of human blood samples, respectively. Validation of the methodology was confirmed by spiking and ICP-Ms analysis as CRM to samples. The proposed procedure was successfully used to speciation and separation of Cr (III) and Cr (VI) in human blood samples.

## 6. References

[1] Y. Wang, H. Su, Carcinogenicity of chromium and chemoprevention: a brief update, Onco. Targets Ther., 10 (2017) 4065–4079.

[2] P. Singh, D.K. Chowdhuri, Environmental presence of hexavalent but not trivalent chromium causes neurotoxicity in exposed drosophila melanogaster, Mol Neurobiol., 54 (2017) 3368-3387.

[3] A. Swaroop, M. Bagchi, H.G. Preuss, S. Zafra-Stone, T. Ahmad, D. Bagchi, Benefits of chromium (III) complexes in animal and human health, the nutritional biochemistry of chromium (III), Cambridge, MA: Elsevier, pp. 251-78, 2019.

[4] J.B. Vincent JB, New evidence against chromium as an essential trace element, J. Nutr., 147 (2017) 2212-2219.

[5] E.M. Hamilton, S.D. Young, E.H. Bailey, M.J. Watts, Chromium speciation in foodstuffs: A review, Food Chem., 250 (2018)105-12.

[6] K. Yatera, Y. Morimoto, S. Ueno, S. Noguchi, T. Kawaguchi, F. Tanaka, H. Suzuki, T. Higashi, Cancer risks of hexavalent chromium in the respiratory tract, J. UOEH., 40 (2018) 157–172.

[7] P.L. Abreu, T. Cunha-Oliveira, L.M.R. Ferreira, A.M. Urbano, Hexavalent chromium, a lung carcinogen, confers resistance to thermal stress and interferes wif heat shock protein expression in human bronchial epithelial cells, Biometals, 31 (2018) 477–487.

[8] World Health Organization. Inorganic Cr(VI) compounds., concise international chemical assessment document, Geneva, World Health Organization,78, 2013.

[9] American Conference of Governmental Industrial Hygienists (ACGIH), U.S documentation of the threshold limit values and biological exposure indices, 7th Edition, 2011.

[10] Agency for Toxic Substances and Disease Registry (ATSDR), Chromium, public health service, US Atlanta GA, 2018.

[11] Q.y. Zhu, L.y. Zhao, Speciation analysis of chromium by carboxylic group functionalized mesoporous silica with inductively coupled plasma mass spectrometry, Talanta, 195 (2019) 173-180.

[12] A. Islam, H. Ahmad, N. Zaidi, S. Kumar, A graphene oxide decorated with triethylenetetramine-modified magnetite for separation of chromium species prior to their sequential speciation and determination via FAAS, Microchim. Acta, 183 (2016) 289–296.

[13] T.S. Munonde, N.W. Maxakato, P.N. Nomngongo, Preconcentration and speciation of chromium species using ICP-OES after ultrasound-assisted magnetic solid phase extraction with an amino-modified magnetic nanocomposite prepared from $Fe_3O_4$, $MnO_2$ and $Al_2O_3$, Microchim. Acta, 184 (2017) 1223– 1232.

[14] H. M. Huang, L. J. Zhao, B. S. Chen, B. Hu, Advanced functional materials in solid phase extraction for ICP-MS determination of trace elements and their species: A review, Anal. Chim. Acta, 973 (2017) 1–24.

[15] L.A. Meira, Multi-element determination of Cd, Pb, Cu, V, Cr, and Mn in ethanol fuel samples using energy dispersive X-ray fluorescence spectrometry after magnetic solid phase microextraction using $CoFe_2O_4$ nanoparticles, J. Microchem., 142 (2018) 144–151.

[16] Z. Sarikhani, M. Manoochehri, Determination of Ultra Trace Cr(III) and Cr(VI) species by electrothermal atomic absorption spectrometry after simultaneous Magnetic solid phase extraction with the aid of a novel imidazolium-functionalized magnetite graphene oxide nanocomposite, Bull. Chem. Soc. Jpn., 90 (2017) 746–753.

[17] N. Campillo, P. Viñas, J. Sandrejova, V. Andruch, Ten years of dispersive liquid-liquid microextraction and derived techniques, Appl. Spect. Rev., 52 (2017) 267–415.

[18] B. Hu, M. He, B. Chen, In solid phase extraction, (ed Colin, F. Poole) Elsevier, pp. 235–284, 2020.

[19] M. Ghorbani, M. Aghamohammad hassan, M. Chamsaz, H. Akhlaghi, T. Pedramrad, Dispersive solid phase microextraction, TrAC, Trends Anal. Chem., 118 (2019) 793–809.

[20] K. M. Diniz, C. R. Teixeira Tarley, Speciation analysis of chromium in water samples through sequential combination of dispersive magnetic solid phase extraction using mesoporous amino-functionalized $Fe_3O_4$/ $SiO_2$ nanoparticles and cloud point extraction, J. Microchem., 123 (2015)185–195.

[21] L. Zhiyong, Y. Feng, L. Xiaomin, W. Huiyong, P. Yuanchao, H.Q. Nimal Gunaratne, W. Jianji, Light-triggered switchable ionic liquid aqueous two-phase systems, ACS Sustain. Chem. Eng., 8 (2020) 15327-15335.

[22] S. M. Yousefi, F. Shemirani, Carbon nanotube-based magnetic bucky gels in developing dispersive solid-phase extraction: application in rapid speciation analysis of Cr(VI) and Cr(III) in water samples, Int. J. Environ. Anal. Chem., 97 (2017) 1065–1079.

[23] M. H. Mashhadizadeh, M. Amoli-Diva, Atomic absorption spectrometric determination of $Al^{3+}$ and $Cr^{3+}$ after preconcentration and separation on 3-mercaptopropionic acid modified silica coated-$Fe_3O_4$ nanoparticles, J. Anal. At Spectrom., 28 (2013) 251–258.

[24] A. Saboori, A nanoparticle sorbent composed of MIL-101(Fe) and dithiocarbamate-modified magnetite nanoparticles for speciation of Cr(III) and Cr(VI) prior to their determination by electrothermal AAS, Microchim. Acta, 184 (2017) 1509–1516.

[25] S. Periyasamy, V.Gopalakannan, N. Viswana, Fabrication of magnetic particles imprinted cellulose based biocomposites for chromium(VI) removal, Carbohydr. Polym., 174 (2017) 352–359.

[26] M.B. HosseinAbadi, H. Shirkhanloo, J. Rakhtshah, The evaluation of TerphApm@MWCNTs as a novel heterogeneous sorbent for benzene removal from air by solid phase gas extraction, Arab. J. Chem., 13 (2020) 1741-1751.